ADDIS ABABA UNIVERSITY
SCHOOL OF GRADUATE STUDIES
FACULTY OF TECHNOLOGY
DEPARTMENT OF MECHANICAL ENGINEERING

LARGE SCALE APPLICATION OF SOLAR WATER HEATING SYSTEM IN ETHIOPIA

A thesis submitted to the School of Graduate Studies of Addis Ababa University in partial fulfillment of the Degree of Masters of Science in Mechanical Engineering

(Thermal Engineering Stream)

By: ***Addisu Bekele***

Advisor: ***Dr. -Ing. Demiss Alemu***

July 2007

ADDIS ABABA UNIVERSITY
SCHOOL OF GRADUATE STUDIES

LARGE SCALE APPLICATION OF SOLAR WATER HEATING SYSTEM IN ETHIOPIA

By: Addisu Bekele

Faculty of Technology

Approved by board of Examiners

Ato Hamssasew Moges	
Chairman	*Signature*
Dr.-Ing. Demiss Alemu	
Adviser	*Signature*
Dr.-Ing. Abebayehu Assefa	
Internal Examiner	*Signature*
Dr. Tesfaye Dama	
External Examiner	*Signature*

ACKNOWLEDGMENT

I would like to express my sincere gratitude to my advisor Dr.-Ing. Demiss Alemu for giving me the opportunity to work on this project and for his guidance and encouragement without which this work could have not been completed. He has been a constant source of inspiration through out my study period.

I am also grateful to Dr.-Ing Abebayehu Assefa for his kind help on different occasions.

Last but not least, I would like to thank my family and friends who were always besides me and played a great role in completion of my work.

ABSTRACT

In this thesis the investigation of the possible use of solar energy for large scale water heating system is conducted for the following sites in Ethiopia: Addis Ababa Tannery, Dire Tannery, Modjo Tannery, and Jimma Hospital.

The thesis focuses on simulation of large-scale solar water heating system and its economic analysis. Transient performance of the system is computed using a numerical heat transfer model of a single glass cover flat plate collector solar water heater with riser and header type active system. The various design parameters are gathered from the inside country solar water heater manufacturers and dealer companies and also from the world experience. The meteorological data for simulation was prepared by taking the average of five years starting from 2001 - 2005.

From the annual contribution of solar energy to the heating load and the estimated investment cost, the unit solar energy cost and the pay back period of the system for each case were calculated.

The result obtained indicates that the unit solar energy cost for all cases are less than that of unit cost of fuel heating. Hence the solar energy is the viable alternative source of energy for large-scale water heating systems in Ethiopia.

TABLE OF CONTENTS

LIST OF FIGURES

LIST OF TABLES

CHAPTER 1

INTRODUCTION

1.1 Problem Background

Ethiopia, in addition to the persistent food insecurity, is suffering from energy under utilized. It is observed through studies and recent data, energy consumption increases proportionally to the gross national product. One of the possible methods of overcoming energy crisis is by increasing the use of renewable energy sources such as solar energy, which is freely available.

The country, because of its proximity to the equator, receives adequate sunshine throughout the year. The average daily radiation intensity on the horizontal surface is 5.2 kWh/m^2 [17]. Hence Ethiopia can use solar energy for domestic and commercial applications.

Many hospitals and tanneries use fuel for water heating system. However, energy costs for heating water is increasing at considerable rate by increasing operating costs and reducing profitability due to continuous escalating of fuel price. Hence, this thesis is going to explore solar energy as sustainable alternative for large scale water heating in tanneries and hospitals.

In this thesis, the performance and economic visibility of the solar water heating system for hospitals and tanneries are analyzed using computer simulation.

This thesis is an attempt to ameliorate large-scale solar water heating systems and a step forward to reduce dependency on imported oils.

1.2 Objectives

The general objective of this thesis is to apply solar water heating system in Hospitals and tanneries in a large scale as an alternative method for heating water rather than using fossil fuel and demonstrate its economic feasibility inputting meteorological data of selected areas in Ethiopia in order to support policy decisions in applying a large scale solar water heaters in Ethiopia.

The specific objectives of this thesis are, therefore,

- Simulation of solar water heating system using FORTRAN.
- Determining the size and number of collectors needed to cover the energy demand for water heating of the specific site.
- Cost optimization of the system using computer simulation.
- Determine the unit cost, pay back period, life cycle cost (LCC) and life cycle saving (LCS) of the system from simulated performance.
- Finally, the analysis compares the conventional water heating system with the solar water heating system in different major cities in Ethiopia.

1.3 Out line of the Report

A brief introduction on the contents of the thesis report is outlined as follows. Literature review of solar water heating system is briefed in chapter two. Chapter three focuses on the types of solar collectors used for solar water heating system with special attention given to flat plate collectors. The hot water consumption pattern for different selected cases are discussed in chapter four followed by the discussion of how the solar radiation data used in simulation of solar water heating system will be determined in chapter five. Chapter six discusses the energy balance for liquid flat plate solar collector in detail. In chapter seven the transient analysis of solar water heating system is discussed. Chapter eight comprises the various results and their discussions. The control element used in controlling the solar water heating system is discussed in chapter nine, while the last two chapters, chapter ten and eleven discuses the economic analysis and conclusions and recommendations for future work respectively.

CHAPTER 2

LITERATURE REVIEW

Solar water heating systems use the sun to heat either water or a heat transfer fluid, such as water-glycol antifreeze mixture in the collectors. The heated water is then stored in a tank similar to a convectional gas or electric water tank. Some systems use an electric pump to circulate the fluid through the collectors [9].

The Performance of solar water heaters varies depending on how much energy is available and how cold the water is coming into the system.

➢ The amount of hot water a solar water heater produces depends on:

- The type and size of the system,
- The amount of sun available at the site,
- Proper installation, and
- The tilt angle and orientation of the collectors.

Solar water heaters are made up of collectors, storage tanks, and depending on the system, pumps and controllers.

Some solar water heaters use pumps to re-circulate warm water from storage tanks through collectors and exposed piping. This is generally to protect the pipes from freezing when outside temperatures drop to freezing or below.

2.1 Types of Solar Water Heaters

2.1.1 Active Systems

Active systems use pumps, valves, and controllers to circulate water or other heat-transfer fluids through the collectors. They are usually more expensive than passive systems but are also more efficient. Active systems are usually easier to retrofit than passive systems because their storage tanks do not need to be installed above or close to the collectors. But because they use electricity for pumping, they will not function in a power outage.

2.1.1.1 Open-Loop Active Systems

Open-loop active systems use pumps to circulate water through the collectors. There is no anti-freeze solution used in this type of system. These systems, also known as "**Direct System**" and are the most common systems in use in tropical and sub-tropical climates where temperatures do not often go below 0°C [9, 18, 16].

Recirculation Systems

These are a specific type of open-loop system that provides freeze protection. They use the system pump to circulate warm water from storage tanks through collectors and exposed piping when temperatures approach freezing [9].

Photovoltaic Operated Systems

This type of solar water heaters is not much different to the ones discussed above. The main difference comes from the fact that the energy to power the pump is provided by a photovoltaic (PV) panel. The PV panel converts the sunlight into electricity, which then drives the pump. In this way water flows through the collector when the sun is shining.

The pump and the PV panel have to be suitable matched in order to ensure optimum performance of the system. The pump starts when there is sufficient solar radiation available to heat the solar collector.

Timers also used in order to control solar system operation. Most of them have a battery back up in case of power failure. The timers operate during the day when solar radiation is available to heat water. In order to avoid loss of energy from the tank during cloudy days, the collector lines are connected to the bottom of the storage tank with a special valve [9, 18].

2.1.1.2 Closed-Loop Active Systems

Closed-loop active systems also called "**Indirect Systems**" are designed for use in climates where freezing weather can occur more frequently. These systems, also known as closed loop systems, are the most commonly used in cold climates where temperatures often go below 0°c. A solar collector, filled with an anti-freeze solution (heat-transfer fluids), is used to collect the thermal energy in sunlight. Typically a propylene glycol or ethylene glycol and water mixture is used [9, 18, 16].

A pump circulates the solution through the collector and into a storage tank where a heat exchanger is fitted. The heat exchanger transfers the heat into the water stored in the tank.

The tube is designed to transfer the heat into the coldest water in the tank. The heat exchanger is a coil of tubing that wraps around inside the perimeter of the storage tank.

Drain Back Systems

Drain back systems are an indirect closed loop system that uses water as the heat-transfer fluid in the collector loop. There is no contact between the heat transfer liquid and the water in the system.

Drain back systems are used in cold climates to reliably ensure that the collectors and the piping never freeze. This protection is achieved when the system is operated in drain mode. In drain mode all of the liquid in the system's collectors and piping is drained back into an insulated reservoir tank when the system is not producing heat. An indicator on the reservoir tank shows when the collector is completely drained. Each time the pump shuts off the solution in the collector is drained into the reservoir tank [9].

2.1.2 Passive Systems

Passive systems move water or a heat-transfer fluid through the system without pumps. Passive systems have no electric components to break. This makes them generally more reliable, easier to maintain, and possibly longer lasting than active systems [9, 18, 16]. Passive systems can be less expensive than active systems, but they can also be less efficient.

Passive systems may be:

- Thermosiphon system, or
- Batch heater.

Passive systems that circulate water through thermosiphoning action are called Thermosiphon system and passive systems, whose collector and storage is one and the same, are called Batch Heater.

2.1.2.1 Thermosiphon Systems

A thermosiphon system relies on warm water rising, a phenomenon known as natural convection, to circulate water through the collectors and to the tank.

The collector absorbs the sun's energy and the water inside the collector flow-tubes is heated. As it heats, the water expands and becomes lighter than the cold water in the solar storage tank mounted above the collector. Gravity then pulls heavier, cold water down from the tank and into the collector inlet. The cold water pushes the heated water through the collector outlet and into the top of the tank, thus heating the water in the tank [9, 18].

A thermosiphon system requires neither pump nor controller. Cold water flows directly to the tank on the roof. Solar heated water flows from the rooftop tank to the auxiliary tank installed at ground level. This system features a thermally operated valve that protects the collector from freezing. It also includes isolation valves, which allow the solar system to be manually drained in case of freezing conditions, or to be bypassed completely.

2.1.2.2 Batch Heaters

Batch heaters (also known as "bread box" or integral collector storage systems) are simple passive systems consisting of one or more storage tanks placed in an insulated box that has a glazed side facing the sun.

In the integral collector storage solar system, the hot water storage system is the collector. Cold water flows progressively through the collector where it is heated by the sun. Hot water is drawn from the top, which is the hottest, and replacement water flows into the bottom [18, 16]. Some batch heaters use "selective" surfaces on the tank(s). These surfaces absorb sun well but inhibit radiative loss.

This system is simple because pumps and controllers are not required. On demand, cold water from the house flows into the collector and hot water from the collector flows to a standard hot water auxiliary tank within the house.

2.2 Benefits of Solar Water Heater

A solar water heater is a long-term investment that will save you money and energy for many years. Like other renewable energy systems, solar water heaters minimize the environmental effects of enjoying a comfortable, modern lifestyle. In addition, they provide insurance against energy price increases, help reduce our dependence on imported oil, and are investments in everyone's future.

2.3 International Experience

Figure2.1 shows a brief review of international experience in solar water heating system in the year of 2001. In terms of collector density per inhabitant, International Energy Agency (IEA) statistics show Israel is well ahead of any other country, with Greece and Austria also having relatively high densities [14].

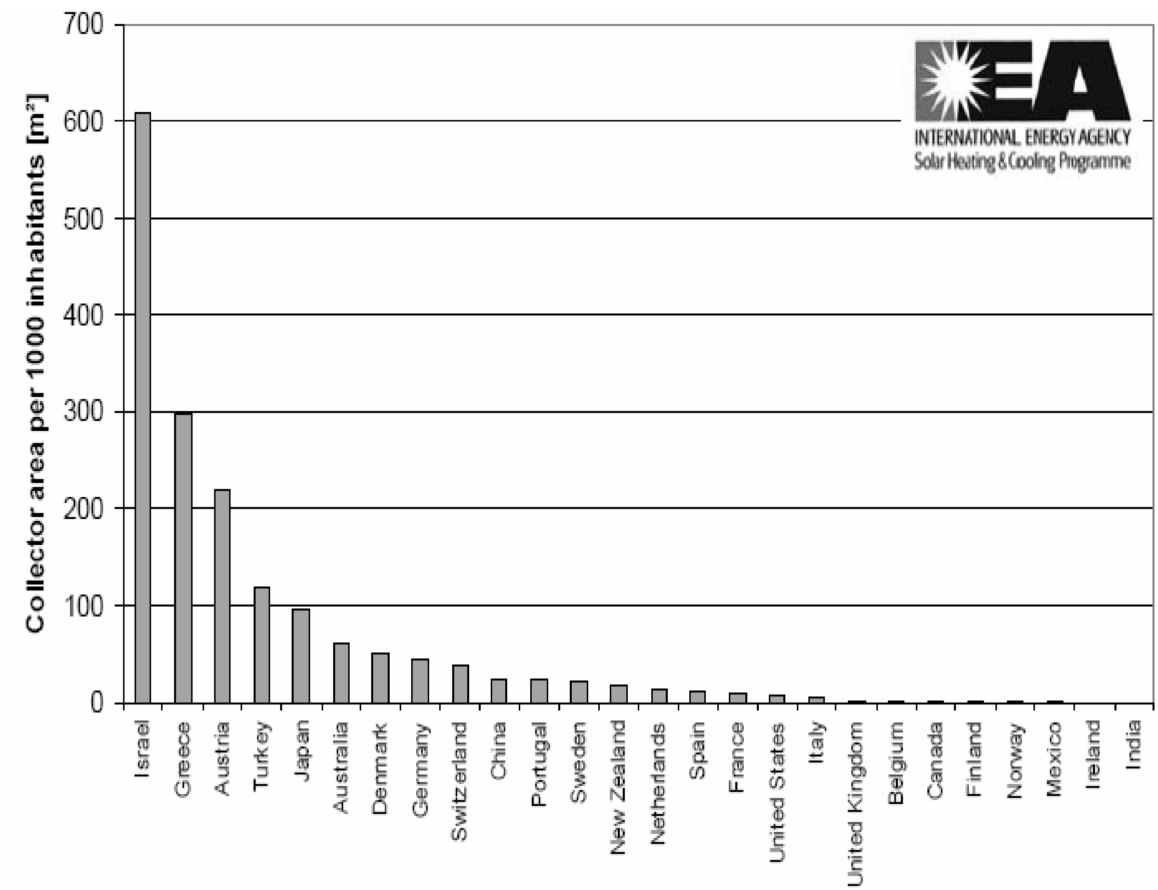

Figure 2. 1 Glazed Flat Plate and Evacuated Tube Collectors in Operation in the Year 2001 per 1000 Inhabitants.

In European countries, the most common applications for larger scale SWH include [14]:

- Government and other public buildings.
- Apartments and multi-family/person housing – are a common form of larger scale SWH applications across most European countries, and in Israel.
- Hotels and other accommodation - hotels have proven to be a prime focus of larger scale SWH. The reasons are that accommodation trends tend to be seasonal with the highest accommodation over the summer - large quantities of hot water are required for guests, laundry, kitchen etc. when solar gain is at a maximum.
- District heating schemes – there has been growing use of solar water heating particularly in the colder climates of northern Europe and Scandinavia.
- Industrial applications.

In Israel over 80% of Israeli families have solar water heaters, representing over 1.3 million installations. The solar contribution is equivalent to 21% of the electricity used by the domestic sector, 5.2% of national electricity consumption and 3% of Israel's primary energy consumption [14].

Israel has extensive experience in the installation of large scale systems including commercial buildings and hospitals, a variety of agricultural purposes (greenhouses, drying and water heating), minerals extraction at the Dead Sea works and water heating/steam production in many educational/commercial buildings [14].

The law requiring the installation of solar heater in Israel was introduced in 1980. The "Solar Law" is an amalgam of different legislative measures, all designed to lay down national standards and regulations. The Planning and Building Law requires the installation of solar water heaters for all new buildings (including residential buildings, hotels and institutions, but not industrial buildings, workshops, hospitals or high-rise buildings in excess of 27 meters (height), dictating the size of the installation required for a particular type of building. Furthermore, Israel is the only country in the world that legally requires the education of energy managers to include solar energy [14].

CHAPTER 3

SOLAR COLLECTORS

3.1 Types of Solar Collectors

- There are basically three types of collectors used for water heating system:

  - Flat plate,
  - Evacuated-tube, and
  - Concentrating.

3.1.1 Flat Plate Collectors

Flat plate collectors (figure 3.1) are the most common collectors for water heating and also it is simple and effective means of collecting solar energy for applications that require heat at temperatures below about 100 ºc. In simple words a flat plate collector is an insulated metal box with glass cover, which is called "glazing". The dark colour plate is called the "absorber plate" because it absorbs the sun radiation. The glazing can be "transparent" or "translucent" [18].

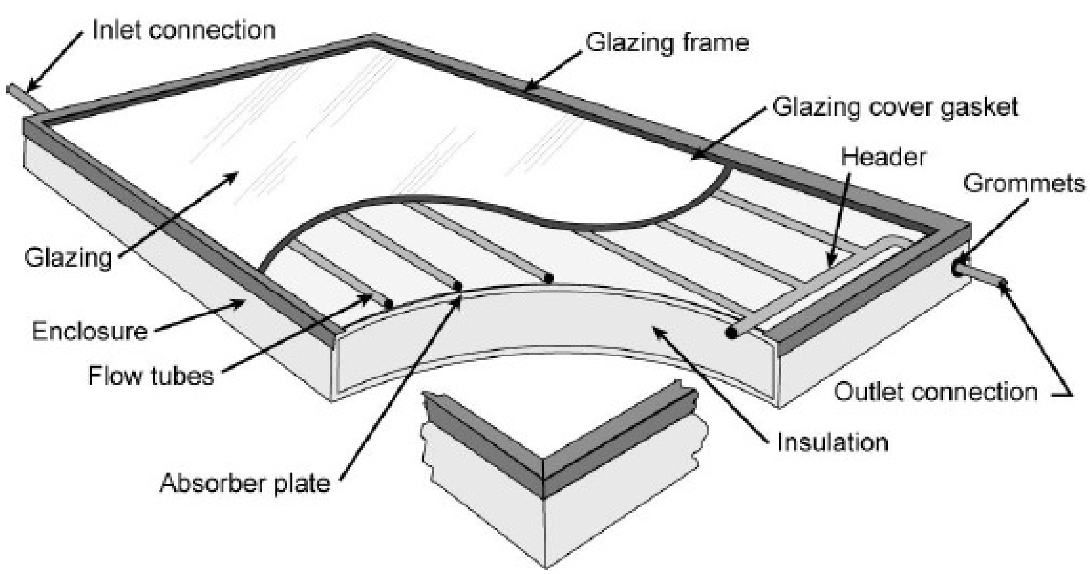

Figure 3.1 Flat Plate Solar Collector

Translucent (transmitting light only), low iron glass is a common glazing material for flat-plate collectors because low iron glass transmits a high percentage of the available solar energy.

The roles of glazing in a solar collector are:

- To transmit as much solar energy as possible to the absorber plate;
- To minimize heat loss from the absorber plate to the environment;
- To shield the absorber plate from direct exposure to weathering.

Usually the sides and the bottom of the plate are insulated to minimize the heat losses. The absorber plate is usually black. The reason is that dark colours absorb a higher percentage of sunlight than light colours.

The working principles of flat plate collector is, the sunlight passes through the glazing and strikes the absorber plate. The absorber plate then starts to heat up concentrating solar radiation into heat energy. The heat then is transferred to the water passing through the flow tubes [18].

Flat-plate collectors have the following main components:

- A transparent cover or sheet of glass.
- Tubes, fins, passages or channels are connected to the collector absorber plate.
- The absorber plate, normally metallic or with a black surface, although a wide variety of other materials can be used.
- Insulation, which should be provided at the back and sides to minimize the heat losses.
- The casing or container, which encloses the other components and protects them from the weather.

3.1.2 Evacuated Tube Collectors

Evacuated tube collectors are mostly used to heat water in residential applications that require higher temperatures. Sunlight enters through the outer glass tube and strikes the absorber tube(s) and changes to heat. The heat is transferred to the liquid flowing through the absorber tube. The collector consists of rows of parallel transparent glass each tube contains an absorber tube with selective coating. In such type of solar collectors, tubes can be either added or removed [18].

3.1.3 Concentrating Collectors

Concentrating collectors use mirror surfaces to collect sunlight on an absorber called receiver. They can achieve high temperatures but like evacuated tube collectors, this happens when direct sunlight is available. The sun's energy is collected over a large area onto a smaller absorber area to achieve high temperatures.

Concentrating collectors can reach much higher temperatures compared to flat plate collectors. However they can only focus direct solar radiation, which affects the performance of the collectors especially in cloudy days [18].

3.2 Selection of Materials for Flat-Plate Collectors

To design and construct solar collectors for water heating, detailed knowledge of the properties of the materials and the characteristics of the various components is necessary to predict the performance and durability of the collector.

Needed property data can generally be classified into three categories:

- Thermo physical
- Physical, and
- Environmental properties.

Thermo physical properties: - include thermal conductivity, heat capacity and radiant heat transfer characteristics.

Physical properties: - include density, tensile strength, melting point, and modulus of elasticity.

Environmental properties: - include resistance to ultraviolet degradation, moisture penetration and degradability due to pollutants in the atmosphere.

a) Absorber Plate: - The collector absorber plate should have high thermal conductivity, adequate tensile and comprehensive strength, and good corrosion resistance. The current liquid flat-plate solar collectors manufactured in Ethiopia are made from steel absorber plates and copper tubes.

b) Cover Plate: - The most critical factors for the cover plate-materials are strength, durability, non-degradability and solar energy transmission. Therefore, Tempered glass of thickness 3.2 mm is used as a covering material because of its proven durability and because it is not affected by ultraviolet radiation from the sun.

c) Casing: - The choice of the material for casing is largely one of cost and mild steel is used for the casing material.

d) Seal: - Sealing materials are applied to ensure the solar collector is not affected from weather conditions. The most common material used is EPDM. This sealing material is applied in solid form.

e) Absorber Insulation: - A layer of insulating material can reduce heat losses from the back and edge of an absorber plate and should be able to withstand the collector stagnation temperatures.

Mineral fibre is selected for the back and edge of absorber plate insulation because it presents no fire hazards compared to other polymeric foams and can resist the high collector stagnation temperature.

3.3 Selection of Materials for Heat Management and Storage

a) Pipes and Connection.

The pipe work in a solar system must be able to withstand circulating fluid at high temperatures without corroding.

b) Storage Tank

The primary task of the storage tank is to store the hot water without corroding, and must withstand the pressures involved.

CHAPTER 4

HOT WATER CONSUMPTION PATTERN OF SELECTED CASES

The study areas of this thesis are tanneries and hospitals located in Addis Ababa, Modjo, and Jimma. This is due to their great demand for hot water.

4.1 Addis Ababa Tannery

Hot water is used for tanning process, retanning process and also during testing in the test drum.

Source of Hot Water: The boiler is used to generate steam and the steam is directly mixed with the cold water in the tank to heat the water at different place and at required temperature.

Tanning Process: This is done in four drums. A total daily hot water required is, 27,800 litters per day.

Re tanning Process: This is done in four drums. A total daily hot water required is, 4600 litters per day.

Test Drum: 200 litters per day of hot water are consumed.

$$\text{The daily hot water consumption} = 27{,}800 + 4{,}600 + 200 = 32{,}600 \text{ liters per day}$$
$$= 32.6 \text{ m}^3 \text{ per day.}$$

Working Temperature: Of the total daily hot water consumptions 9.45 % will be heated from 50°c – 60°c and the rest will be heated below 50 °c.

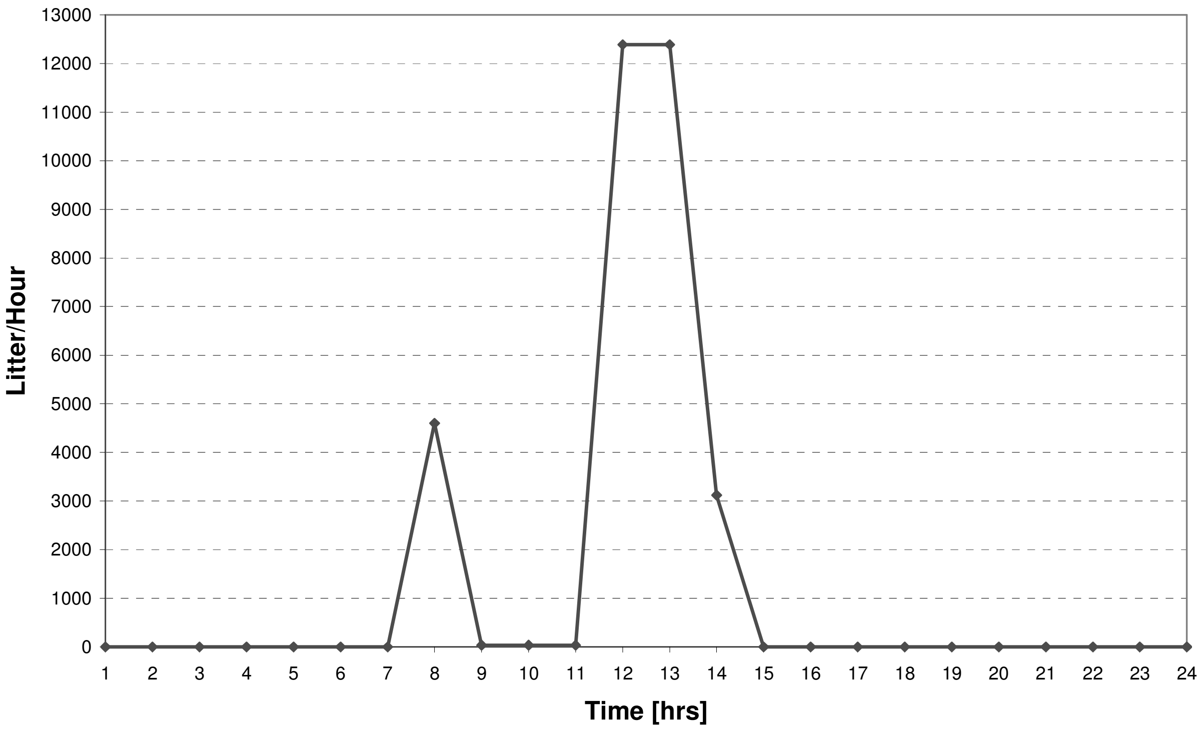

Figure 4.1 Addis Ababa Tannery Daily Hot Water Consumption Pattern

4.2 Dire Tannery

Hot water is used for tanning process, retaining process and also during testing in the test drum.

Source of Hot Water: The boiler is used to generate steam and the steam is directly mixed with the cold water in the tank to heat the water at different place and at required temperature.

Tanning Process: This is done in four drums. A total daily hot water required is, 6,300 litters per day.

Retanning Process: This is done in four drums. A total daily hot water required is, 11,930 litters per day.

Test Drum: 300 litters per day of hot water are consumed.

The daily hot water consumption = 6,300 + 11,930 + 300 = 18,530 litters per day = **18.53 m^3** per day.

Working Temperature: Of the total daily hot water consumptions 20.23 % will be heated from 50°c – 60°c and the rest will be heated below 50 °c.

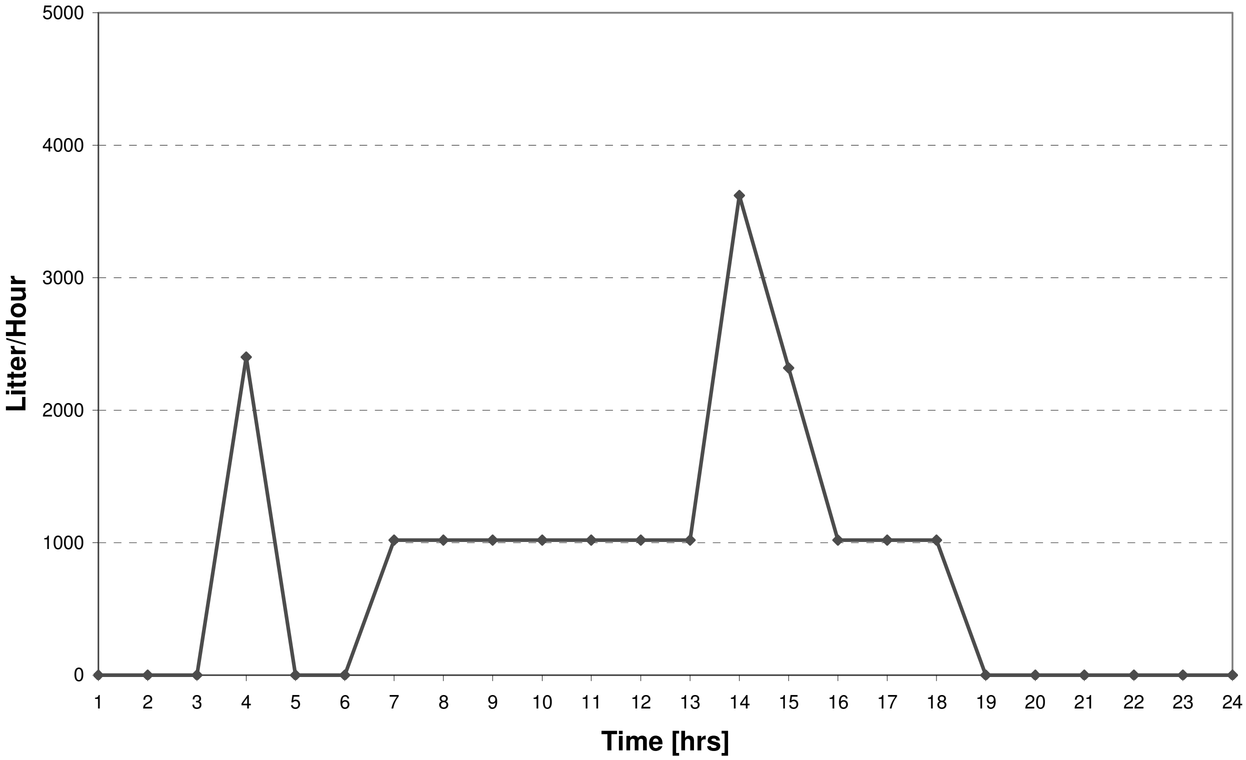

Figure 4.2 Dire Tannery Daily Hot Water Consumption Pattern

4.3 Ethiopian Tannery

It is one of the biggest tanneries in East Africa which is found In Ethiopia near koka hydro electric power station which is 10 Km from modjo on the way to Hawassa.

The factory consumes a total of 2500 m^3 per day of cold and hot water out of this the total hot water consumption is **250 m^3 per day**. The most common processes which use this hot water are tanning process and re tanning process and in the test drum during testing.

- ❖ Of the total hot water consumption 100 m^3 per day is used for skin tannery and 150 m^3 per day is for Hide tannery**.**

Source of Hot Water: The factory uses the boiler to generate steam and using the 1-2 shell and tube (quantity 5 two at a time working) heat exchanger the cold water can be heated up to 90°c which is then used by different processes at a range of 40°c – 60°c.

Working Temperature: Of the total daily hot water consumptions 24.54% will be heated from 50°c – 60°c and the rest will be heated below 50 °c.

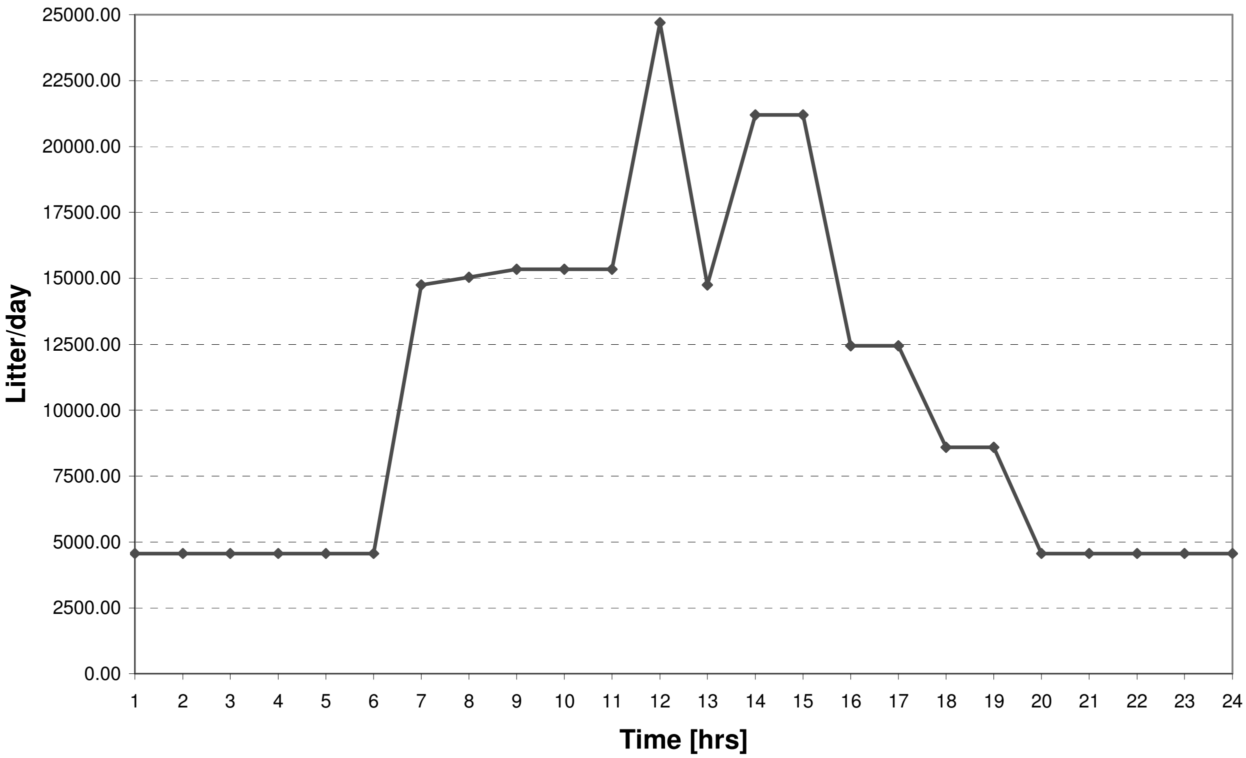

Figure 4.3 Ethiopian Tannery Daily Hot Water Consumption Pattern

4.4 Jimma Hospital

For hospitals the hot water is required for:

- Tubs and showers
- Wash basing
- Kitchen equipment
- Food service to the patients and pantry service for guests
- Laundry service

For developed countries, as a preliminary estimate, some designers use a rule of thumb of 125 gallons of 140 ºF water per bed per day as basis for the hot water requirement [18].

Depending on our country condition it is good to assume that the daily hot water requirement for Jimma hospital will be half of the developed countries requirement. Therefore, the daily hot water requirement for Jimma hospital will be 62.5 gallons per bed at 140 ºF (60ºc).

The total number of beds in Jimma hospital is 504. Therefore the total daily hot water requirement of the hospital is $504 * 62.5 gallons = 31{,}500 gallons = 119.24 \text{ m}^3$.

This daily hot water consumption can be distributed as 35 % in the morning, 15% at the mid day, 15% in the evening and the rest 35 % will be distributed over the day time.

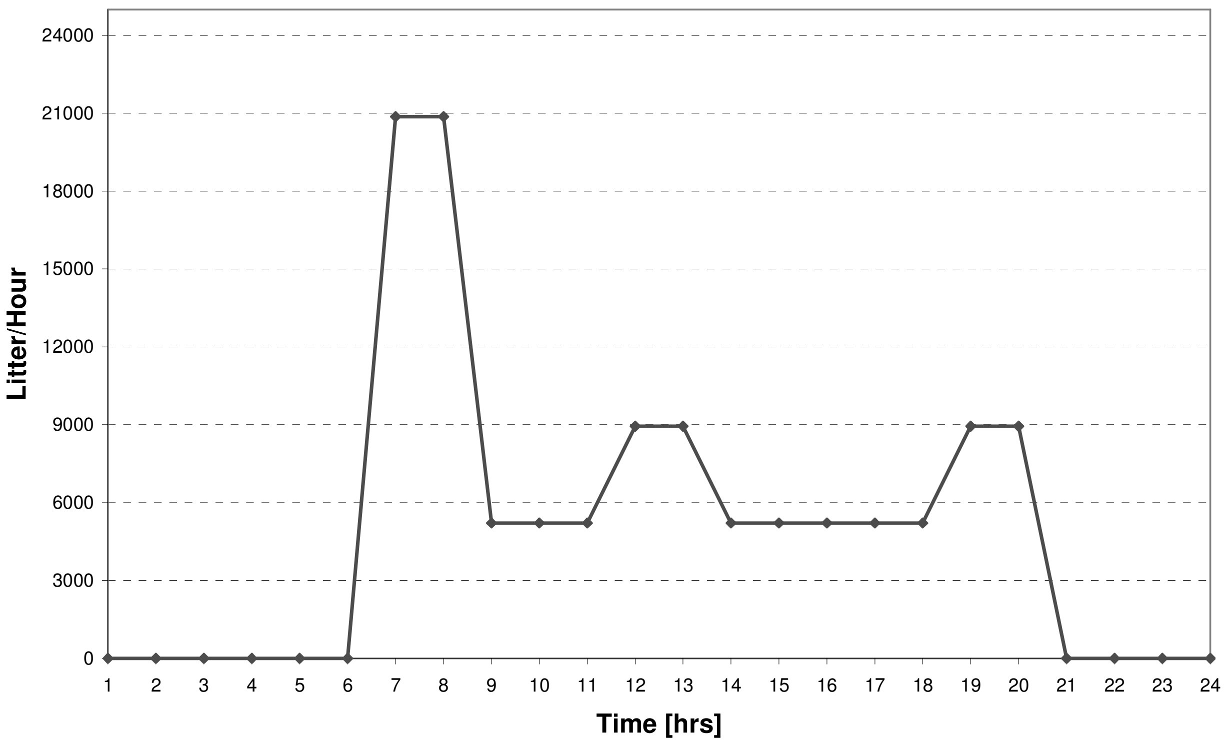

Figure 4.4 Jimma Hospital Daily Hot Water Consumption pattern

Table 4. 1 Summary of the Daily Hot Water Consumption of the Project Sites

Project Site	**Daily Hot Water Consumption** [m^3]
Addis Ababa Tannery	32.6
Dire Tannery	18.53
Ethiopian Tannery	250
Jimma Hospital	119.24

CHAPTER 5

ESTIMATION OF SOLAR RADIATION DATA

5.1 Introduction

The design of a solar water heating system requires precise knowledge regarding the availability of global solar radiation and its components at the location of interest. Since the solar radiation reaching the earth's surface depends upon climatic conditions of the place, a study of solar radiation under local climatic conditions is essential.

In developing countries such as Ethiopia, due to absence or malfunction of measuring instruments, reliable solar radiation data is not available. In the absence and scarcity of trustworthy solar radiation data, the use of an empirical model to predict and estimate solar radiation seems inevitable. These models use climatological parameters of the location under study. Among all such parameters, sunshine hours are the most widely and commonly used.

5.2 Prediction of Monthly Average Daily Global Radiation on a Horizontal Surface

The first empirical correlation using the idea of employing sunshine hours for the estimation of global solar radiation was proposed by Angstrom. The Angstrom correlation was modified by Prescott and Page. The simplest model used to estimate monthly average daily solar radiation on horizontal surface is the well-known Angstrom equation [10].

$$\frac{\bar{H}}{\bar{H}_O} = a + b\frac{\bar{n}_s}{\bar{N}_s} \qquad (5.1)$$

Where: $\bar{H}$ - Monthly average daily radiation on horizontal surface.

$\bar{H}_O$ - Monthly average radiation out side of the atmosphere (ETR on the horizontal surface) for the same location.

a, b – empirical constants, (Values are obtained by regression).

$\bar{n}_s$ - Monthly average daily hours of bright sunshine.

$\bar{N}_s$ - Monthly average of the maximum possible daily hours of bright sunshine.

The regression parameters a and b can be determined from:

$$a = -0.110 + 0.235\cos\phi + 0.323\left(\frac{\bar{n}_s}{\bar{N}_s}\right)$$

$$b = 1.449 - 0.533\cos\phi - 0.694\left(\frac{\bar{n}_s}{\bar{N}_s}\right)$$

$\bar{H}_O$ Can be obtained by the Klein relationship:

$$\bar{H}_o = \left[\frac{24*3600}{\pi}I_{sc}\right]\left[1.0 + 0.033\cos\left(\frac{360N}{365}\right)\right]\left[\cos\phi\cos\delta\sin\varpi_s + \frac{\pi}{180}\varpi_s\sin\delta\sin\phi\right]$$

------------------------------- (5.2)

Where: ϖ_s = sunrise hour angle

$\bar{H}_O$ in $Wh/m^2 day$

I_{sc} = $1367 W/m^2$, (Solar constant)

The length of sun shine hours ($\bar{N}_s$) are computed from Cooper's formula:

$$\bar{N}_s = \left(\frac{2}{15}\right)\varpi_s \quad \text{------------------------------- (5.3)}$$

$$\varpi_s = \cos^{-1}(-\tan\phi\tan\delta)$$

$$\delta = 23.45\sin\left[\frac{360}{365}(284 + N)\right] \quad \text{------------------------------- (5.4)}$$

Where: N is recommended average days for the month.

5.3 Prediction of Monthly Average Daily Diffuse Radiation on a Horizontal Surface

The monthly average daily diffuse radiation on a horizontal surface can be determined from the monthly average daily global radiation on a horizontal surface and the number of bright sunshine hours [10].

$$\frac{\bar{H}_d}{\bar{H}} = 0.931 - 0.814\left(\frac{\bar{n}_s}{\bar{N}_s}\right) \quad \text{---} \; (5.5)$$

5.4 Prediction of Monthly Average Hourly Global Radiation on a Horizontal Surface

The monthly average hourly global radiation on a horizontal surface can be calculated from the knowledge of the monthly average daily global radiation on a horizontal surface [10].

$$\frac{\bar{I}}{\bar{H}} = \frac{\pi}{24}\left(a + b\cos\varpi\right)\frac{\cos\varpi - \cos\varpi_s}{\sin\varpi_s - \frac{\pi}{180}\varpi_s\cos\varpi_s} \quad \text{-------------------------------------} \; (5.6)$$

Where:

$$a = 0.409 + 0.5016\sin\left(\varpi_s - 60\right)$$

$$b = 0.6609 - 0.4767\sin\left(\varpi_s - 60\right)$$

5.5 Prediction of Monthly Average Hourly Diffuse Radiation on a Horizontal Surface

The monthly average hourly diffuse radiation on a horizontal surface can be calculated from the knowledge of the monthly average daily diffuse radiation on a horizontal surface [10].

$$\frac{\bar{I}_d}{\bar{H}_d} = \frac{\pi}{24}\frac{\cos\varpi - \cos\varpi_s}{\sin\varpi_s - \frac{\pi}{180}\varpi_s\cos\varpi_s} \quad \text{---} \; (5.7)$$

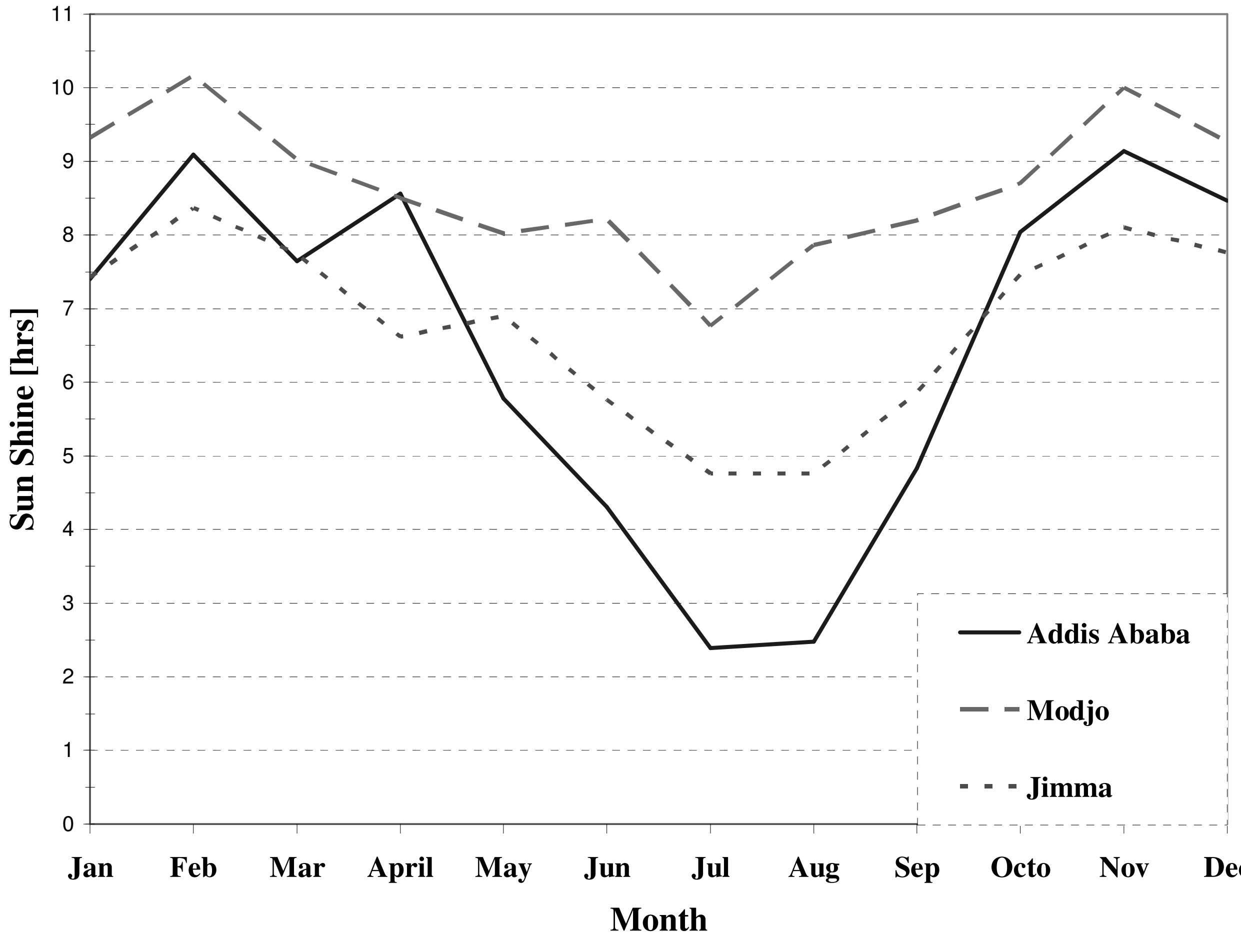

Figure 5. 1 Monthly Average Daily Sunshine Duration

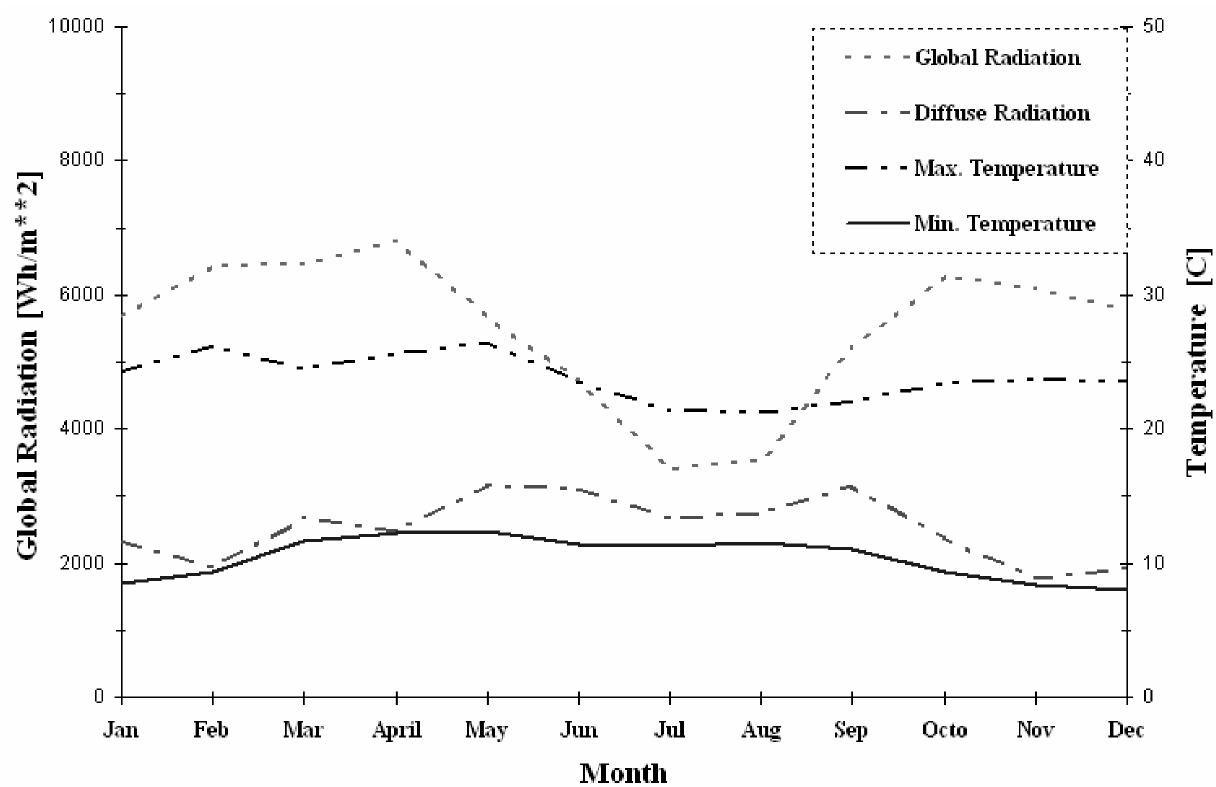

Figure 5. 2 Monthly Averages of Daily Mean Global and diffuse Radiation on the Horizontal Surface and Maximum and Minimum Temperature for Addis Ababa

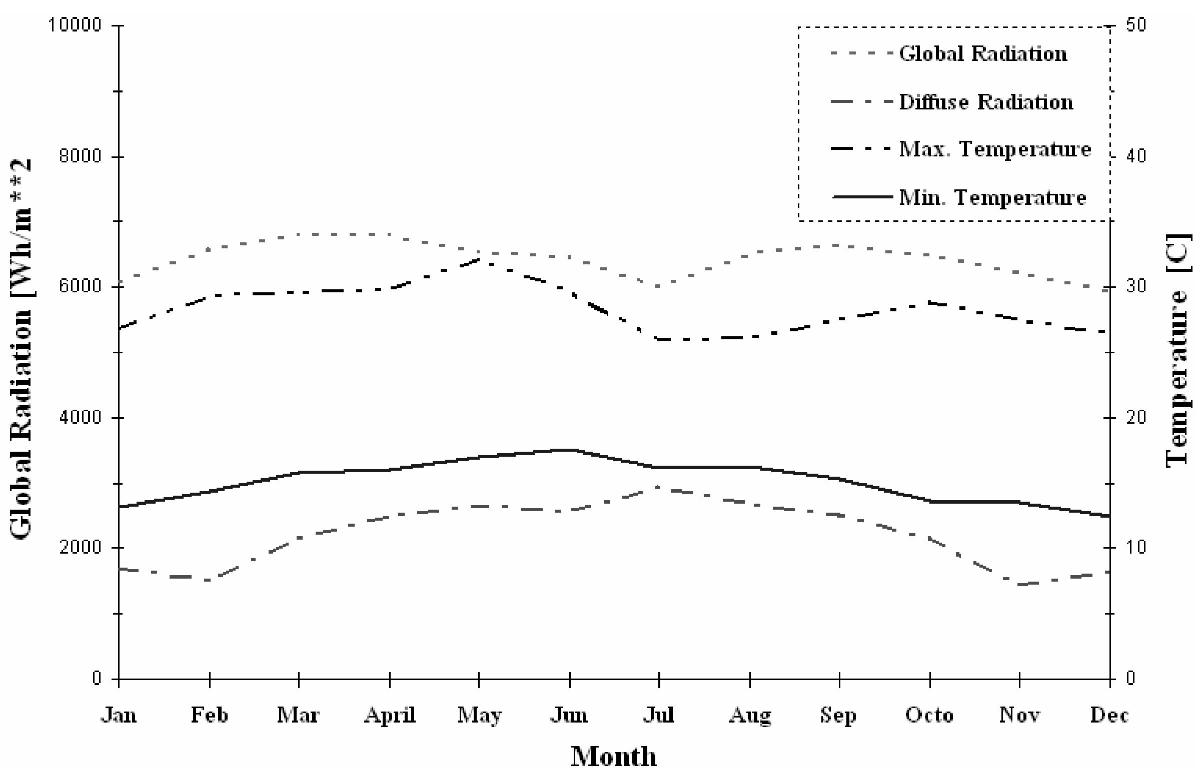

Figure 5. 3 Monthly Averages of Daily Mean Global and diffuse Radiation on the Horizontal Surface and Maximum and Minimum Temperature for Modjo

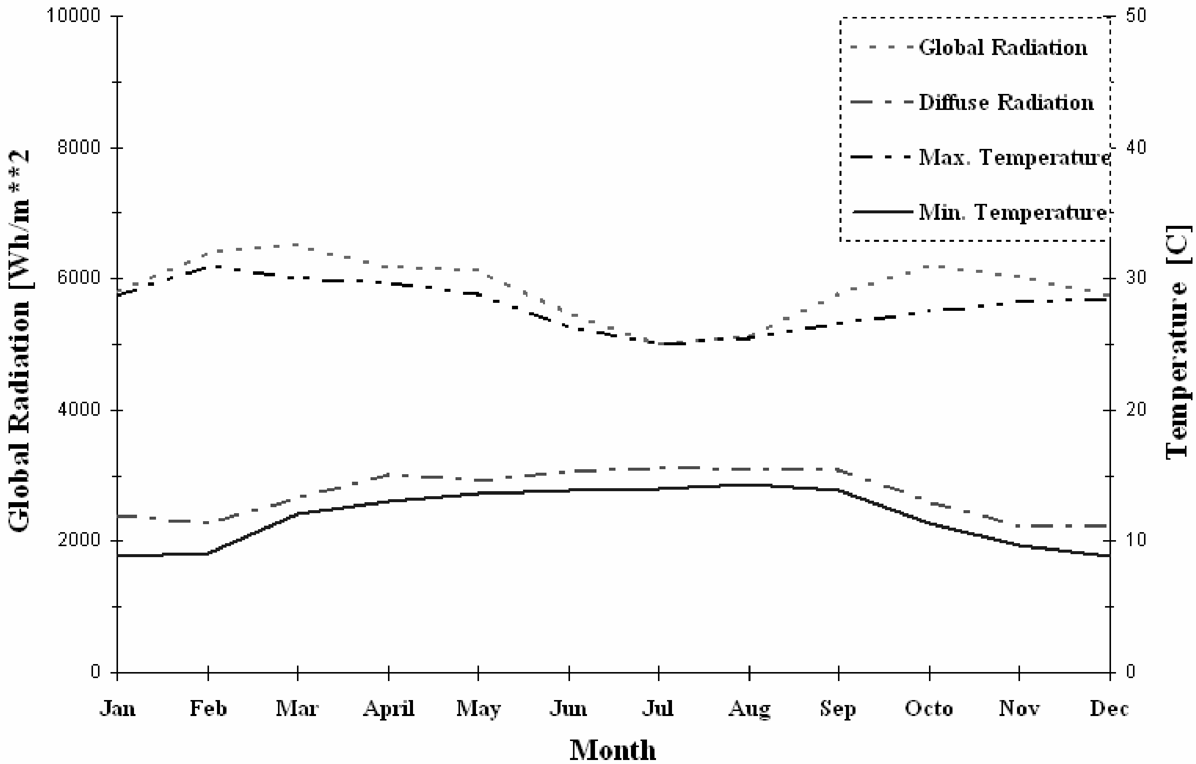

Figure 5. 4 Monthly Averages of Daily Mean Global and diffuse Radiation on the Horizontal Surface and Maximum and Minimum Temperature for Jimma

5.6 Prediction of Hourly Variation of Temperature

The hourly variation of temperatures can be predicted from the daily maximum and daily minimum temperatures using the sine-exponential model [15].

This model describes the diurnal cycle by a sine function during daytime connected to a decreasing exponential function during nighttime. For a given day, it has three free parameters, T_{min} and T_{max} on day t and T_{min} on day t + 1 denoted as T'_{min}. In an uninterrupted series of days, two free parameters for each day remain because of double use of T_{min}. The model assumes that T_{max} occurs somewhere during the daytime hours and T_{min} occurs within a few hours before or after sunrise. The phase shift α between the time of the maximum temperature h_{max} and midday is defined as $\alpha = h_{max} - \frac{1}{2}(h_r + h_s)$, where: h_r and h_s are the times of sunrise and sunset respectively.

The phase shift β between the time of the minimum temperature $h_{\min}$ and h_r is defined by $\beta = h_{\min} - h_r$. Then, the sine-exponential model is given by:

$$T(h) = \begin{cases} T_{\min} + (T_{\max} - T_{\min})\sin\left[\dfrac{\pi(h - h_r - \beta)}{l + 2(\alpha - \beta)}\right] & h_{\min} \le h \le h_s \\ \tau + [T(h_s) - \tau]\exp\left[-\dfrac{\gamma(h - h_s)}{24 - l + \beta}\right] & h_s \le h \le h'_{\min} \end{cases} \quad \text{---------------- (5.8)}$$

Where day length l is defined as $l = h_s - h_r$, γ is an exponential decay coefficient, and $h'_{\min}$ is the time of the minimum temperature at day $t+1$. All times are in hours and *in* this equation τ is taken as τ = $T'_{\min}$. The variables $h_{\min}$, $h'_{\min}$, $h_{\max}$ are climatological parameters, calculated per month, and h_r and h_s are astronomical quantities. The decay coefficient γ can also be treated as a climatological parameter, but better results are obtained if γ is adjusted to the observations [15].

$$\tau = \frac{T'_{\min} - T(h_s)\exp\left[-\dfrac{\gamma(h'_{\min} - h_s)}{24 - l + \beta}\right]}{1 - \exp\left[-\dfrac{\gamma(h'_{\min} - h_s)}{24 - l + \beta}\right]} \quad \text{--- (5.9)}$$

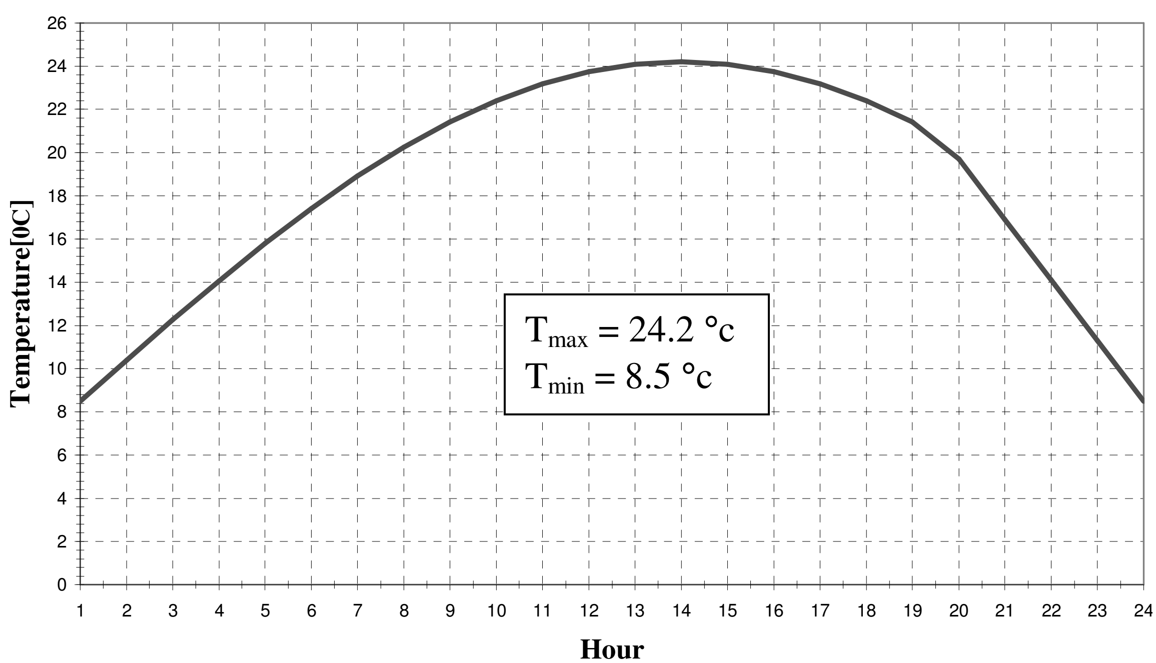

Figure 5. 5 Hourly Ambient Temperature pattern for Addis Ababa on January 17

CHAPTER 6

ENERGY BALANCE FOR LIQUID FLAT-PLATE SOLAR COLLECTOR

6.1 Overall Loss Coefficient and Heat Transfer Correlations

It is convenient from the point of view of analysis to express the heat lost from the collector in terms of an overall loss coefficient defied by the equation.

$$\dot{Q}_L = U_L A_C (T_{pm} - T_a) \quad (6.1)$$

Where: U_L = overall loss coefficient

A_C = area of the collector

T_{pm} = average temperature of the absorber plate

and T_a = temperature of surrounding air (assumed to be the same on all sides of the collector).

The heat lost from the collector is the sum of the heat lost from the top, the bottom and the sides. Thus,

$$\dot{Q}_L = \dot{Q}_t + \dot{Q}_b + \dot{Q}_s \quad (6.2)$$

Where $\dot{Q}_t$ = rate at which heat is lost from the top

$\dot{Q}_b$ = rate at which heat is lost from the bottom

and $\dot{Q}_s$ = rate at which heat is lost from the sides

Each of these loses is also expressed in terms of coefficients called the top loss coefficient, the bottom loss coefficient and the side loss coefficient and defined by the equations:

$$\dot{Q}_t = U_t A_C (T_{pm} - T_a) \text{ ---------- } (6.3)$$

$$\dot{Q}_b = U_b A_C (T_{pm} - T_a) \text{ ---------- } (6.4)$$

$$\dot{Q}_s = U_s A_C (T_{pm} - T_a) \text{ ---------- } (6.5)$$

The losses can also be pictured in terms of thermal resistances as shown below.

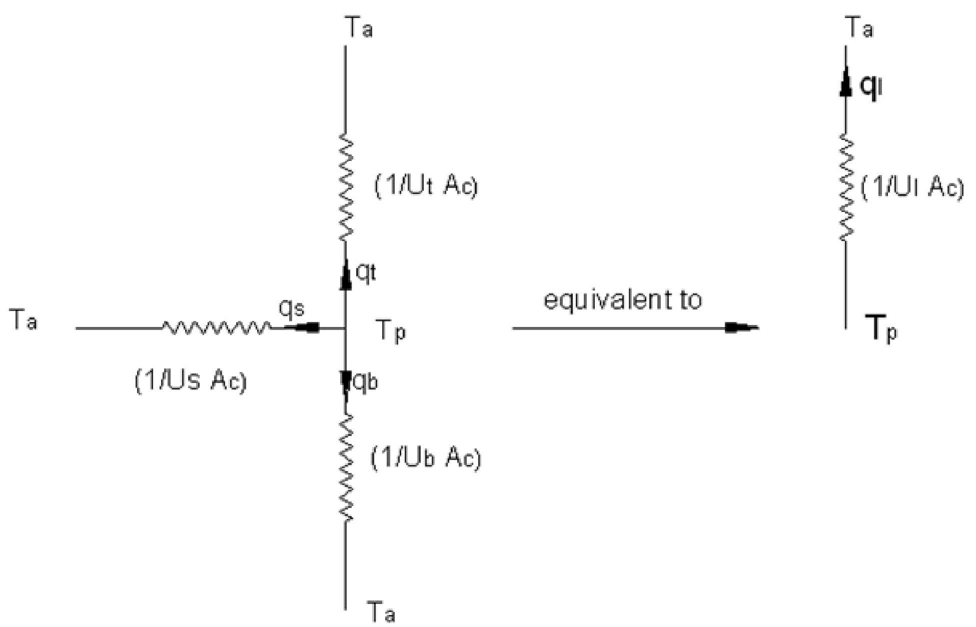

Figure 6.1 Thermal Resistance Network Showing Collector Losses

6.1.1 Top Loss Coefficient

The top loss coefficient U_t is evaluated by considering convection and re-radiation losses from the absorber plate in the upward direction.

For the purpose of calculation, it is assumed that the transparent cover and the absorber plate constitute a system of infinite parallel surfaces and that the flow of heat is one-dimensional and steady [13].

It is further assumed that the temperature drop across the thickness of the cover is negligible and that the interaction between the incoming solar radiation absorbed by the cover and the outgoing lose may be neglected. The outgoing re-radiation is of long wavelengths. For these wavelengths, the transparent cover will be assumed to be almost opaque.

Convective Heat Transfer Coefficient

a) From the plate to the cover

For the prediction of the top loss coefficient, the evaluation of natural convection heat transfer between two parallel plates tilted at some angle to the horizontal is of obvious importance. The natural convection heat transfer coefficient h_{1c} is related to three dimensionless parameters, the Nusselt number Nu, the Rayleigh number Ra, and the Prandtl number Pr, that are given by:

$$N_u = \frac{h_{1c} L}{K}, \qquad R_a = \frac{g \beta_v \Delta T L^3}{\upsilon \alpha}, \qquad P_r = \frac{\upsilon}{\alpha} \text{ -------------------------------- (6.6)}$$

Where: L – is the plate spacing,

g – the gravitational constant,

ΔT – Temperature difference between the plate and the glass, and

β_v – is the volumetric coefficient of expansion of air.

Hollands et al. suggested the relationship between the Nusselt number and Rayleigh number for tilt angle β from 0 to 75° as:

$$N_u = 1 + 1.44\left[1 - \frac{1708 \sin(1.8\beta)^{1.6}}{R_a \cos\beta}\right]\left[1 - \frac{1708}{R_a \cos\beta}\right]^{+} + \left[\left(\frac{R_a \cos\beta}{5830}\right)^{1/3} - 1\right]^{+} \text{ -------- (6.7)}$$

- "+" exponent means only the positive value of the term in square bracket is to be considered.
- Zero is to be used for negative values.

b) From the Glazing cover to the ambient

The convective heat transfer coefficient (h_{2c}) at the glass cover is calculated from the following empirical correlation.

$$h_{2c} = 5.7 + 3.8V \text{ -- (6.8)}$$

Where: h_{2c} is in W/m^2 k, and

V is the wind speed in m/s.

2. Radiative Heat Transfer Coefficient

a) From the plate to the cover

- The radiative heat transfer coefficient from the plate to the glass cover is expressed as:

$$h_{1r} = \varepsilon_{eff}\sigma\left\{\frac{(T_p + 273)^4 - (T_g + 273)^4}{T_p - T_g}\right\} \text{--- (6.9)}$$

- The effective emissive of plate-glazing system is given by:

$$\varepsilon_{eff} = \left[\frac{1}{\varepsilon_p} + \frac{1}{\varepsilon_g} - 1\right]^{-1} \text{-- (6.10)}$$

b) From the Glazing Cover to the ambient

Sky Temperature

The effective temperature of the sky is usually calculated from the following simple empirical relation in which temperatures are expressed in Kelvin

$$T_{sky} = T_a - 6$$

- The radiative heat transfer coefficient from the glass cover to the ambient is expressed as:

$$h_{2r} = \varepsilon_g\sigma\left\{\frac{(T_g + 273)^4 - (T_{sky} + 273)^4}{T_g - T_a}\right\} \text{-- (6.11)}$$

- The total heat transfer coefficient from collector plate to cover h_1 is expressed as:

  $h_1 = h_{1c} + h_{1r}$

- The total heat transfer coefficient from the cover to ambient h_2 is expressed as:

  $h_2 = h_{2c} + h_{2r}$

- The effective heat transfer coefficient from plate to ambient (i.e. the top loss coefficient) is given by:

$$U_t = \left[\frac{1}{h_1} + \frac{1}{h_2}\right]^{-1} \text{--- (6.12)}$$

6.1.2 Bottom Loss Coefficient

The bottom loss coefficient U_b is evaluated by considering conduction and convection losses from the absorber plate in the downward direction through the bottom of the collector.

It will be assumed that the flow of heat is one dimensional and steady. In most cases, the thickness of insulation provided is such that the thermal resistance associated with conduction dominates. Thus, neglecting the convective resistance at the bottom surface of the collector casing, we have:

$$U_b = \frac{K_i}{\delta_b} \quad \text{------------------------------------} \quad (6.13)$$

Where: K_i = thermal conductivity of the insulation

δ_b = back insulation thickness

6.1.3 Side Loss Coefficient

As in the case of the bottom loss coefficient, it will be assumed that the conduction resistance dominates and that the flow of heat is one-dimensional and steady. The one-dimensional approximation can be justified on the grounds that the side loss coefficient is always much smaller than the top loss coefficient.

$$U_s = \frac{A_1}{A_C}\frac{k_i}{\delta e} \quad \text{------------------------------------} \quad (6.14)$$

Where: $A_1 = P * d_e$

P = perimeter of the absorber plate.

d_e = height of the edge.

δ_e = edge insulation thickness.

6.1.4 Overall Heat Loss Coefficient

The overall heat loss coefficient U_L is the sum of the top, bottom and edge loss coefficient. That is:

$$U_L = U_t + U_b + U_s \quad \text{------------------------------------} \quad (6.15)$$

6.2 Thermal Analysis of Flat Plate Collector and Useful Heat Gained by the Fluid

The procedure for calculating the overall loss coefficient is described in the above section. If the average plate temperature or mean plate temperature T_{pm} is known, then the heat lost from the collector can be calculated.

T_{pm} can be related to the value of the inlet fluid temperature T_{fi} by considering the flow of heat in the absorber plate and across the fluid tubes to the fluid.

In order to simplify the problem, a number of one-dimensional analyses will be conducted. The one-dimensional flow of heat in the absorber plate in the direction of fluid will be first considered, and then it will be followed by a consideration of the heat flow from the plate to the fluid across the tube wall. Finally, the one-dimensional heat transport inside the tube will be considered.

6.2.1 Collector Efficiency Factor

The collector efficiency factor, $F^{'}$, represents the ratio of the actual useful heat collection rate to the useful heat collection rate when the collector absorber plate (Tp) is at the local fluid temperature (T_f).

Figure 6.2 illustrates the absorber plate-tube configuration of the present collector model. Let us assume temporarily the negligible temperature gradient in the fin in the flow direction; the collector efficiency factor can be obtained by solving the classical fin problem [18].

Let W be the distance between the tubes, D is the tube diameter and δ is the sheet thickness as shown in the Figure 6.3 (a). Because the sheet material is a good conductor, the temperature gradient through the sheet is negligible. Assume the sheet above the bond to be at some local base temperature T_b. The region between the center line separating the tubes and the tubes base can then be considered as a classical fin problem.

The fin length is equal to $\frac{W-D}{2}$, as shown in the Figure 6.3 (a), and $\frac{W}{2}$ is the distance from the center of the collector to the center of the tube.

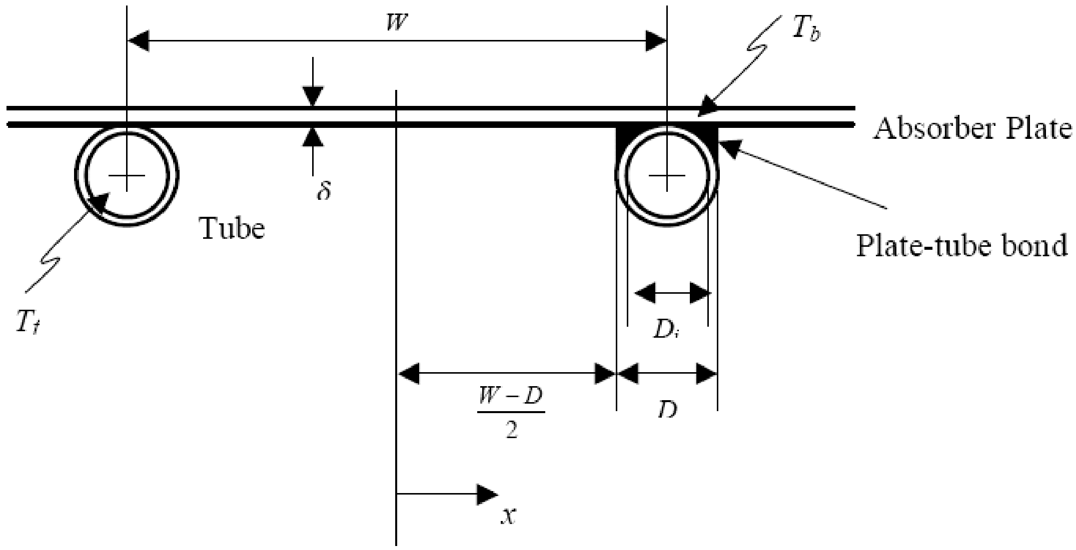

Figure 6.2 Geometric Configuration of the Absorber Plate-Tube

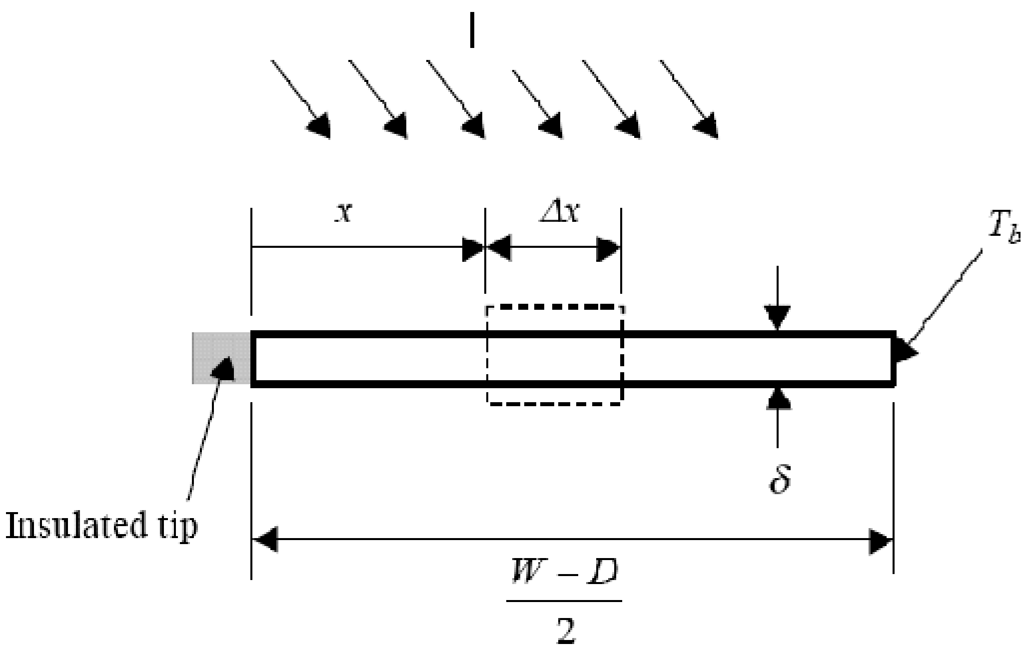

(a) Fin with Insulated Tip

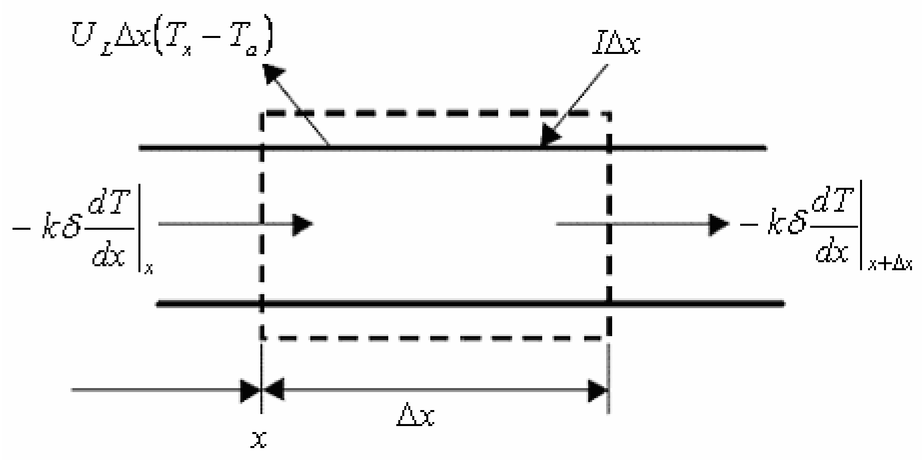

(b) Energy Balance over Finite Volume

Figure 6.3 Fin Configuration and Energy Balance

Considering heat transfer occurring in the x-direction. For an elemental region Δx and unit length in the flow direction, energy balance yields:

$$I\Delta x - U_L \Delta x (T - T_a) + \left(-k\delta \frac{dT}{dx}\bigg|_x \right) - \left(-k\delta \frac{dT}{dx}\bigg|_{x+dx} \right) = 0 \quad \text{------------------ (6.16)}$$

Or $$I\Delta x + U_L (T_a - T)\Delta x - k\delta \frac{dT}{dx} - \left[-k\delta \frac{d}{dx}(T + dT)\Delta x \right] = 0$$

Or $$I\Delta x + U_L (T_a - T)\Delta x - k\delta \frac{dT}{dx} + k\delta \frac{dT}{dx} + k\delta \frac{d^2T}{dx^2}\Delta x = 0$$

$$I\Delta x + U_L (T_a - T)\Delta x = -k\delta \frac{d^2T}{dx^2}\Delta x$$

$$I + U_L (T_a - T) = -k\delta \frac{d^2T}{dx^2}$$

$$-\frac{d^2T}{dx^2} = \frac{U_L}{k\delta}(T_a - T) + \frac{I}{k\delta}$$

$$\frac{d^2T}{dx^2} = \frac{U_L}{k\delta}\left(T - T_a - \frac{I}{U_L} \right) \quad \text{-- (6.17)}$$

Expression 6.17 is of second order differential equation, the two boundary conditions are

(i) $\left.\dfrac{dT}{dx}\right|_{x=0} = 0$

(ii) $\left.T\right|_{x=\frac{W-D}{2}} = T_b$

Let $m^2 = \dfrac{U_L}{k\delta}$

$$\Psi = T - T_a - \frac{I}{U_L}$$

Then equation 6.17 becomes

$$\frac{d^2\Psi}{dx^2} - m^2\Psi = 0 \text{ --- } (6.18)$$

This has the boundary conditions

$$\left.\frac{d\Psi}{dx}\right|_{x=0} = 0, \qquad \left.\Psi\right|_{x=\frac{W-D}{2}} = T_b - T_a - \frac{I}{U_L}$$

The general solution is

$$\Psi = C_1 \sinh mx + C_2 \cosh mx \text{ -- } (6.19)$$

The constants C_1 and C_2 are found by substituting boundary conditions.

Differentiating equation (6.19)

$$\frac{d\Psi}{dx} = C_1 m \cosh mx + C_2 m \sinh mx$$

Condition, $\dfrac{d\Psi}{dx} = 0$ at x = 0, gives $C_1 = 0$

From the second condition

$$\frac{T - T_a - I/U_L}{T_b - T_a - I/U_L} = \frac{\cosh mx}{\cosh m\left(\frac{W-D}{2}\right)} \text{ -- } (6.20)$$

The energy conducted to the region of the tube per unit length in the flow direction is,

(i.e. The energy transferred from the fin per unit of length in the flow direction)

$$\dot{Q}_{fin\ base} = -k\delta \left.\frac{dT}{dx}\right|_{x=\frac{W-D}{2}}$$

From equation 6.20,

$$\frac{dT}{dx} = \left(T_b - T_a - \frac{I}{U_L}\right)\frac{m \sinh mx}{\cosh m\left(\frac{W-D}{2}\right)}$$

$$\therefore \qquad \dot{Q}_{fin\ base} = \frac{k\delta m}{U_L}\left[I - U_L(T_b - T_a)\right]\tanh\left(\frac{W-D}{2}\right)m \quad \text{------------------------- (6.21)}$$

Equation 6.21 accounts for the energy collected to only one side of a tube; for both sides

$$\dot{Q}_{fin\ base} = 2\frac{k\delta m}{U_L}\left[I - U_L(T_b - T_a)\right]\tanh m\left(\frac{W-D}{2}\right)$$

$$= 2\frac{1}{m}\left[I - U_L(T_b - T_a)\right]\tanh m\left(\frac{W-D}{2}\right)$$

$$\left[\therefore \qquad m^2 = \frac{U_L}{k\delta}, \qquad \therefore \qquad \frac{k\delta m}{U_L} = \frac{1}{m}\right]$$

$$= 2\left(\frac{W-D}{2}\right)\left[I - U_L(T_b - T_a)\right]\frac{\tanh m\left(\frac{W-D}{2}\right)}{m\left(\frac{W-D}{2}\right)}$$

$$\dot{Q}_{fin\ base} = (W-D)\eta_f\left[I - U_L(T_b - T_a)\right] \quad \text{-- (6.22)}$$

Where: η_f is the fin efficiency for straight fins with rectangular cross section and defined as:

$$\eta_f = \left\{\frac{\tanh m\left(\frac{W-D}{2}\right)}{m\left(\frac{W-D}{2}\right)}\right\} \text{--- (6.23)}$$

6.2.2 Useful Heat Gain

Basic Energy Balance Equation

The performance of a flat-plate solar collector can be described by the useful gain from the collector per unit time of a collector area A_c and it is the difference between the absorbed solar radiation and the thermal loss or the useful energy output of a collector.

$$\dot{Q}_u = A_c\,\dot{q}_u = A_c\left[\dot{q}_{ab} - U_L\left(T_p - T_a\right)\right] \quad (6.24)$$

Where: $\dot{q}_{ab} = (\tau_o \alpha_o) I_T(t)$

τ_0 and α_o are the transimissivity of the glass cover and the absorptivity of the absorber respectively.

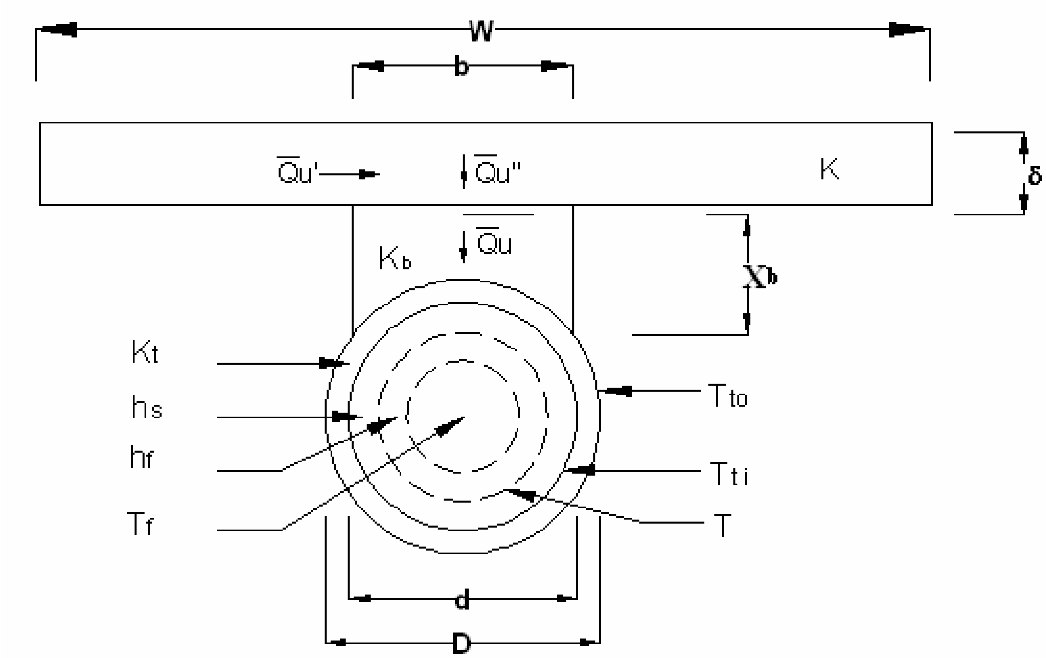

Figure 6.4 Schematic Representation of a Section through a Typical Finned-Tube

The useful gain of the collector also includes the energy collected above the tube region. The solar energy absorbed just above the tube per unit of length in the flow direction can be calculated by:

$$\dot{Q}_{tube} = D\left[\dot{Q}_{ab} - U_L\left(T_b - T_a\right)\right] \quad (6.25)$$

Hence, the total energy gain of the collector tubes per unit length in the flow direction may be expressed as:

$$\dot{Q}_u = \dot{Q}_{fin\ tube} + \dot{Q}_{tube\ section}$$

$$= \left[(W - D)\eta_f + D\right]\left[\dot{q}_{ab} - U_L(T_b - T_a)\right] \text{ ---------------------------------- (6.26)}$$

Ultimately, the useful gain from equation (6.25) must be transferred to the fluid. The resistance to heat flow from the plate to the tube may be consisted of the following components.

- The resistance due to the bonding material between the plate and the tube;
- The resistance due to the temperature gradient in the fluid at the tube wall;
- The resistance due to the wall thickness of the tube.

Hence $\dot{q}_U = \dfrac{T_b - T_f}{\dfrac{1}{C_b} + \dfrac{1}{\pi d h_f} + \dfrac{1}{C_w}}$ --- (6.27)

Where: C_b = the conductance of the bond

C_w = the conductance of the tube wall

h_f = the forced-convection heat transfer coefficient inside of tubes

T_f = the local fluid temperature

The bond conductance is given as:

$C_b = \dfrac{K_b b}{X_b}$, and $C_w = \dfrac{\pi A_{mw} K_t}{X_t}$ --- (6.28)

Where: K_b = bond conductivity

b = bond length

X_b = bond average thickness

$A_{mw} = \dfrac{D/d}{\ln D/d}$ = Mean wall area

$X_t = \dfrac{(D - d)}{2}$ = Thickness of the tube

The bond conductance can be very important in accurately describing collector performance. Simple wiring or clamping of the tubes to the sheet results in a significant loss of performance. It is necessary to have good metal to metal contact so that the bond resistance is less than 0.03 m ºC /W.

The useful energy gain per unit flow length transferred to the flowing fluid can then be expressed in terms of the known dimensions, the physical parameters and the local fluid temperature by solving the equation (6.27) for T_b and subsisting to obtain $\dot{Q}_u$ from equation (6.26).

$$\dot{Q}_u = WF'\left[\dot{q}_{ab} - U_L\left(T_f - T_a\right)\right] \quad \text{-- (6.29)}$$

Where: $$F' = \frac{1/U_L}{W\left[\frac{1}{U_L\left[D + (W-D)F_e\right]} + \frac{1}{C_b} + \frac{1}{C_w} + \frac{1}{\pi d h_f}\right]} \quad \text{-------------------------- (6.30)}$$

F' is called the collector efficiency factor. Physical interpretation of F', for most collector geometries will be clear from equation (6.30). The denominator is the heat transfer resistance from the fluid to the ambient air, which is equal to $\frac{1}{U_o}$. The numerator is the heat transfer resistance from the absorber plate to the ambient air, which is equal to $\frac{1}{U_L}$. Thus F' is the ratio of these two heat transfer coefficients.

$$F' = \frac{1/U_L}{1/U_o} = \frac{U_o}{U_L}$$

F' is essentially constant for any collector design and fluid flow rate.

The heat transfer coefficient inside the tube (h_f) may be assumed:

- 300 W/m^2 ºC for natural convection (Thermosiphon heaters), and
- 1500 W/m^2 ºC for forced circulation.

6.2.3 Temperature Distribution in Flow Direction

The temperature of fluid varies along the tube with a certain temperature profile. Consider the steady state energy balance on a fluid element flowing through a pipe of length Δx, which is receiving a uniform heat flux $\dot{q}_u$, so that:

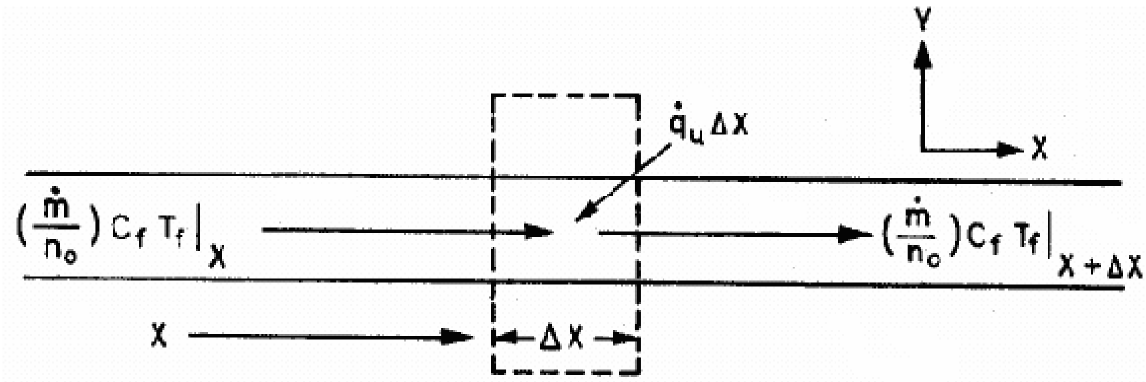

Figure 6.5 Energy Balance on Fluid Element

$$\left[\frac{\dot{m}}{n_o}\right] C_p T_f \Big|_x - \left[\frac{\dot{m}}{n_o}\right] C_p T_f \Big|_{x+dx} + \dot{q}_u \, \Delta x = 0 \text{ -- } (6.31)$$

Where: $\dot{m}$ - is the total collector flow rate,

n_o - is the number of riser tubes, and

C_p - is the specific heat of fluid.

Dividing throughout by Δx and finding the limit as $\Delta x \rightarrow 0$, and substituting in equation (6.29) for $q_u^{'}$

$$\left[\frac{\dot{m}}{n_o}\right] C_p \frac{dT_f}{dx} - WF^{'} \left[\dot{q}_{ab} - U_L \left(T_f - T_a\right)\right] = 0 \text{ -- } (6.32)$$

If the assumption is made that $F^{'}$ and U_L are constant and independent of x, then the solution of the differential equation for the temperature at any position (if subjected to the condition that inlet fluid temperature is T_{fi}) is:

$$\frac{T_f - T_a - \dot{q}_{ab}/U_L}{T_{fi} - T_a - \dot{q}_{ab}/U_L} = e^{-\left(U_L n_o W F' X / \dot{m} C_p\right)} \quad \text{-- (6.33)}$$

If the collector has length L in the flow direction, then the outlet fluid temperature T_{fo} is found by substituting L for X in the equation (6.33).

$$T_{fo} = T_a + \left(\dot{q}_{ab}/U_L\right) - \left[\left(\frac{\dot{q}_{ab}}{U_L} - T_{fi} + T_a\right) e^{-U_L F' A_c / \dot{m} C_p}\right] \text{---------------- (6.34)}$$

Where: $A_c = n_o WL$, the area of collector.

6.2.4 Collector Heat Removal Factor

It is an important design parameter since it is a measure of the thermal resistance encountered by the absorbed solar radiation in reaching the collector fluid.

It represents the ratio of the actual useful heat gain rate to the gain which would occur if the collector absorber plate was at the temperature T_{fi} everywhere. Its value will range between 0 and 1.

The total useful energy collection rate $\dot{Q}_u$ may be expressed as:

$$\dot{Q}_u = \dot{m} C_p \left(T_{fo} - T_{fi}\right) \quad \text{--- (6.35)}$$

Substitution of T_{fo} already derived, gives

$$\dot{Q}_u = A_c F_R \left[\dot{q}_{ab} - U_L \left(T_{fi} - T_a\right)\right] \text{--- (6.36)}$$

Equation (6.36) is known as the actual useful heat energy gain.

This equation is often referred to as the Hottel-Whillier-Bliss [10].equation and it is a very convenient expression for calculating the useful energy gain because the inlet fluid temperature is usually a known quantity.

$$F_R = \left[\frac{\dot{m} C_p}{A_c U_L}\right] \left[1 - e^{-A_c U_L F' / \dot{m} C_p}\right] \text{-- (6.37)}$$

Where: F_R is the heat removal factor of the collector.

Physically the collector heat removal factor is equivalent to the effectiveness of a conventional heat exchanger.

From equation (6.36) the instantaneous thermal efficiency of flat plate collector is given by:

$$\eta_i = \frac{\dot{Q}_{useful}}{A_c I(t)} = F_R\left[(\alpha\tau) - \frac{U_L (T_{fi} - T_a)}{I(t)}\right] \text{-- (6.38)}$$

6.3 Effects of Various Parameters on Collector Performance

A large number of parameters influence the performance of liquid flat-plate collector. These parameters could be classified as:

- Design parameters,
- Operational parameters,
- Meteorological parameters, and
- Environmental parameters

6.3.1 Effects of Design Parameters

a) Selective Absorber coatings

An effective way to reduce thermal losses from the absorber plate of a solar heating panel is by using selective absorber coatings. An ideal selective coating is one that is a perfect absorber of solar radiation while being a perfect reflector of thermal radiation. Such a coating will make a surface, a poor emitter of thermal radiation. Hence a selective coating increases the temperature of an absorbing surface.

Absorber plate surface which exhibit the characteristics of a high value of absorptivity for incoming solar radiation and a low value of emissivity for out-going re-radiation are called **selective surfaces**. Such surfaces are desirable because they maximize the absorption of solar energy and minimize the emission of the radiative losses.

A large number of non-selective coatings are available and are in widespread use as flat-plate collector coatings. These are primarily organic coatings such as flat black coatings. Most of these coatings have absorptances exceeding 0.95 and emittances of 0.90-0.95. Although the emittances are high, use of these coatings may be justified economically in some applications where high collector temperatures are not required, such as hot water system or swimming pool heaters.

The possibility of having selective absorber plate surface for flat-plate collectors was suggested first by Tabor and then by Gier and Dunkle [18].

A selective surface should posses the following characteristics in addition to the above-mentioned spectral characteristics:

i) Its properties should not change with use. A significant degradation in the value of α and ε_p has been observed in the case of some selective coatings, largely due to the effect of exposure to atmospheric humidity.

ii) It should be able to withstand the temperature levels associated with the absorber plate surface of a collector over extended periods of time. It should be able to with stand any short-term temperature rise which may occur when no useful heat is being removed.

iii) It should be able to withstand atmospheric corrosion and oxidation.

iv) It should be of reasonable cost.

For this design condition black chrome electroplated with Absorptance of α_p= 0.96 and Emittance of ε_p 0.1 is used.

b) Number of Covers

The number of covers (glazing) used in a collector is usually one or two. As the number of cover increases the value of $\tau\alpha$ decrease. Thus, the flux $\dot{q}_{ab} = (\tau\alpha)I(t)$ absorbed in the absorber plate decreases.

The addition of more covers also causes the value of U_t, and hence the heat loss, to decrease. However, the amount of decrease is not the same in both cases. For this *reason,* the efficiency goes through a maximum. This kind of result is obtained with all collectors, a maximum efficiency being usually obtained with one or two covers. Since the flat-plate collectors currently available in our country are single glass this design is based on this parameter.

c) Spacing

The proper spacing has to be kept between the absorber plate and the cover. From the point of view of the heat loss from the top, it is evident that the spacing must be such that the values of the convective heat transfer coefficients are minimized.

Effect of Shading

The main problem associated with the use of larger spacing is that Shading of the absorber plate by the side walls of the collector casing increases. Whenever the angle of incidence is not normal, some of the structure will intercept the solar radiation. Some of this radiation will be reflected to the absorbing plate if the side walls are of a high reflectance material. Some shading always occurs in every collector and needs to be corrected for. The shading is particularly important in the early morning and late evening hours. It is estimated that for most designs using spacing of 2 to 5 cm between the cover and the plate, shading reduces the radiation absorbed by about 3 percent [18].

Accordingly, Hottel and Woertz [18] recommend that the absorbed flux $\dot{q}_{ab}$ is to be calculated in the usual manner but with the multiplying factor of 0.97. Similarly for the case of this design let us assume that for the spacing of 5 cm to consider the shading effect $\dot{q}_{ab}$ is to be multiplied by a factor of 0.97.

d) Collector Tilt

The tilt of a collector is the angle between the collector and the local horizontal. In most solar water heating applications, a tilt of approximately latitude plus 10º to 15º is near optimum because it is necessary to favor the summer season, when the collector operates under adverse conditions (due to lower ambient temperature) and load is greatest [18].

For the case of Addis Ababa, the collector tilt is 20º.

For the case of modjo, the collector tilt is 19º.

For the case of Jimma, the collector tilt is 18º.

e) Collector Azimuth

The azimuth is the angle the collector faces relative to south. The maximum heating performance is occurred at azimuth of 0º.

f) Number of Tubes

As the number of tubes increases, the tube-to-tube spacing W decreases and the collector heat removal factor F_R increases while the value of $(\tau\alpha)$ remains constant. Thus, the instantaneous efficiency improves with the increase of the number of tubes.

The degree of improvement decreases and there exists the optimum number of tubes for the collector considering the manufacturing cost. For the case of this design the flat plate collector contains 8 tubes.

6.3.2 Effects of Operational Parameters

The fluid inlet temperature is operational parameters which strongly influence the performance of a flat-plate collector. Various experiments have been conducted and give that the efficiency of the collector decreases sharply as the inlet fluid temperature T_{fi} increases. This decrease is because of the higher temperature level at which the collector as a whole operates when the fluid inlet temperature increases. Because of this, the top loss coefficient as well as the temperature difference with the surrounding increases, the heat lost increases and useful heat gain decreases.

6.3.3 Effects of Meteorological Parameters

Various experiments show that the collector efficiency increases with the flux, the increase being more pronounced at lower values of flux. Since the fluid inlet temperature and the ambient temperature essentially determines the loss from the collector, if these quantities are constant and the incident flux increases, the useful heat gain and the efficiency must increase. It should be noted that the incident flux is composed of beam, diffuse, and reflected radiation.

6.3.4 Effects of Environmental Parameters

The preceding calculations of the flux transmitted through the covers of the collector have been done under the assumption that the top cover is clean and has no dust accumulated on it. This assumption is acceptable only if the cover is continuously cleaned. However, in any practical situation, this is not possible. Cleaning is generally done once every few days. For this reason, it is recommended that the incident flux be multiplied by a correction factor which accounts for the reduction in intensity because of the accumulation of dust.

The rate of deposition of the dust depends on the graphical and metrological parameters. The dust factor is related to the dust layer transmissivity, hence the dust factors reported by investigators depend on places of investigations. A comparison and correlation of the finding of the above investigators is possible only if the transmissivity of the dust layer is known as a function of:

a) Angle of incidence
b) Deposit rate, and
c) Ratio of diffuse to total radiation.

Therefore, a systematic study of the reduction in transmissivity due to dust with reference to above variable is needed.

- The results of two studies are as follows:
  a) For collector inclined at 30º in Boston, U.S.A., Hottel and Woertz found a reduction of less than 1 percent in transmitted radiation and accordingly recommended a correction factor of 0.99. However this recommendation seems to be on the higher side [18].
  b) Garg conducted studies in Roorkee on glass covers inclined at various angles. The experiments were performed during May and June, which are relatively dusty months. For a collector inclined at 45 º, Garg obtained a correction factor of 0.92 for a cleaning frequency of 20 days [18].

The above two studies represent some what extreme situations. In general, a value for the correction factor between 0.92 and 0.99 seems to be indicated and for design purpose, it is suggested that radiation absorbed by the plate be reduced by a factor of (1-d), where d is 0.02 to account for dust. (I.e. a correction factor = 0.98) [18].

- Considering the effect of dust and shading the collected incident flux is corrected by

$$\dot{q}_{ab} = (\tau\alpha) I_T(t)(1-d)(1-s)$$

Where: d = 0.02 to account for dust.

S = 0.03 to account for shading.

Thus, $\dot{q}_{ab} = 0.951(\tau\alpha) I_T(t)$

6.4 Determining Design Parameters

The data of some collector which can be used for water heating system design is given as follows.

Table 6.1 Collector Parameters and Important Properties of Fluid

Parameter	Vonal.Com	GPG Solar	S-Series	G-Series
Collector Area [m^2]	2 *	2.09	2.53	2.53
Collector Perimeter [m]	6 *	6	6.8	6.8
Back Insulation Thickness[m]	0.05 *	0.05	0.025	0.025
Edge Insulation Thickness[m]	0.025 *	0.025	0.025	0.025
Depth of the Collector [m]	0.095	0.09	0.086	0.086
Depth of the Edge [m]	0.054 *			
Emissivity of the Panel	0.1 *	0.1	0.29 painted 0.15selective	0.25 painted 0.15selective
Absorbtivity of the Panel	0.90	0.96coated with black-chrome *	0.95 painted 0.92selective	0.95 painted 0.92selective
Emissivity of the Glass	0.88 *	0.88	0.88	0.88
Transmissivity of the Glass	0.9 *	0.9	0.898	0.898
Number of Glass Cover	1 *	1	1	1
Insulation Material	Mineral wool *	Mineral wool	Fiberglas AF530	Fiberglas AF530
Conductivity of Insulation Material [w/m K]	0.045 *	0.045	0.036	0.036
Panel Material	Steel *	copper	Aluminium	Aluminium
Panel Height [m]	2 *	1.9	2.3	2.3
Panel Width [m]	1 *	1.1	1.1	1.1
Thickness of the Panel [m]	0.002 *	0.0004	0.0005	0.0005
Tube Material	Copper *	Copper	Copper	Copper
No.of Tubes per m of Panel Width	8 *	7	8	8
Tube Diameter [m]	0.022 * (circular)	0.016 (circular)	0.008 (rhombus)	0.012 (rhombus)
Space b/n Collector Panel & Glass	0.05 *	0.05	0.02 – 0.025	0.02 – 0.025
Thermal Conductivity of the Absorber [W/m K]	54 *	385	205	205
Fluid capacity of the Panel Tubes [kg/m2]	3.04 *			
Mass*Sp Heat of the Panel [J/K]	14112.0 *			
Mass*Sp Heat of the Glass [J/K]	18417.067 *			
Wind Velocity[m/s]	3.0 *			

Reynolds Number	733.0	*
Prandtl Number	4.772	*
Average Density of Water [kg/m^3]	991	*
Sp. Heat of water [J/kg K]	4180	*
Thermal Conductivity of Water [W/m K]	0.625	*
Thermal Conductivity of Air [W/m K]	0.026	*
Mass Flow Rate of Fluid Flow, $\dot{m}$ [kg/s m^2]	0.03	*
Sealing Material	EPDM	*

Remark: * Parameters selected for this paper.

Vonal.Com – Manufacturer of solar water heater in Ethiopia.

GPG Solar – Dealer of solar water heater in Ethiopia (Manufacturer: Israel).

S-Series – Canada standard type solar water heater.

G-Series – Canada standard type solar water heater.

CHAPTER 7
TRANSIENT ANALYSIS OF SOLAR WATER HEATER

7.1 Mathematical Model

In order to determine the feasibility of the solar water heating system, it is necessary to determine the annual heat gain which is found by simulating the heating system inputting climatic data and design parameters. Hence in this chapter the development of the simulation model will be discussed.

7.1.1 Absorbed Radiation

The solar radiation energy incident on the collector surface which is inclined at an angle of β to the horizontal, defined in terms of the global radiation (G_r), the diffuse radiation (D_r), the beam radiation factor (R_b) and the ground reflectivity factor (ρ) is given by:

$$I_T = R_b(G_r - D_r) + 0.5(1+\cos\beta)D_r + 0.5\rho(1-\cos\beta)G_r \quad \text{------------------------------ (7.1)}$$

Where: $R_b = \dfrac{\cos\theta_i}{\cos\theta_z}$ θ_i - angle of incident, and

θ_z - Zenith angle

$$\begin{aligned}\cos\theta_i = &(\cos\phi\cos\beta + \sin\phi\sin\beta\cos\gamma)\cos\delta\cos\varpi \\ &+ \cos\delta\sin\varpi\sin\beta\sin\gamma \\ &+ \sin\delta(\sin\phi\cos\beta - \cos\phi\sin\beta\cos\gamma)\end{aligned} \quad \text{-- (7.2)}$$

$$\cos\theta_z = \cos\phi\cos\delta\cos\varpi + \sin\delta\sin\phi \quad \text{--- (7.3)}$$

The flux collected per unit time is given by:

$$\dot{q}_{ab} = (\tau\alpha)I_T(t)(1-d)(1-s)$$

Where: d = 0.02 to account for dust.

S = 0.03 to account for shading.

Thus, $\dot{q}_{ab} = 0.951(\tau\alpha)I_T(t)$ -- (7.4)

7.1.2 Absorber Plate

The temperature of the absorber plate varies across the width of the fin, having a maximum on the centerline between the fluid ducts. If for high fin efficiencies it is assumed that the temperature variation is linear as shown in the figure (7.1), then for fin efficiency η_f and for a maximum plate temperature of T_{pO}, the temperature adjacent to the water tube is $F_w \times T_{pO}$, where $F_w = 2\eta_f - 1$. The average plate temperature is $\eta_f \times T_{pO}$.

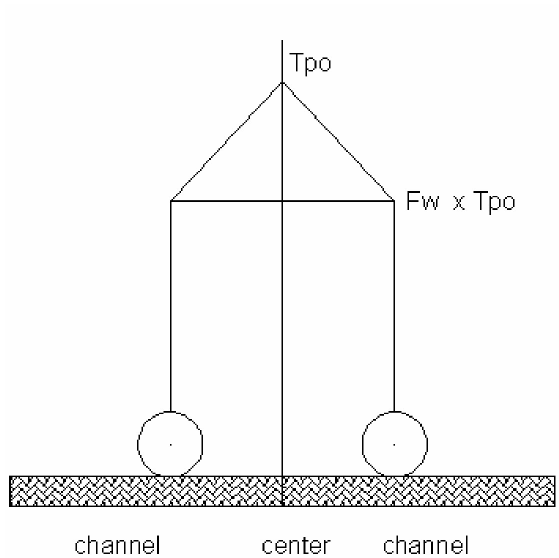

Figure 7. 1 Linear Temperature Variation in the Absorber Plate

The plate temperature T_p at any time $(t + \Delta\tau)$ can be determined from conditions at time t and the energy absorbed by the plate and energy losses.

$$\begin{aligned}(mc_p)_p \frac{dT_p}{dt} = A_c I_c - A_c U_{pg}(\eta_f T_p - T_g) - A_w U_{pw}\left\{F_w T_p - \frac{T_{wo} + T_{wi}}{2}\right\} \\ - A_c U_{pab}(\eta_f T_p - T_a) - A_1 U_{pae}(\eta_f T_p - T_a)\end{aligned} \quad \text{--- (7.5)}$$

$$T_{p1} = \underbrace{\frac{1}{\eta_f}\frac{A_c I_c}{(mc_p)_p}\Delta\tau}_{a_{11}} + \underbrace{\left\{1.0 - \left(\frac{A_c U_{pg}}{(mc_p)_p} + \frac{F_w}{\eta_f}\frac{A_w U_{pw}}{(mc_p)_p} + \frac{A_c U_{pab}}{(mc_p)_p} + \frac{A_1 U_{pae}}{(mc_p)_p}\right)\Delta\tau\right\}}_{a_{12}} T_{pO}$$

$$+ \underbrace{\frac{1}{\eta_f}\left(\frac{A_c U_{pg}}{(mc_p)_p}\Delta\tau\right)}_{a_{13}} T_{gO} + \underbrace{\frac{1}{\eta_f}\left(\frac{A_w U_{pw}}{2(mc_p)_p}\Delta\tau\right)}_{a_{14}} T_{woO} + \underbrace{\frac{1}{\eta_f}\left(\frac{A_w U_{pw}}{2(mc_p)_p}\Delta\tau\right)}_{a_{15}} T_{wiO}$$

$$+ \underbrace{\left\{\frac{1}{\eta_f}\left(\frac{A_c U_{pab}}{(mc_p)_p} + \frac{A_1 U_{pae}}{(mc_p)_p}\right)\Delta\tau\right\}}_{a_{16}} T_{aO}$$

$$T_{p1} = a_{11} + a_{12}T_{pO} + a_{13}T_{gO} + a_{14}T_{woO} + a_{15}T_{wiO} + a_{16}T_{aO} \quad \text{------------------- (7.6)}$$

7.1.3 Glass Cover

Making an energy balance for the glass cover its temperature at any time $(t + \Delta\tau)$ is determined from data at time t as follows:

$$(mc_p)_g \frac{dT_g}{dt} = A_c I_T (1 - \tau_g) + A_c U_{pg}(\eta_f T_p - T_g) - A_c U_{ga}(T_g - T_a) \quad \text{------- (7.7)}$$

$$T_{g1} = \underbrace{\frac{A_c I_T (1 - \tau_g)}{(mc_p)_g}\Delta\tau}_{a_{21}} + \underbrace{\left\{1.0 - \left(\frac{A_c U_{pg}}{(mc_p)_g} + \frac{A_c U_{ga}}{(mc_p)_g}\right)\Delta\tau\right\}}_{a_{22}} T_{gO}$$

$$+ \underbrace{\left(\frac{A_c U_{pg}}{(mc_p)_g}\Delta\tau\right)\eta_f}_{a_{23}} T_{pO} + \underbrace{\left(\frac{A_c U_{ga}}{(mc_p)_g}\Delta\tau\right)}_{a_{24}} T_{aO}$$

$$T_{g1} = a_{21} + a_{22}T_{gO} + a_{23}T_{pO} + a_{24}T_{aO} \quad \text{--- (7.8)}$$

7.1.4 Water Stream

Making an energy balance for the water stream, the temperature of the water leaving the solar collector at any time $(t + \Delta\tau)$ is determined from data at time t as follows:

$$\left(mc_p\right)_w \frac{dT_{wo}}{dt} = A_w U_{pw} \left\{ F_w T_p - \frac{T_{wo} + T_{wi}}{2} \right\} - \left(\dot{m} c_p\right)_w \left(T_{wo} - T_{wi}\right) \text{---------} \quad (7.9)$$

$$T_{wo1} = \underbrace{\left\{ \frac{A_w U_{pw}}{\left(mc_p\right)_w} \Delta\tau \right\} F_w}_{a_{31}} T_{pO} + \underbrace{\left\{ 1.0 - \left(\frac{A_w U_{pw}}{2\left(mc_p\right)_w} + \frac{\left(\dot{m} c_p\right)_w}{\left(mc_p\right)_w} \right) \Delta\tau \right\}}_{a_{32}} T_{woO}$$

$$\underbrace{- \left\{ \left(\frac{A_w U_{pw}}{2\left(mc_p\right)_w} \right) - \left(\frac{\left(\dot{m} c_p\right)_w}{\left(mc_p\right)_w} \right) \right\} \Delta\tau}_{a_{33}} T_{wiO}$$

$$T_{wo1} = a_{31} T_{pO} + a_{32} T_{woO} + a_{33} T_{wiO} \text{ ---} \quad (7.10)$$

Equations (7.6), (7.8), (7.10) are derived from energy balance on the absorber plate, the glass cover and the water stream, respectively. The given sets of equations are non-linear due to temperature dependent radiant and convective heat transfer coefficients. The solutions are, therefore, determined by an integration scheme that linearises these equations within a set time step.

7.1.5 Storage Tank

The heat balance in the storage tank for the model shown in the figure (9.1) is given by the following expression:

$$\rho V_s C \frac{dT_s}{dt} = \dot{Q}_U - \dot{Q}_{Loss} - \dot{Q}_{LOAD} \text{ --} \quad (7.11)$$

Where the left-hand side term corresponds to the heat energy stored in the tank and the three terms on the right-hand side of the above expression represent the rate of the net solar energy gain, the rate of heat loss from the storage tank and the rate of heating Load required respectively.

- The net solar useful heat gain is given by:

$$\dot{Q}_U = \left(\dot{m}C_P\right)_W \left(T_{WO} - T_{WI}\right)$$

- The storage tank heat loss is given by:

$$\dot{Q}_{Loss} = A_S U_{LS}\left(T_S - T_a\right) \text{ --- } (7.12)$$

Where: A_S is the storage tank heat transfer area.

U_{LS} is the heat transfer coefficient of the storage tank.

Hot water supply rate is given by:

$$\dot{Q}_{LOAD} = ALOAD\left(T_S - T_{WS}\right) \text{ --- } (7.13)$$

Where: $ALOAD = \left(\rho C_P\right)_W DWC * PP(j)$

DWC is the total daily hot water consumption.

$PP(j)$ is the fraction of daily hot water consumption.

T_{WS} is the temperature of supply water.

By considering that $T_{S0} = T_{WI0}$ and $T_{S1} = T_{WI1}$ equation (7.11) can be simplified as:

$$T_{S1} = \left(\frac{\left(\rho C_P\right)_W V_S - ALOAD}{\left(\rho C_P\right)_W V_S}\right) T_{S0} + \left(\frac{ALOAD}{\left(\rho C_P\right)_W V_S}\right) T_a + \frac{\dot{Q}_U - \dot{Q}_{Loss}}{\left(\rho C_P\right)_W V_S} \text{ ----------- } (7.14)$$

7.2 Flow Chart of Simulation Program

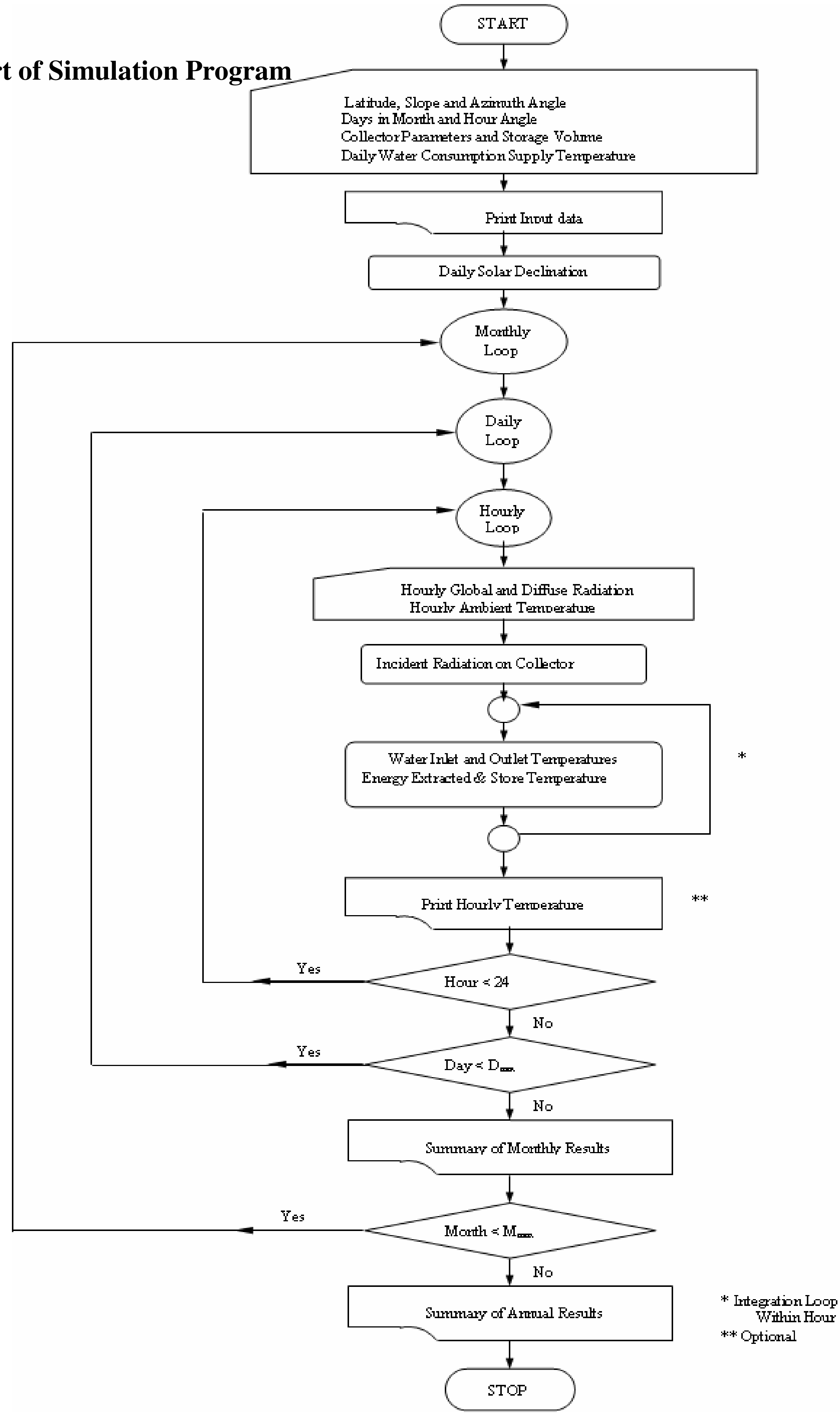

The parameters read from input files at the beginning of the simulation process include:

- Latitude of the site, azimuth and slope of the solar collector,
- Geometric dimensions and thermophysical properties of the absorber plate, the glazing and the insulation,
- Thermophysical properties of water,
- Storage capacity, daily hot water consumption pattern and hot water delivery and cold water supply temperatures, and
- Global and diffuse solar radiation and ambient temperature for every hour of the day.

CHAPTER 8

RESULTS AND DISCUSSION

8.1 Thermal Storage and Insulation

Storage tank is one of the major components in large scale solar water heating system. It is used in most solar systems to provide a thermal inertia or capacitance effect. This thermal capacitance is required to damp out fluctuations of energy collection and demand in solar system. The amount of thermal storage is usually subjected to economic constraint, since very large storage, which could produce a nearly uniform system output, is generally very expensive.

The shapes of the storage tanks are a right circular cylinder with height to diameter ratio of 2:1.

- For the climatic condition of Addis Ababa city the volume of storage tank for a single collector is assumed to be 0.1 m^3 and the daily heating capacity of a single collector is assumed 0.125 m^3.
- For the climatic condition of Modjo town the volume of storage tank for a single collector is assumed to be 0.125 m^3 and the daily heating capacity of a single collector is assumed 0.15 m^3.
- For the climatic condition of Jimma town the volume of storage tank for a single collector is assumed to be 0.125 m^3 and the daily heating capacity of a single collector is assumed 0.15 m^3.

Therefore, the volume of storage tank needed to heat the total daily hot water consumption is:

$$\text{Total volume of storage tank needed} = \text{Daily Hot Water Consumption} * \frac{\text{assumed volume of storage tank for one collector}}{\text{assumed volume of water heated by one collector per day}}$$

$$\text{Total volume of storage tank} = 32.6m^3 * \frac{0.1m^3}{0.125m^3} = 26.08m^3 \text{ (for A.A. tannery)}$$

$$\text{Total volume of storage tank} = 18.53.m^3 * \frac{0.1m^3}{0.125m^3} = 14.824m^3 \text{ (for Dire tannery)}$$

Total volume of storage tank = $250m^3 * \dfrac{0.125m^3}{0.15m^3} = 208.33m^3$ (for Ethiopia tannery)

Total volume of storage tank = $119.24m^3 * \dfrac{0.125m^3}{0.15m^3} = 99.37m^3$ (for Jimma hospital)

For $\dfrac{h}{D_i} = 2$, Volume of a single storage tank is:

$$V_s = \pi \frac{D^2{}_i}{4} h = \pi \frac{D_i^3}{2}$$

Surface area of the storage tank is:

$$A_s = \pi D_i h + 2 * (\frac{\pi D_i^2}{4}) = \frac{5}{2} \pi D_i^2$$

Storage Tank Insulation Thickness Determination

The exterior of a storage tank should be well insulated to retain heat. Heat losses from the storage tank have great impact on the economic utilization of the system as a whole. For this reason thickness of insulation should be determined by considering it as one part of the storage tank design. The determination of the storage tank insulation can be made by using different consideration. In one case for example, the insulation thickness is taken as an utilizable parameter and then determined by considering the economic trade-off between the cost of the added insulation and the benefit gained from the saved solar heat.

The other way of calculating the insulation thickness is as follows: The overall heat transfer coefficient U across the storage tank is assumed first. Then, the thickness of the insulation is determined. For simplification of the problem, the second method is used for the determination of the required insulation thickness for some assumed value of the overall heat transfer coefficient U. Neglecting the effect of the storage tank material on heat transfer, the temperature difference across the insulation is taken as ΔT .

The rate of heat loss from the tank is then given by:

$$\dot{Q} = \frac{2\pi L\left(T_{1-}T_{\infty,0}\right)}{2/D_o h_o + 1/k \; Ln\left(D_o/D_i\right)} \qquad \text{-- (8.1)}$$

Where: T_o - temperature of water in the tank.

$T_{\infty,0}$ - Ambient temperature.

T_2 - Surface temperature of the storage tank.

h_o - Convective heat transfer coefficient of ambient air.

k - Thermal conductivity of insulation.

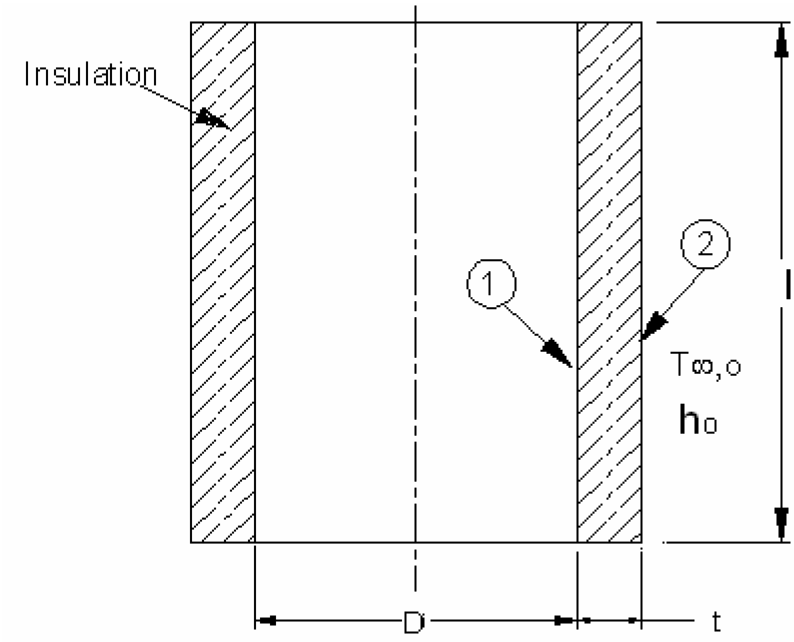

Figure 8.1 Side Insulation of the Storage Tank

$$D_o = D_i + 2t \qquad \text{------------------------} \; (8.2)$$

The rate of heat transfer can also be given by:

$$\dot{Q} = UA\Delta T \qquad \text{------------------------} \; (8.3)$$

Where: U - overall heat transfer coefficient.

A – Surface area of the insulation.

$$\Delta T = T_1 - T_{\infty,0}$$

Equating and simplifying equation (8.1) and (8.3) gives:

$$D_o = D_i * \exp[2k(1/U - 1/h_o)1/D_o] \qquad \text{------------------------} \; (8.4)$$

Taking: k = 0.032 W/mk (for Glass fiber)

U [W/m^{2}k] (assumed)

ho = 12 W/m^{2}k

Gives: $$t = 0.5\left[D_i * \exp\left[\frac{2k}{D_i + 2t}\left(\frac{1}{U} - \frac{1}{h_o}\right)\right] - D_i\right] \qquad \text{------------------------} \; (8.5)$$

Considering the tank inside plate thickness of 2 mm and insulation cover plate thickness of 1 mm, the out side tank diameter is:

$$D_o = D_i + 2t + 2*0.002 + 2*0.001$$

Table 8.1 Technical Data of Storage Tank

Storage Tank				
	Addis Ababa Tannery	**Dire Tannery**	**Ethiopia Tannery**	**Jimma Hospital**
Daily hot water consumption	32.6 m^3	18.53 m^3	250 m^3	119.24 m3
Number of storage tanks	4	2	4	4
Single storage tank volume, Vs	6.5 m^3	7.4 m^3	52.1 m^3	24.8 m^3
Internal surface area, A_s	20.3 m^2	22.1 m^2	81.1 m^2	49.5 m^2
Height, L	3.2 m	3.44 m	6.4 m	5.0 m
Inside diameter, D_i	1.6m	1.7 m	3.2 m	2.5 m
Outside diameter, D_o	1.8 m	1.9 m	3.8 m	3.1 m
Insulation material	Glass fiber (k=0.032 w/mk)	Glass fiber (k=0.032 w/mk)	Glass fiber (k=0.032 w/mk)	Glass fiber (k=0.032 w/mk)
Insulation thickness, t	0.1076 m	0.0984 m	0.2672 m	0.267 m
Mild steel plate thickness (internal cover)	2 mm	2 mm	2 mm	2 mm
Galvanized pre painted steel jacket (outer cover)	0.8 mm	0.8 mm	0.8 mm	0.8 mm

8.2 Solar Contribution to the Heating Load

For the storage tank hot water delivery temperature of 50ºc the maximum solar contribution to the heating load is archived during the winter season in the month of February and the minimum is achieved during the summer season in the month of July.

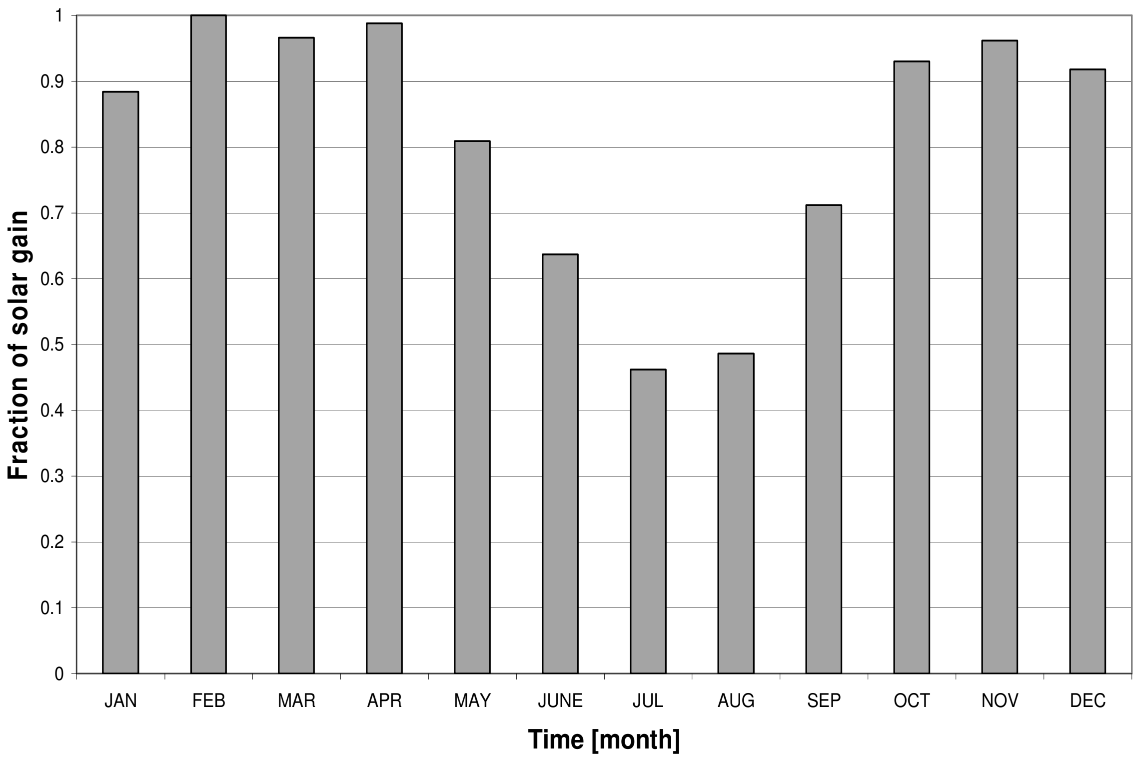

Figure 8. 2 Fraction of Solar Gain for Addis Ababa Tannery

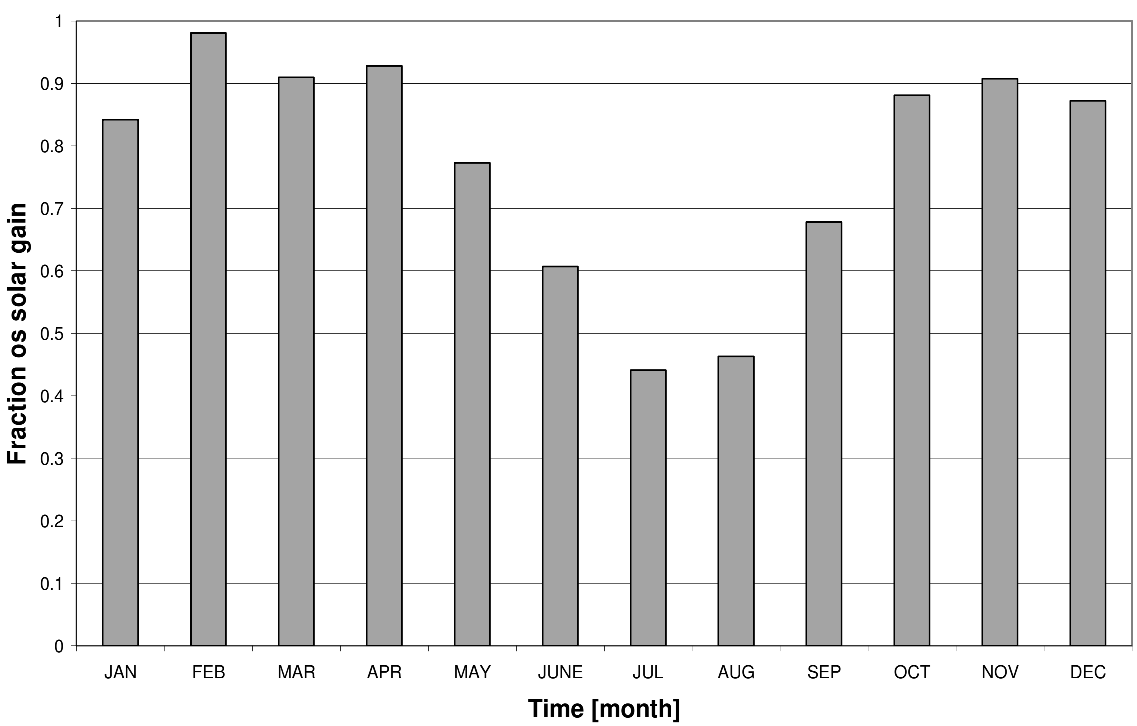

Figure 8. 3 Fraction of Soar Gain for Dire Tannery

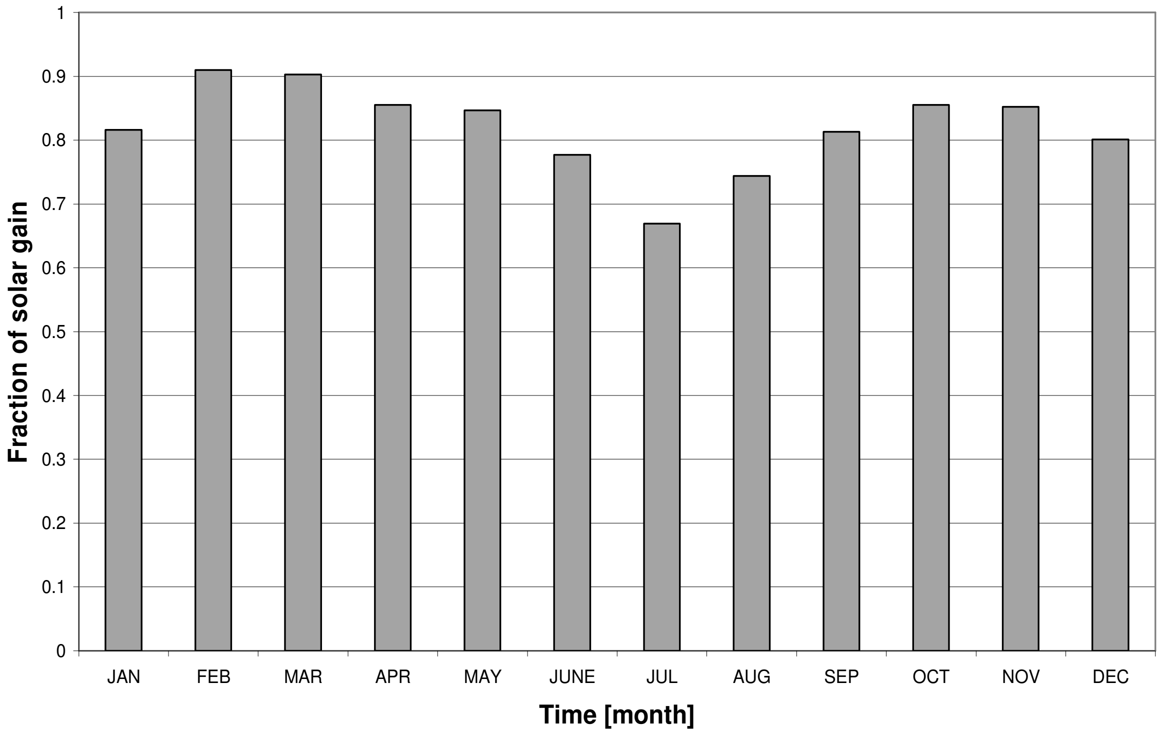

Figure 8. 4 Fraction of Solar Gain for Ethiopian Tannery

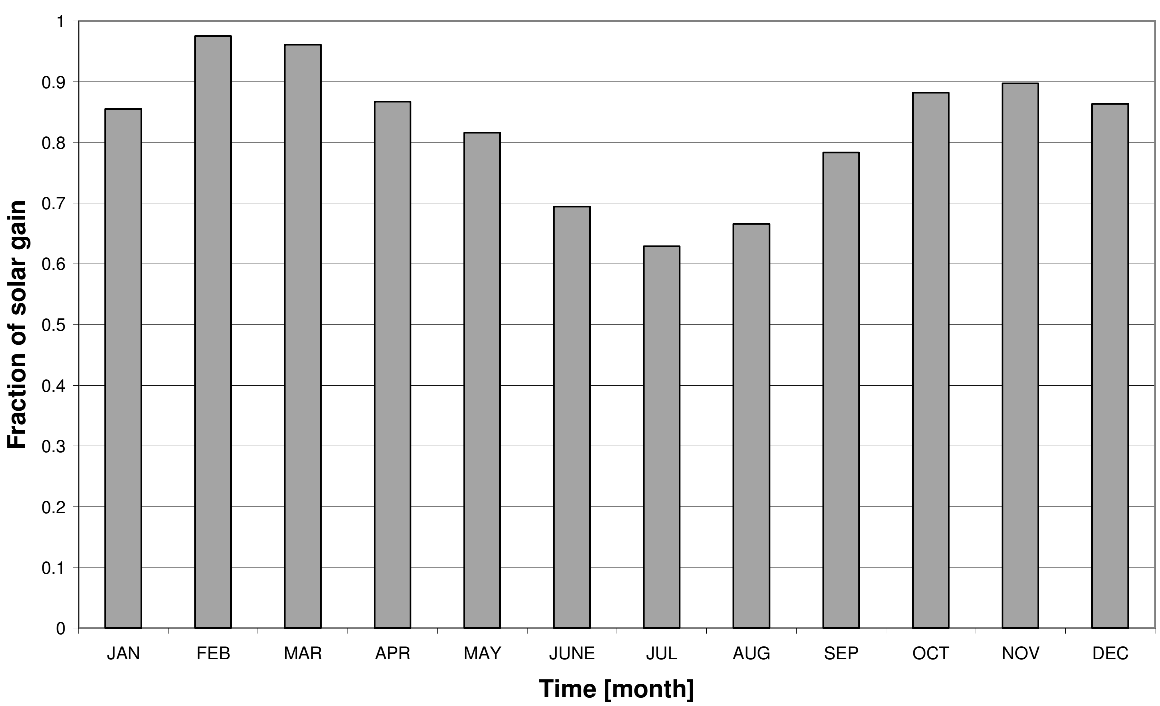

Figure 8. 5 Fraction of Solar Gain for Jimma Hospital

❖ The annual solar contribution to heating load is summarized in the table below.

Table 8. 2 Summery of Annual Fraction of Solar Contribution to Load

Project Site	**Annual Fraction of Solar Contribution**	**Annual Solar Contribution to Heating Load [KWh]**
Addis Ababa Tannery	0.809	1355.467
Dire Tannery	0.762	1311.903
Ethiopian Tannery	0.816	1361.764
Jimma Hospital	0.818	1449.115

Temperatures of the water in the storage tank at various seasons of a year are plotted in the figure below.

a) Addis Ababa Tannery

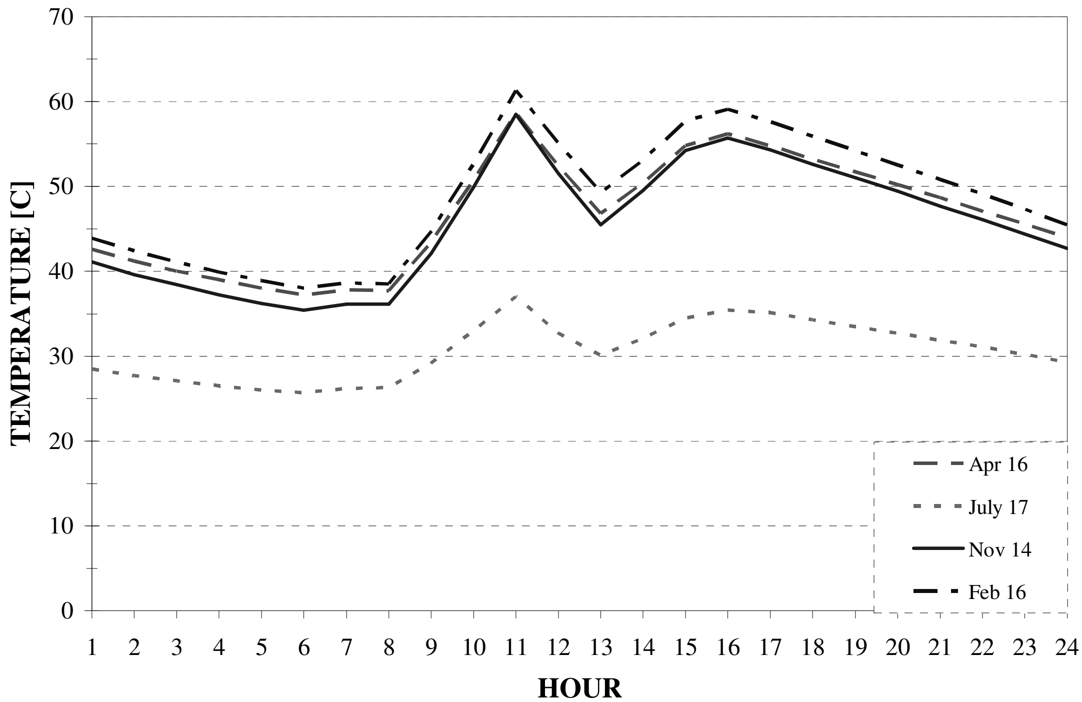

b) Dire Tannery

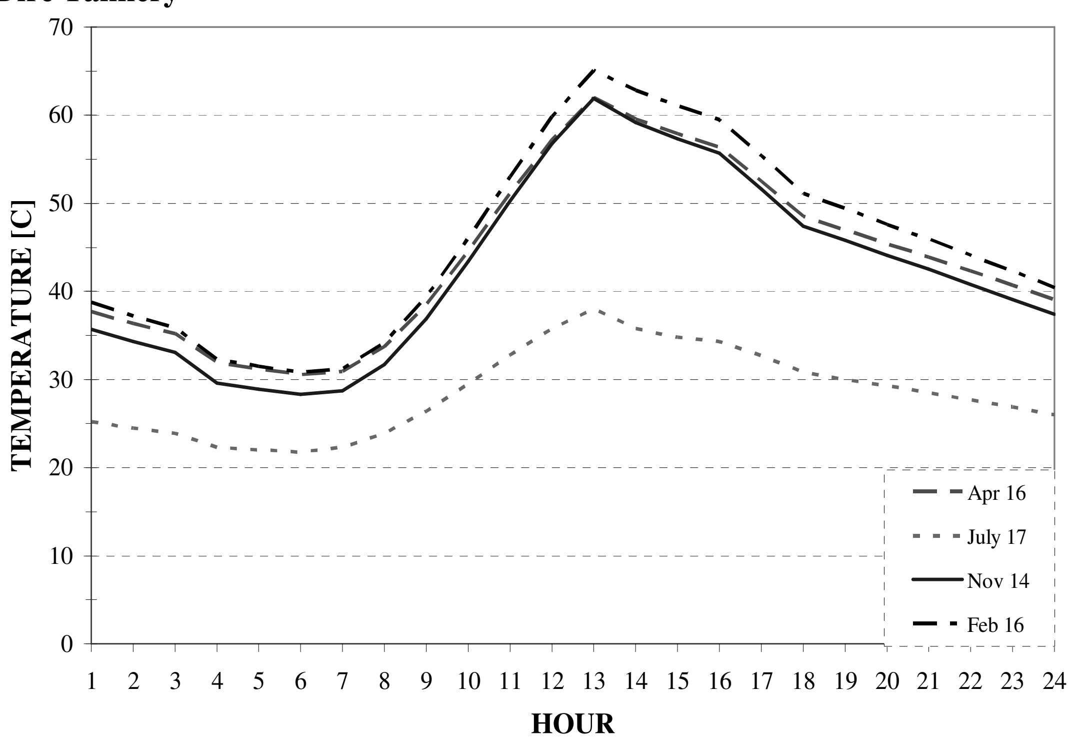

c) Ethiopian Tannery

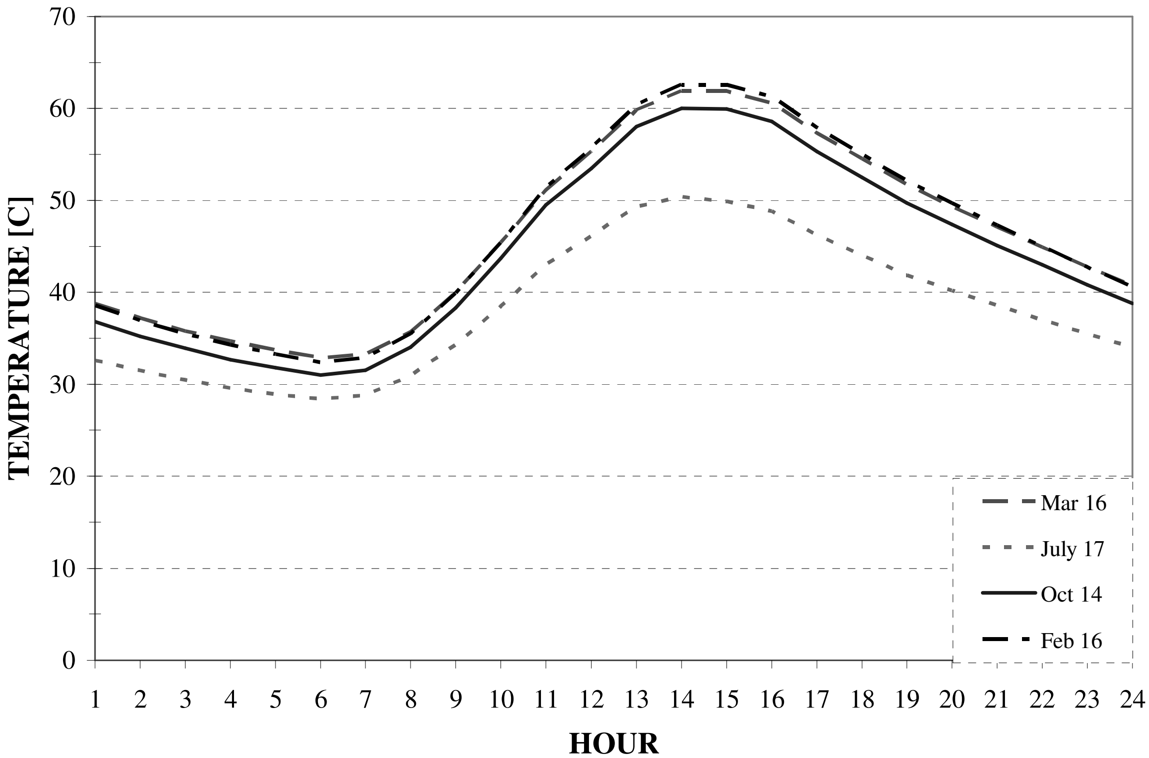

d) Jimma Hospital

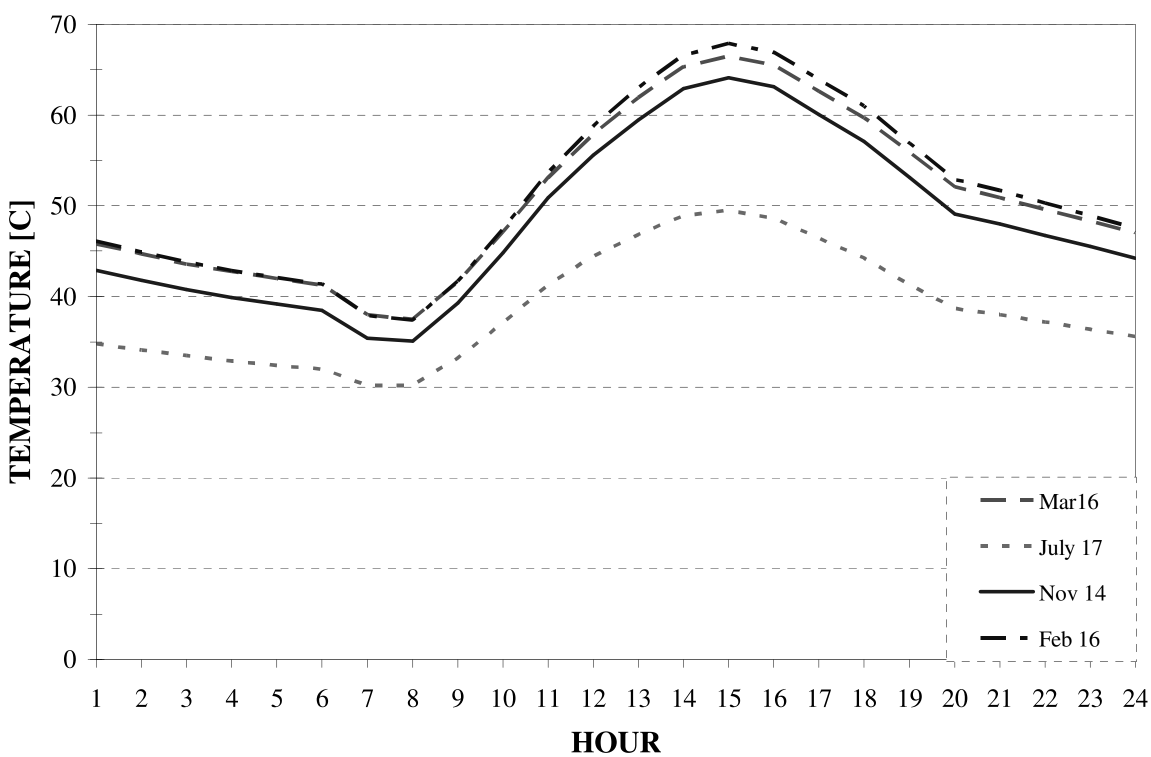

Figure 8. 6 Simulated Hourly Variation of Temperature of Water in the Storage Tank

8.3 Pressure Drop in the Collector

Based on the designed diameter of tube, number of riser tubes, mass flow rate and flow pattern the pressure drop inside the collector can be calculated with the help of the schematic diagram shown below.

At average temperature of 38 ºc of the property of water is:

ρ = 991 kg/m^3

μ = 6.87 *10^{-4} kg/m^3

$\dot{m}$ = 0.03 kg/s m^2 = 0.03 kg/s m^2 * 2 m^2 = 0.06 kg/s

Volume flow rate $\dot{Q} = \dfrac{\dot{m}}{\rho} = 6.05 * 10^{-5}\ m^3/s$

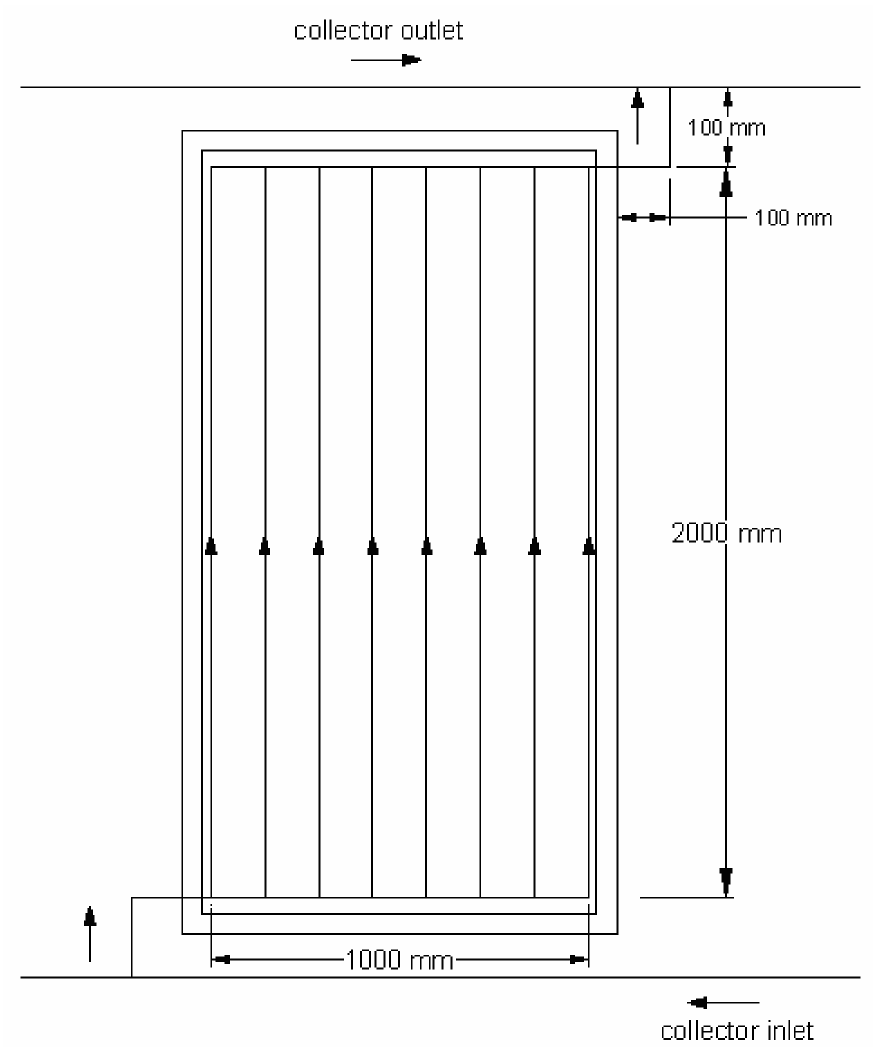

Figure 8. 7 Schematic Representation of the flow in the collector

a) Pressure drop inside the risers

Assuming uniform flow rate in each risers the volume flow rate per riser is:

$\dot{Q}_i = \frac{\dot{Q}}{N} = 7.57 * 10^{-6}\, m^3/s$; Where N is the number of risers.

Average velocity in a riser $V_{avr} = \frac{\dot{Q}_i}{A_r} = 0.02\, m/s$

Reynolds Number $R_e = \frac{\rho V_{avr} d}{\mu} = 634.702$

Since the $R_e < 2300$ it is laminar flow

For laminar flow $\Delta P_r = f \frac{L}{d} \frac{\rho V_{avr}^2}{2}$, $f = \frac{64}{R_e}$

$\Delta P_R = \underline{\underline{1.817 Pa}}$

b) Pressure drop inside the header

Taking the average volume flow rate

$\dot{Q}_{av} = \frac{\dot{Q}}{2} = 3.025 * 10^{-5}\, m^3/s$

Average velocity in the header

$V_{avh} = \frac{\dot{Q}_i}{A_h} = 0.03144\, m/s$

Reynolds Number $R_e = \frac{\rho V_{avh} D}{\mu} = 1587.33$

Since the $R_e < 2300$ it is laminar flow

For laminar flow $\Delta P_h = f \frac{L}{D} \frac{\rho V_{avh}^2}{2}$, $f = \frac{64}{R_e}$

$\Delta P_h = 0.564 Pa$

For the two headers, $\Delta P_H = 2 * \Delta P_h = \underline{\underline{1.1285 Pa}}$

c) Pressure drop inside the fittings

Based on the figure (8.2) there are 20 bends.

Pressure loss in the fitting, $\Delta P_f = K_f \dfrac{\rho V_1^2}{2}$

Where: K_f = pressure loss factor

V_1 = average velocity in the tube up stream of the fitting.

For 90º bend, laminar flow $K_f = 0.9$

$\Delta P_f = \underline{\underline{6.717 Pa}}$

d) Pressure drop inside the connection pipes

The total connection pipes length for a single collector is $L = 0.35m$

Pressure drop in the pipe is given by:

$$\Delta P_c = f \frac{L}{D} \frac{\rho V_{avh}^2}{2} = \underline{\underline{0.1975 Pa}}$$

The total pressure loss due to viscous effect of the fluid in a single collector is the sum of all the above losses.

$$\Delta P_{TC} = \Delta P_R + \Delta P_H + \Delta P_f + \Delta P_c$$
$$= \underline{\underline{9.86 Pa}}$$

8.4 Arrays of Collectors

According to the results of computer simulation, the daily hot water demand of the Addis Ababa tannery is fulfilled by the use of 261collectors, Dire tannery is fulfilled by the use of 149 collectors, and Ethiopian tannery is fulfilled by the use of 1667 collectors and Jimma hospital is fulfilled by the use of 795collectors.

a) Addis Ababa Tannery

These collectors are arranged in parallel with arrays. Each of the four storage tanks is connected with 6 arrays of collector. Where for all storage tanks of the six arrays the first five of them contains 12 collectors each and for 2 storage tanks the last array contains 6 collectors each and for the left 2 storage tanks the last array contains 5 collectors for the one storage tank and 4 collectors for the other storage tank.

Thus two of the four storage tanks each are connected to 66 collectors and the other two storage tanks are connected to 65 and 64 collectors.

b) Dire Tannery

In this tannery there are four storage tanks, where the first storage tank is connected to 75 collectors and the other storage tank is connected to74 collectors. These collectors are arranged in parallel with arrays. Each of the two storage tanks is connected with 6 arrays of collector. Where for both storage tanks of the six arrays the first five of them contains 12 collectors each and for the 75 collector storage tank the last array contains 15 collectors and for the 74collector storage tank, the last array contains 14 collectors.

c) Ethiopian Tannery

In this tannery, there are four storage tanks, where each of the three storage tanks are connected to 417collectors and the other storage tank is connected to 416 collectors. Where for all storage tanks, 209 collectors are on one side and on the other side, the first three storage tank each contains 208 collectors and the last storage tank contains 207 collectors.

d) Jimma Hospital

For this case there are four storage tanks, where each of the three storage tanks are connected to 199 collectors where there are 100 collectors are on one side and the other 99 collectors are on the other sides of the storage tank. And the last storage tank is connected to198 collectors where there are 99 collectors on both sides of the storage tanks.

For all storage tanks there are 8 arrays on each side. Of which the first 2 arrays contains 14 collectors and the last 6 array contains 12 collectors for the total of 100 collectors but for the 99 collector the last array contains 11 collectors.

8.5 Selection of Pump

An active system uses a pump or circulator to move the heat transfer fluid from the storage tank to the collector. In pressurized systems, the system is full of fluid and a circulator is used to move hot water or heat transfer fluid from the collector to the tank.

Pumps are sized to overcome static and head pressure requirements in order to meet specific system design and performance flow rates.

Drain-back and other unpressurized solar water heating systems require a high head pump to lift the water from the storage vessel to the collector and force the air out of the collector or collector array. This requires a centrifugal pump or other pump that will provide adequate pressure.

Most active solar systems use centrifugal pumps. Pump selection depends on the following factors:

- System type (direct or indirect).
- Heat collection fluid.
- Operating temperatures.
- Required fluid flow rates.
- Head or vertical lift requirements.
- Friction losses.

The most common pump (circulator) used in solar systems is the "wet rotor" type in which the moving part of the pump, the rotor, is surrounded by liquid. The liquid acts as a lubricant during pump operation, negating the need for manual lubrication.

8.5.1 Addis Ababa Tannery

The pump that circulates water through each collector is related based on the total pressure drop that occurs following the longest path to the farthest collector.

a) Pressure drop on the line from the pump up to the collector array

Approximating the length from the pump to the collector as 20 m, the total closed loop length will be 40 m.

The total volume flow rate in the storage outlet and inlet pipes is:

$$\dot{Q} = 66 * \dot{Q} = 4 * 10^{-3}\, m^3/s$$

For 63 mm diameter pipe, the average velocity is:

$$V_{av} = \frac{\dot{Q}}{A} = 1.28\, m/s$$

Reynolds number, $R_e = \dfrac{\rho V_{av} D}{\mu} = 116.323 * 10^3$, the flow is turbulent

For the tube material of galvanized steel the equivalent roughness is, $\varepsilon = 0.15mm$

$\dfrac{\varepsilon}{D} = 0.00238$, therefore, from the Moody Chart or by using the explicit Haaland formula with the corresponding Reynolds number $f = 0.0255$

$$\Delta P_m = f \frac{L}{D} \frac{\rho V_{av}^2}{2} = \underline{\underline{13{,}143.87 Pa}}$$

b) Pressure drop in the main manifold connecting the all arrays together

Average flow rate in the manifold is:

$$\dot{Q}_{av} = 66 * \left(\frac{\dot{Q}}{2} \right) = 2 * 10^{-3}\, m^3/s$$

With 52 mm manifold diameter, the average velocity is:

$$V_{av} = \frac{\dot{Q}_{av}}{A} = 0.94\, m/s$$

Reynolds number, $R_e = \dfrac{\rho V_{av} D}{\mu} = 70{,}509.58$ the flow is turbulent

For the tube material of galvanized steel the equivalent roughness is, $\varepsilon = 0.15mm$

$\dfrac{\varepsilon}{D} = 0.0029$, therefore, from the Moody Chart or by using the explicit Haaland formula with the corresponding Reynolds number, $f = 0.0273$

i) *The pressure drops in the supply main manifolds*

Length of the manifold leaving a space of 0.5 m between two arrays for easy maintenance is $L = 13m$.

$$\Delta P_{ms} = f \frac{L}{D} \frac{\rho V_{av}^2}{2} = \underline{\underline{2{,}988.15 Pa}},$$

ii) The pressure drops in the return main manifolds

$L = 10.8m$

$$\Delta P_{mr} = f \frac{L}{D} \frac{\rho V_{av}^2}{2} = \underline{\underline{2{,}482.46 Pa}}$$

iii) Pressure drop in the bend

Based on the layout there are 2 bends on the main manifolds.

Pressure loss in bends, $\Delta P_b = K_f \frac{\rho V_1^2}{2}$

Where: K_f = pressure loss factor

V_1 = average velocity in the tube up stream of the fitting.

For 90º standard elbow, $K_f = 0.9$

$$\Delta P_b = K_f \frac{\rho V_1^2}{2} = \underline{\underline{788.08 Pa}}$$

c) Pressure drop in the array manifold

i) Pressure drop in the supply array manifold

$L = 7.25m$

Average volume flow rate through the manifold is:

$$\dot{Q}_{av} = 6 * \frac{\dot{Q}}{2} = 1.815 * 10^{-4} \, m^3/s$$

Average velocity for the 41 mm manifold diameter is:

$$V_{av} = \frac{\dot{Q}_{av}}{A} = 0.1375 \, m/s$$

Reynolds number, $R_e = \frac{\rho V_{av} D}{\mu} = 8{,}132.114$, the flow is turbulent.

Similarly, $\varepsilon = 0.15mm$

$\frac{\varepsilon}{D} = 0.0037$, and $f = 0.0368$

The pressure drops in the supply manifold is:

$$\Delta P_{ms} = f \frac{L}{D} \frac{\rho V_{av}^2}{2} = \underline{\underline{60.96 Pa}}$$

ii) Pressure drop in the return array manifold

$L = 7.9m$

The pressure drops in the return manifold is:

$$\Delta P_{ms} = f\frac{L}{D}\frac{\rho V_{av}^{2}}{2} = \underline{\underline{66.43 Pa}}$$

d) Pressure drop through the collector

Pressure drop through a single collector is:

$\Delta P_h = \underline{\underline{9.86 Pa}}$

e) Pressure drop due to the inclination of the collector to the horizontal

$\Delta P_h = \rho g h = \underline{\underline{6{,}650.04 Pa}}$

So, total pumping pressure needed for design is the sum of all the above pressure drops.

$\Delta P_{total} = \underline{\underline{26{,}189.832 Pa}}$

Total specific work $Y = \frac{\Delta P_{TP}}{\rho} = 26.44\ \mathrm{m^2/s^2}$

Total Head $H = \frac{Y}{g} \approx 3m$

The total volume flow rate for the pump is:

$\dot{Q} = 66 * \dot{Q} = 4 * 10^{-3}\ m^3/s = 14.4\ \mathrm{m^3/h}$

The proper centrifugal electric drive pump satisfying the requirement of Head = 4 m and Flow rate = 14.4 m^3/ h is:

Type	Caprari Electric Drive Pump	➢ The proper motor data	
Model	MEC-A 1/40A	Frequency	50 Hz
Normal Speed	1450 rpm	Rated Voltage	400 V
Shaft Power	0.39 KW	Rated power	0.55 KW
Efficiency	42.3 %	Motor Type	3~

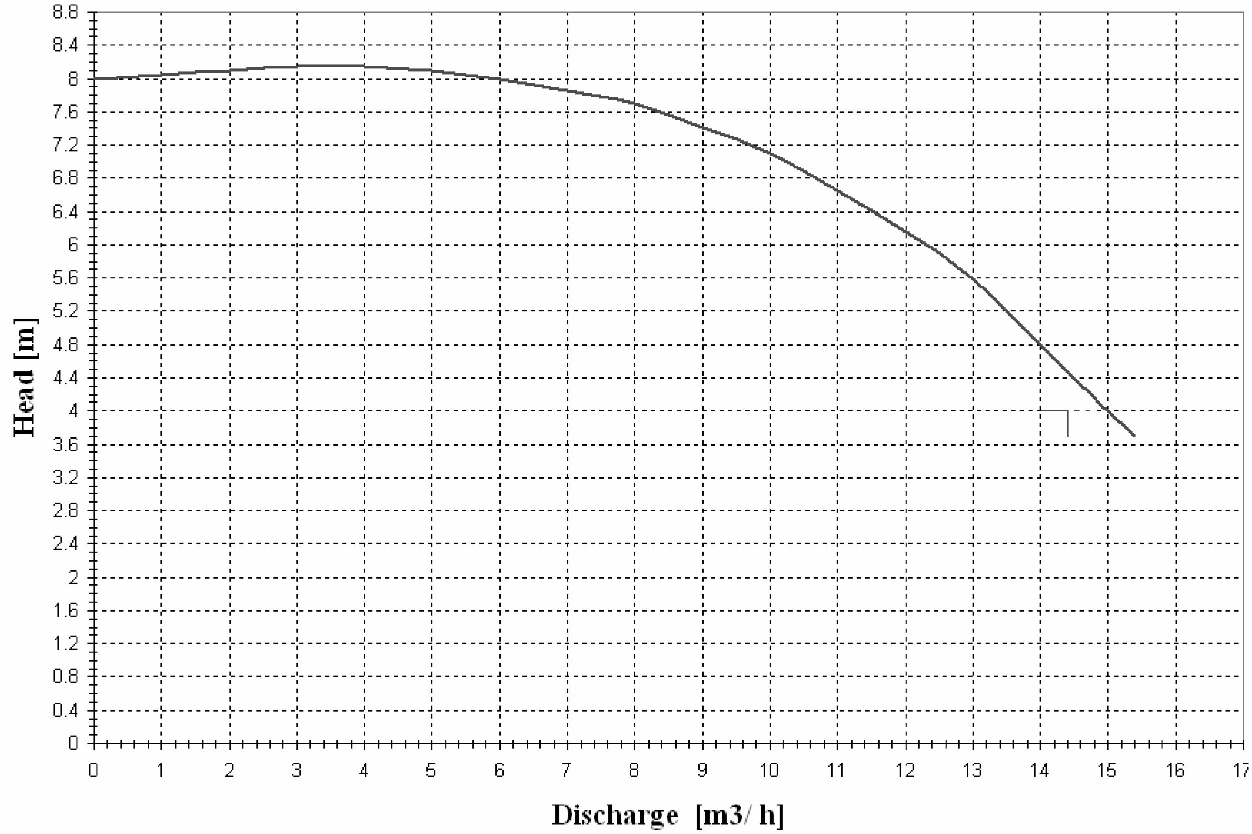

Figure 8. 8 Performance Curve for **MEC-A 1/40A C**entrifugal Pump.

8.5.2 Dire Tannery

The pump that circulates water through each collector is related based on the total pressure drop that occurs following the longest path to the farthest collector.

a) Pressure drop on the line from the pump up to the collector array

Approximating the length from the pump to the collector as 20 m, the total closed loop length will be 40 m.

The total volume flow rate in the storage outlet and inlet pipes is:

$$\dot{Q} = 75 * \dot{Q} = 4.54 * 10^{-3}\, m^3/s$$

For 63 mm diameter pipe, the average velocity is:

$$V_{av} = \frac{\dot{Q}}{A} = 1.456\, m/s$$

Reynolds number, $R_e = \dfrac{\rho V_{av} D}{\mu} = 132.283 * 10^3$, the flow is turbulent.

For the same material as the others pipes $\varepsilon = 0.15mm$

$\frac{\varepsilon}{D} = 0.00238$, therefore, from the Moody Chart or by using the explicit Haaland formula with the corresponding Reynolds number $f = 0.02535$

$$\Delta P_m = f\frac{L}{D}\frac{\rho V_{av}^2}{2} = \underline{\underline{16{,}906.25 Pa}}$$

b) Pressure drop in the main manifold connecting the all arrays together

Average flow rate in the manifold is:

$$\dot{Q}_{av} = 75 * \left(\frac{\dot{Q}}{2}\right) = 2.27 * 10^{-3}\, m^3/s$$

With 52 mm manifold diameter, the average velocity is:

$$V_{av} = \frac{\dot{Q}_{av}}{A} = 1.068\, m/s$$

Reynolds number, $R_e = \frac{\rho V_{av} D}{\mu} = 80.177 * 10^{-3}$, the flow is turbulent

For the tube material of galvanized steel the equivalent roughness is, $\varepsilon = 0.15mm$

$\frac{\varepsilon}{D} = 0.0029$, therefore, from the Moody Chart or by using the explicit Haaland formula with the corresponding Reynolds number $f = 0.02714$

i) The pressure drops in the supply main manifolds

Length of the manifold leaving a space of 0.5 m between two arrays in order to maintain it easily is $L = 15.7m$.

$$\Delta P_{ms} = f\frac{L}{D}\frac{\rho V_{av}^2}{2} = \underline{\underline{4{,}631.19 Pa}}$$

ii) The pressure drops in the return main manifolds

$L = 13.5m$

$$\Delta P_{mr} = f\frac{L}{D}\frac{\rho V_{av}^2}{2} = \underline{\underline{3{,}982.23 Pa}}$$

iii) Pressure drop in the bend

Based on the layout there are 2 bends on the main manifolds.

Pressure loss in bends, $\Delta P_b = K_f \frac{\rho V_1^2}{2}$

Where: K_f = pressure loss factor.

V_1 = average velocity in the tube up stream of the fitting.

For 90º standard elbow, $K_f = 0.9$

$$\Delta P_b = K_f \frac{\rho V_1^2}{2} = \underline{\underline{1{,}017.32 Pa}}$$

c) Pressure drop in the array manifold

i) Pressure drop in the supply array manifold

$L = 7.25m$

Average volume flow rate through the manifold is:

$$\dot{Q}_{av} = 6 * \frac{\dot{Q}}{2} = 1.815 * 10^{-4}\, m^3/s$$

Average velocity for the 41 mm manifold diameter is:

$$V_{av} = \frac{\dot{Q}_{av}}{A} = 0.1375\, m/s$$

Reynolds number, $R_e = \frac{\rho V_{av} D}{\mu} = 8{,}132.114$, the flow is turbulent.

Similarly, $\varepsilon = 0.15mm$

$\frac{\varepsilon}{D} = 0.0037$, and $f = 0.0368$

The pressure drops in the supply manifold is:

$$\Delta P_{ms} = f \frac{L}{D} \frac{\rho V_{av}^2}{2} = \underline{\underline{60.96 Pa}}$$

ii) Pressure drop in the return array manifold

$L = 7.9m$

The pressure drops in the return manifold is:

$$\Delta P_{ms} = f \frac{L}{D} \frac{\rho V_{av}^2}{2} = \underline{\underline{66.43 Pa}}$$

d) Pressure drop through the collector

The pressure drop through a single collector is:

$\Delta P_h = \underline{\underline{9.86 Pa}}$

e) Pressure drop due to the inclination of the collector to the horizontal

$\Delta P_h = \rho g h = \underline{\underline{6{,}650.04 Pa}}$

So, total pumping pressure needed for design is the sum of all the above pressure drops.

$\Delta P_{total} = \underline{\underline{\underline{33{,}324.282 Pa}}}$

Total specific work $\mathrm{Y} = \dfrac{\Delta P_{TP}}{\rho} = 33.42\ \mathrm{m}^2/\mathrm{s}^2$

Total Head $H = \dfrac{\mathrm{Y}}{g} \approx 4m$

The total volume flow rate for the pump is:

$\dot{Q} = 75 * \dot{Q} = 4.54 * 10^{-3}\ m^3/s = 16.34\ \mathrm{m}^3/\mathrm{h}$

The proper centrifugal electric drive pump satisfying the requirement of Head = 4 m and Flow rate = 16.34 m^3/ h is:

Type	Caprari Electric Drive Pump
Model	MEC-A 1/100D
Normal Speed	1450 rpm
Shaft Power	0.847 KW
Efficiency	25.6 %

- The proper motor data

Frequency	50 Hz
Rated Voltage	400 V
Rated power	1.1 KW
Motor Type	3~

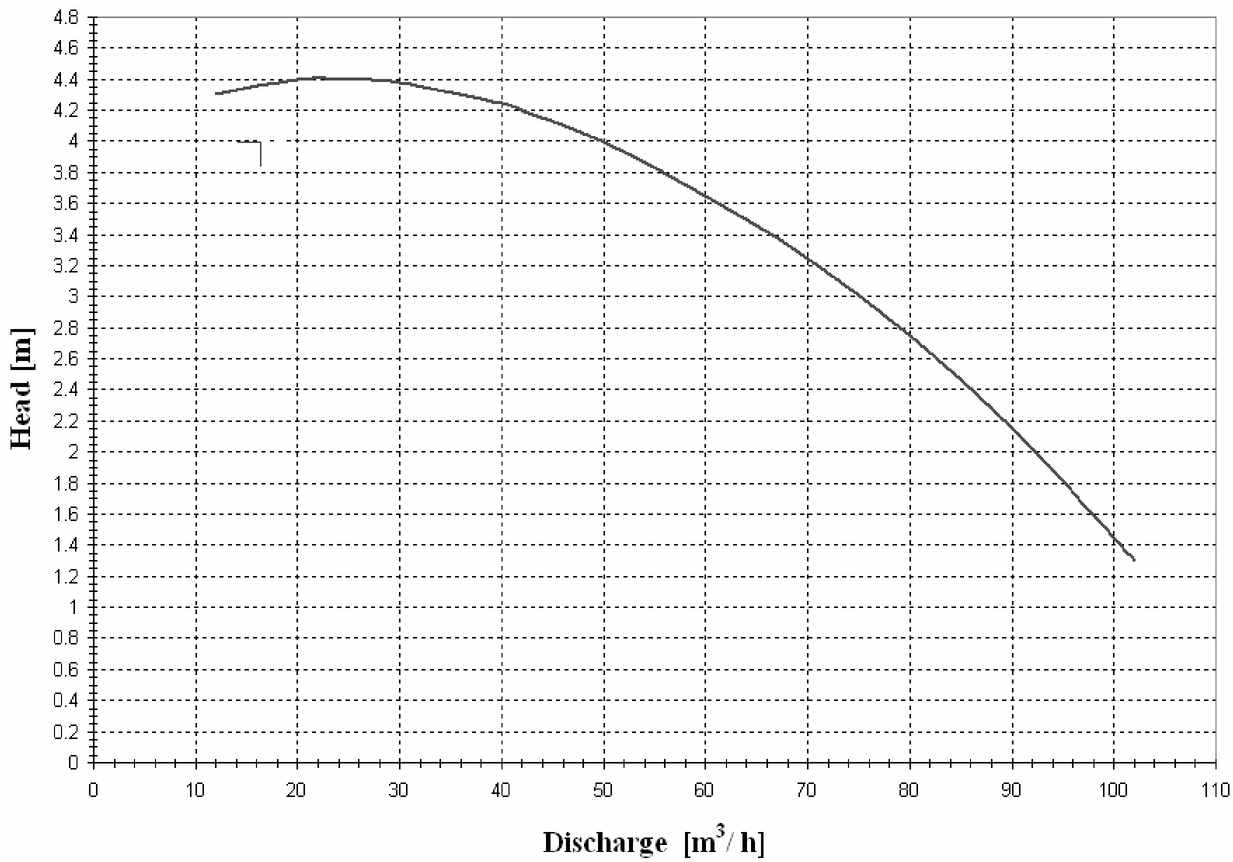

Figure 8. 9 Performance Curve for **MEC-A 1/100D C**entrifugal Pump

8.5.3 Ethiopian Tannery

The pump that circulates water through each collector is related based on the total pressure drop that occurs following the longest path to the farthest collector.

a) Pressure drop on the line from the pump up to the collector array

Approximating the length from the pump to the collector as 20 m, the total closed loop length will be 40 m.

The total volume flow rate in the storage outlet and inlet pipes is:

$$\dot{Q} = 209 * \dot{Q} = 12.645 * 10^{-3}\ m^3/s$$

For 63 mm diameter pipe, the average velocity is:

$$V_{av} = \frac{\dot{Q}}{A} = 4.056\, m/s$$

Reynolds number, $R_e = \dfrac{\rho V_{av} D}{\mu} = 368.63*10^3$, the flow is turbulent.

For the same material similar to the others pipes $\varepsilon = 0.15mm$

$\dfrac{\varepsilon}{D} = 0.00238$, therefore, from the Moody Chart or by using the explicit Haaland formula with the corresponding Reynolds number $f = 0.0247$

$$\Delta P_m = f\,\frac{L}{D}\,\frac{\rho V_{av}^2}{2} = \underline{\underline{127{,}458.9Pa}}$$

b) Pressure drop in the main manifold connecting the all arrays together

Average flow rate in the manifold is:

$$\dot{Q}_{av} = 209*\left(\frac{\dot{Q}}{2}\right) = 6.32*10^{-3}\ m^3/s$$

With 52 mm manifold diameter, the average velocity is:

$$V_{av} = \frac{\dot{Q}_{av}}{A} = 2.976\,m/s$$

Reynolds number $R_e = \dfrac{\rho V_{av} D}{\mu} = 223.23*10^3$, the flow is turbulent.

Assume the tube material is also galvanized iron, so that the equivalent roughness is, $\varepsilon = 0.15mm$

$\dfrac{\varepsilon}{D} = 0.0029$, therefore, from the Moody Chart or by using the explicit Haaland formula with the corresponding Reynolds number, $f = 0.026$

i) The pressure drops in the supply main manifolds

Length of the manifold leaving a space of 0.5 m between two arrays in order to maintain it easily is $L = 40m$.

$$\Delta P_{ms} = f\,\frac{L}{D}\,\frac{\rho V_{av}^2}{2} = \underline{\underline{87{,}768.668Pa}}$$

ii) The pressure drops in the return main manifolds

$L = 37.8m$

$$\Delta P_{mr} = f\frac{L}{D}\frac{\rho V_{av}^2}{2} = \underline{\underline{82{,}941.37Pa}}$$

iii) Pressure drop in the bend

Based on the layout there are 2 bends on the main manifolds.

Pressure loss in bends, $\Delta P_b = K_f\frac{\rho V_1^2}{2}$

Where: K_f = pressure loss factor.

V_1 = average velocity in the tube up stream of the fitting.

For 90º standard elbow, $K_f = 0.9$

$$\Delta P_b = K_f\frac{\rho V_1^2}{2} = \underline{\underline{7{,}899.2Pa}}$$

c) Pressure drop in the array manifold

i) Pressure drop in the supply array manifold

$L = 9.4m$

Average volume flow rate through the manifold is:

$$\dot{Q}_{av} = 7*\frac{\dot{Q}}{2} = 2.12*10^{-4}\,m^3/s$$

Average velocity for the 41 mm manifold diameter is:

$$V_{av} = \frac{\dot{Q}_{av}}{A} = 0.16\,m/s$$

Reynolds number, $R_e = \frac{\rho V_{av}D}{\mu} = 9{,}485.64$, the flow is turbulent.

Similarly, $\varepsilon = 0.15mm$

$\frac{\varepsilon}{D} = 0.0037$, and $f = 0.0357$

The pressure drops in the supply manifold is:

$$\Delta P_{ms} = f\frac{L}{D}\frac{\rho V_{av}^2}{2} = \underline{\underline{103.82Pa}}$$

ii) Pressure drop in the return array manifold

$L = 8.9m$

The pressure drops in the return manifold is:

$$\Delta P_{ms} = f \frac{L}{D} \frac{\rho V_{av}^2}{2} = \underline{\underline{98.3 pa}}$$

d) Pressure drop through the collector

The pressure drop through a single collector is:

$$\Delta P_c = \underline{\underline{9.86 Pa}}$$

e) Pressure drop due to the inclination of the collector to the horizontal

$$\Delta P_h = \rho g h = \underline{\underline{6,650.04 Pa}}$$

So, total pumping pressure needed for design is the sum of all the above pressure drops.

$$\Delta P_{total} = \underline{\underline{312,930.16 Pa}}$$

Using four pumps to satisfy this pressure drop, for a single pump the pressure drop to be considered is $\Delta P_{\sin gle\_pump} = \underline{\underline{78,232.54 Pa}}$

Total specific work $\mathrm{Y} = \frac{\Delta P_{TP}}{\rho} = 78.47\, \mathrm{m}^2/\mathrm{s}^2$

Total Head $H = \frac{\mathrm{Y}}{g} \approx 8m$

The total volume flow rate for each of the four pumps is:

$$\dot{Q} = \frac{209 * \dot{Q}}{4} = 3.16 * 10^{-3}\ m^3/s = 11.38\, \mathrm{m}^3/\mathrm{h}$$

The proper centrifugal electric drive pump satisfying the requirement of Head = 8 m and Flow rate = 11.38 m^3/ h is:

Type	Caprari Electric Drive Pump	➢ The proper motor data	
Model	MEC-A 01/40G	Frequency	50 Hz
Normal Speed	2950 rpm	Rated Voltage	400 V
Shaft Power	0.463 KW	Rated power	0.55 KW
Efficiency	59.4 %	Motor Type	3~

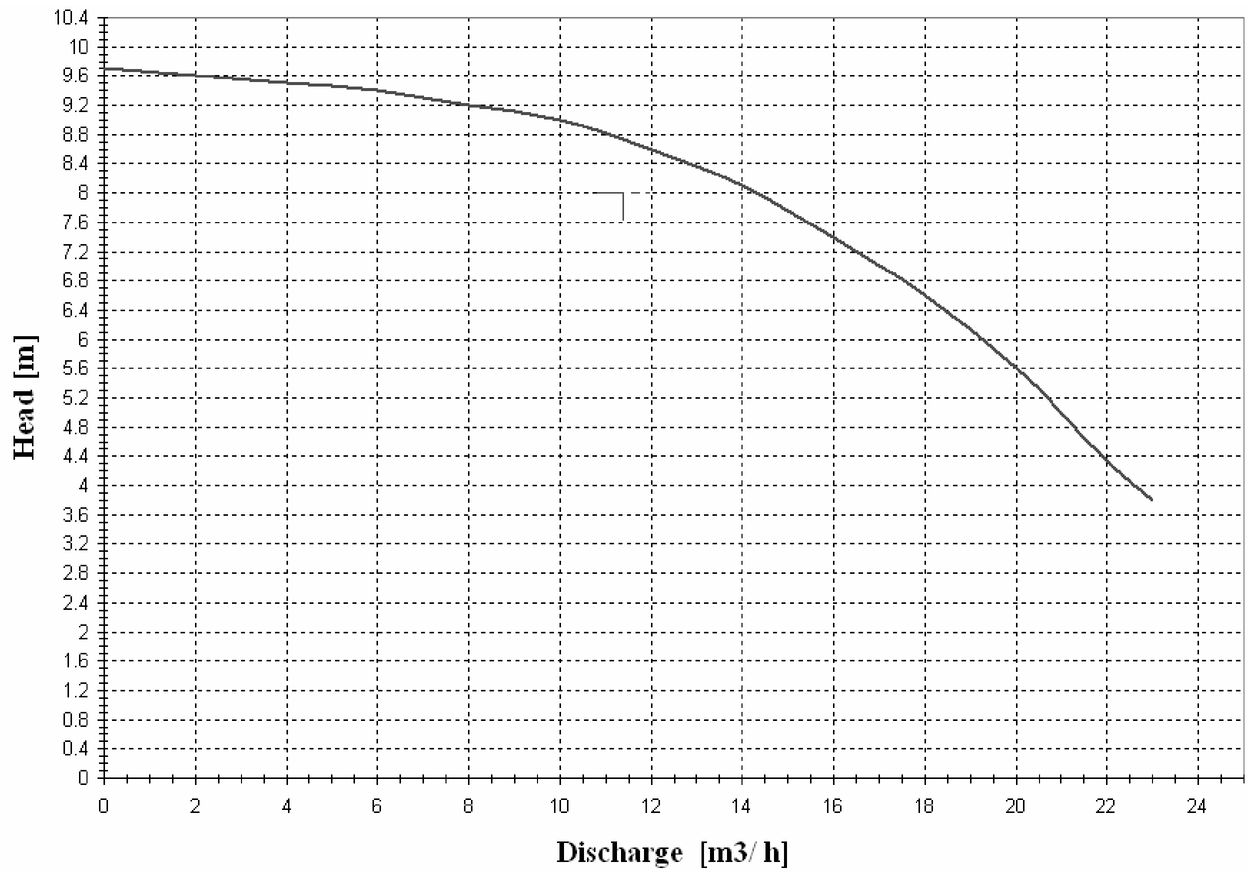

Figure 8.10 Performance Curve for **MEC-A 01/40G** Centrifugal Pump

8.5.4 Jimma Hospital

The pump that circulates water through each collector is related based on the total pressure drop that occurs following the longest path to the farthest collector.

a) Pressure drop on the line from the pump up to the collector array

Approximating the length from the pump to the collector as 20 m, the total closed loop length will be 40 m.

The total volume flow rate in the storage outlet and inlet pipes is:

$$\dot{Q} = 100 * \dot{Q} = 6.05 * 10^{-3}\ m^3/s$$

For 63 mm diameter pipe, the average velocity is:

$$V_{av} = \frac{\dot{Q}}{A} = 1.94\, m/s$$

Reynolds number, $R_e = \frac{\rho V_{av} D}{\mu} = 176.3*10^3$, the flow is turbulent

For the same material as the others pipes $\varepsilon = 0.15mm$

$\frac{\varepsilon}{D} = 0.00238$, therefore, from the Moody Chart or by using the explicit Haaland formula with the corresponding Reynolds number, $f = 0.0251$

$$\Delta P_m = f \frac{L}{D} \frac{\rho V_{av}^2}{2} = \underline{\underline{29{,}724.82 Pa}}$$

b) Pressure drop in the main manifold connecting the all arrays together

Average flow rate in the manifold is:

$$\dot{Q}_{av} = 100 * \left(\frac{\dot{Q}}{2} \right) = 3.025*10^{-3}\, m^3/s$$

With 52 mm manifold diameter, the average velocity is:

$$V_{av} = \frac{\dot{Q}_{av}}{A} = 1.424\, m/s$$

Reynolds number $R_e = \frac{\rho V_{av} D}{\mu} = 106.8145*10^3$, the flow is turbulent.

For the tube material of galvanized steel the equivalent roughness is, $\varepsilon = 0.15mm$

$\frac{\varepsilon}{D} = 0.0029$, therefore, from the Moody Chart or by using the explicit Haaland formula with the corresponding Reynolds number, $f = 0.0268$

i) The pressure drops in the supply main manifolds

Length of the manifold leaving a space of 0.5 m between two arrays in order to maintain it easily is $L = 21.1m$.

$$\Delta P_{ms} = f \frac{L}{D} \frac{\rho V_{av}^2}{2} = \underline{\underline{10.924*10^3\, Pa}}$$

ii) The pressure drops in the return main manifolds

$L = 18.9m$

$$\Delta P_{mr} = f \frac{L}{D} \frac{\rho V_{av}^2}{2} = \underline{\underline{9.787*10^3\, Pa}}$$

iii) Pressure drop in the bend

Based on the layout there are 2 bends on the main manifolds.

Pressure loss in bends, $\Delta P_b = K_f \dfrac{\rho V_1^2}{2}$

Where: K_f = pressure loss factor.

V_1 = average velocity in the tube up stream of the fitting.

For 90º standard elbow, $K_f = 0.9$

$$\Delta P_b = K_f \frac{\rho V_1^2}{2} = \underline{\underline{1{,}808.57 Pa}}$$

c) Pressure drop in the array manifold

i) Pressure drop in the supply array manifold

$L = 7.25m$

Average volume flow rate through the manifold is:

$$\dot{Q}_{av} = 6 * \frac{\dot{Q}}{2} = 1.815 * 10^{-4}\, m^3/s$$

Average velocity for the 41 mm manifold diameter is:

$$V_{av} = \frac{\dot{Q}_{av}}{A} = 0.1375\, m/s$$

Reynolds number, $R_e = \dfrac{\rho V_{av} D}{\mu} = 8{,}132.114$, the flow is turbulent.

Similarly, $\varepsilon = 0.15mm$

$\dfrac{\varepsilon}{D} = 0.0037$, and $f = 0.0368$

The pressure drops in the supply manifold is:

$$\Delta P_{ms} = f \frac{L}{D} \frac{\rho V_{av}^2}{2} = \underline{\underline{60.96 Pa}}$$

ii) Pressure drop in the return array manifold

The pressure drops in the return manifold $L = 7.9m$ is:

$$\Delta P_{ms} = f \frac{L}{D} \frac{\rho V_{av}^2}{2} = \underline{\underline{66.43 Pa}}$$

d) Pressure drop through the collector

The pressure drop through a single collector is:

$$\Delta P_c = \underline{\underline{9.86 Pa}}$$

e) Pressure drop due to the inclination of the collector to the horizontal

$$\Delta P_h = \rho g h = \underline{\underline{6{,}650.04 Pa}}$$

So, total pumping pressure needed for design the pump is the sum of all the above pressure drops.

$$\Delta P_{total} = \underline{\underline{59{,}100.102 Pa}}$$

Total specific work $\mathrm{Y} = \dfrac{\Delta P_{TP}}{\rho} = 59.28\, \mathrm{m}^2/\mathrm{s}^2$

Total Head $H = \dfrac{\mathrm{Y}}{g} \approx 6m$

The total volume flow rate for each of the four pumps is:

$$\dot{Q} = 100 * \dot{Q} = 6.05 * 10^{-3}\ m^3/s = 21.78\, \mathrm{m}^3/\mathrm{h}$$

- The proper centrifugal electric drive pump satisfying the requirement of Head = 6 m and Flow rate = 21.78 m^3/ h is:

Type	Caprari Electric Drive Pump
Model	MEC-A 1/50B
Normal Speed	1450 rpm
Shaft Power	0.571KW
Efficiency	71.5 %

- The proper motor data

Frequency	50 Hz
Rated Voltage	400 V
Rated power	0.75 KW
Motor Type	3~

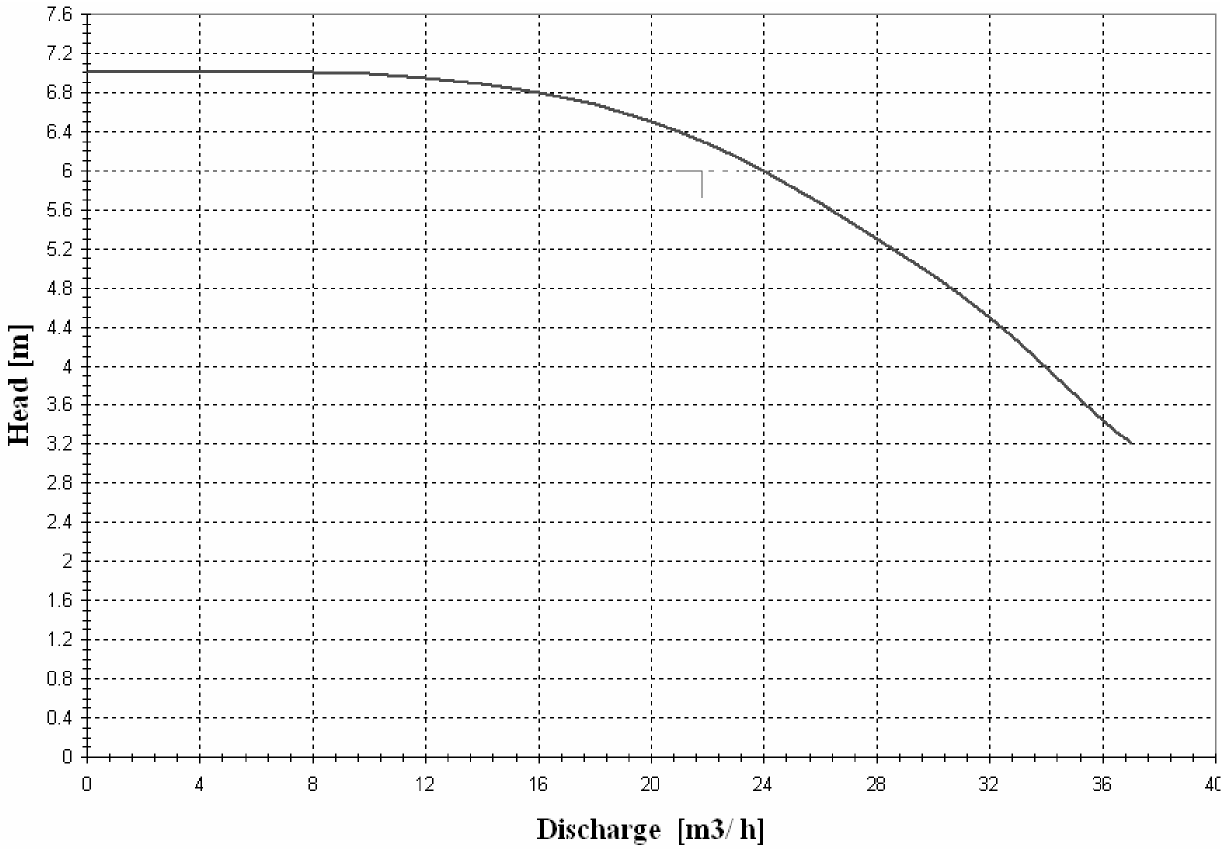

Figure 8.11 Performance Curve for **MEC-A 1/50B** Centrifugal Pump

CHAPTER 9

CONTROL ELEMENT

9.1 Pump Control

The use of pump in thermal collection system increases the efficiency of the system. However the operation of the pump should be designed only when solar collection is feasible. To determine whether solar collection is feasible or not, measuring collector temperature and comparing it with the storage tank bottom temperature is necessary. If the energy obtained from solar collection is not relatively greater than the pumping cost, the pump should be off until sufficient energy is obtained, and on elsewhere. This can be done by the use of differential controller.

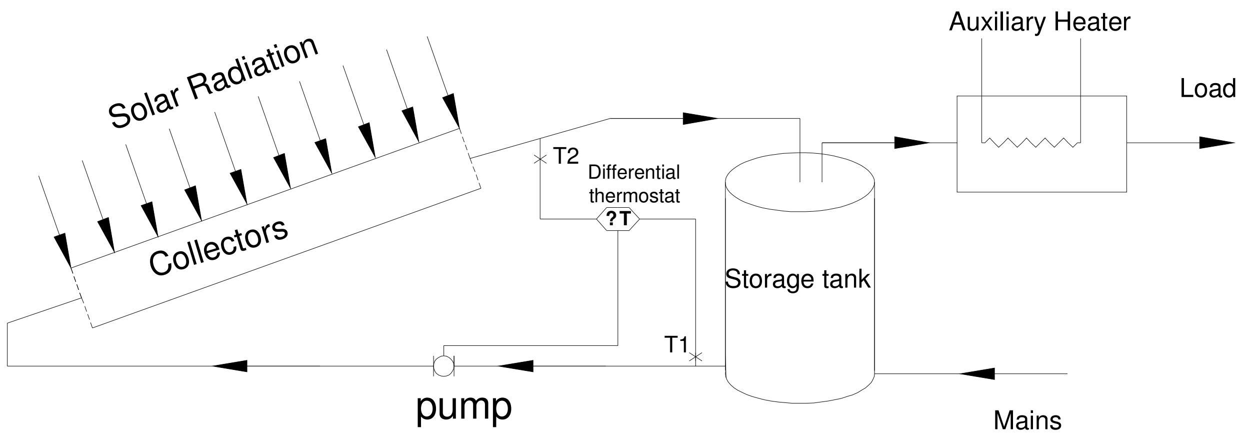

Figure 9.1 Positioning of Differential Controller

For this case the use of a differential thermostat fulfills the requirement.

A thermostat whose electrical resistance varies with temperature messages the differential temperature at a two specified points. The differential thermostat which is presetted for maximum and minimum temperature difference closes or opens the electric pump circuit.

For this model one end of the thermister sensors is placed at the bottom of the storage tank and the other end at the collector outlet pipe and setted to start the pump when the water outlet temperature is 5ºc hotter than the storage medium. The pump will stop its operation when the temperature difference is below 1ºc. In order to avoid continuous off and on operation of the pump, 1 – 3 minutes delay increases the life of the motor.

9.2 Drain Valve and Vacuum Air Vent

Maintenance and avoidance of freezing in cold weather require a water draining system at each collector. A drain valve is installed to fulfill this purpose at the entrance of a collector. For the proper function of the drain valve a vacuum air vent is provided at the headers of the arrays of collectors.

9.3 Pressure Relief Valve

A pressure relief valve is a valve used in liquid systems that opens whenever the pressure in the system is greater than some safe maximum. It guards against destructive pressures that could build up if the system is overheated. The design is based on a spring action for a maximum pressure of 4 bars.

9.4 Air Vent

The amount of air which can be contained in water decreases with the temperature of the water. Therefore, a large amount air from the water may develop a higher pressure in the storage tank and the pipes. Therefore this air should be vented through an air vent. Air vent designed at the header and top of the storage tank is in coincidence with a lighter density of air.

9.5 Check Valves

Check valves allow fluid to flow in only one direction. In solar systems, these valves prevent thermosiphoning action in the system plumbing. Without a check valve, water that cools in the elevated collector at night will fall by gravity to the storage tank, displacing lighter, warmer water out of the storage tank and up to the collector. Once begun, this thermosiphoning action can continue all night, continuously cooling all the water in the tank.

Corrosion and scale may build up on the internal components of a check valve; therefore, a regular service schedule should be maintained.

CHAPTER 10
ECONOMIC ANALYSIS

10.1 Introduction

Economics play a central role in any customer's decision to purchase a solar water heater system. The customer, or a corporation, is unlikely to buy a solar energy system if they know that its only benefits are to the environment. Obviously, any company considering solar power generation is going to look very carefully at economics to ensure that such a project will be profitable to them.

This guide was developed to help illustrate the process involved in completing a Life Cycle Cost (LCC) economic analysis of competing energy solutions. It also introduces the concept of accounting for subsidies and/or externalities in an economic analysis, an increasingly important issue to many policy and other decision makers.

To help illustrate the number of variables that can influence an economic analysis of SWH, the list below has been considered.

a) Performance Variables

- Solar energy available.
- Ambient air temperature & cold water temperature.
- Collector tilt and orientation.
- Collector shading.
- Hot water consumption pattern.
- Hot water delivery temperature.
- Solar energy system size and type.

b) Economic Variables

- Current and future fuel costs.
- Current and future inflation rate.
- Discount rate generally known as interest rate and is also referred to as "time value of money".
- System replacement and maintenance costs over time.

10.2 Economic Indicators

10.2.1 Life Cycle Cost and Unit price of Solar Energy

The life cycle cost includes investment capital and present worth of operating cost during the useful life of the plant. The operating cost of solar water heating system is mainly the maintenance and pumping cost. The life cycle cost of solar water heating system is determined from the investment cost and the present value of maintenance and pumping cost distributed over the life as follows [6, 7].

$$LCC = CI + C_m \frac{1}{i}\left(1 - \frac{1}{(1+i)^n}\right) \quad (10.1)$$

Where: CI is the investment cost of solar water heating system, and

C_m is annual maintenance and pumping cost.

To determine the unit price of solar energy cost, P_e the life cycle cost has to be equal to the life cycle savings of the solar water heater during its life time [7].

The annual energy saving is, $ES = f_a Q_a$ -- (10.2)

The life cycle saving of solar water heater is the energy cost saved due to replacement of fuel by solar.

$$LCS = P_e f_a Q_a \frac{1+i_e}{i-i_e}\left[1 - \left(\frac{1+i_e}{1+i}\right)^n\right] \quad (10.3)$$

To deterimine the unit price:

$LCC = LCS$

$$CI + C_m \frac{1}{i}\left(1 - \frac{1}{(1+i)^n}\right) = P_e f_a Q_a \frac{1+i_e}{i-i_e}\left[1 - \left(\frac{1+i_e}{1+i}\right)^n\right]$$

The unit price of solar energy for water heating is therefore,

$$\Rightarrow \qquad P_e = \frac{CI}{f_a Q_a} \frac{1 + \frac{C_m}{CI}\left(\frac{1}{i}\left(\frac{1}{(1+i)^n}\right)\right)}{\frac{1+i_e}{i-i_e}\left[1 - \left(\frac{1+i_e}{1+i}\right)^n\right]} \quad (10.4)$$

If solar energy has to be economically viable, the unit cost of water heating system must be less than that of other alternatives [7].

10.2.2 Payback Period

To determine the pay-back period, the maintenance cost is neglected. Hence the investment of the solar water heater has to be pay-backed by the life cycle saving of fuel cost.

$$LCCS = C_f f_a Q_a \frac{1+i_e}{i-i_e}\left[1-\left(\frac{1+i_e}{1+i}\right)^n\right] \quad \text{(10.5)}$$

$$LCCS = CI \qquad at \quad n = N_P \quad \text{(10.6)}$$

$$C_f f_a Q_a \frac{1+i_e}{i-i_e}\left[1-\left(\frac{1+i_e}{1+i}\right)^{N_P}\right] = CI$$

$$\Rightarrow \qquad N_P = \frac{\ln\left[1+\dfrac{CI\left(\dfrac{i_e-i}{1+i_e}\right)}{C_f f_a Q_a}\right]}{\ln\left[\dfrac{1+i_e}{1+i}\right]} \quad \text{(10.7)}$$

Where: - LCS is the life cycle saving of a solar water heating system [kWh]

- LCCS is the life cycle saving of fuel cost [Birr].
- C_f is the unit cost of fuel for the first year of analysis [Birr / kWh].
- f_a is annual fraction of load supplied by solar energy .
- Q_a the annual heating load [kWh].
- CI is the initial investment cost, [Birr]
- i is the annual market discount rate.
- i_e is the annual market rate of fuel escalation, and
- n is the years of economic analysis.

10.3 Maintenance& Replacement Costs

Repair and replacement costs are so central to the success of solar water heating. On the other hand they are difficult to obtain. It has to be mentioned that the replacement and repair cost depends on the manufacturer and the type of the system used. The reason for this is the best approximation of the life cycle costing.

a) Pumps

Pumps are the solar water heater components most frequently replaced. Various companies working with solar water heaters recommend that the average age of pumps replaced varies between 5-10 years.

The most common reasons causing a pump failure according to various researches are:

- Plumping leaks, affecting pump and electrical.
- Air in the pump (cavitations).
- Overheating which is a product of poor system design, such as undersize pump or improper collector area to storage volume ratio.

b) Controls

According to controllers manufacturing company's information most controls are a matter of replacement. It could be possible to have the electronic circuit repaired but that happens very rarely. A large part of the repairs involving simple controls had to do with sensors (thermo resistors) replacement and not the control itself. Actual control failures were rather uncommon.

So replacement of thermostats is quite cheap and reasonable and would not cost much.

c) Collectors

In terms of lifetime and replacement this is the most difficult section solar water heating system component to evaluate. From the various companies manufacturing solar collectors just a few of them were notable to give an exact average replacement age. Most of them certified that the solar collectors would last for at least 20-25 years.

d) Storage Tanks

Various companies recommend the average age of tanks replacement varies between 9-12 years.

The following assumptions are taken during the economic analysis of SWH system:

- Life of the plant = 10 years
- Interest rate = 0.10
- Inflation rate = 0.05

10.4 Unit Cost of Fuel

1 liter (or 0.85 kg) furnace oil costs 4.20 birr

The heating value of furnace oil is $9{,}700\ \text{kcal}/\text{kg} = 40{,}604.2\ \text{kJ}/\text{kg}$

So 1 liter furnace oil has a heating value of 34,513.57 kJ

Then the unit price of fuel $= 4.20\ \text{Birr}/34{,}513.57\ \text{kJ} = 121.69 * 10^{-6}\ \text{Birr}/\text{kJ}$

$$= 0.438\ \text{Birr}/\text{kWh}$$

Taking in to account the boiler efficiency = 80 %

The total unit cost of the fuel $= \dfrac{0.438 Birr / kWh}{0.8} = \underline{\underline{0.5475 Birr / kWh}}$

Table 10.1 Unit Price for Solar Water Heating System

No	Item	Specification	Unit Price[birr]
1	Collector	1m*2m flat plate	1,250.00 Birr /m^2
2	Storage Tank		
	Inside Material	2mm Thick Sheet Steel (1m*2m)	175.00 Birr / m^2
	Insulation	Glass Fiber (t = 25 mm W = 2 m, L=1m) (K=0.032 W/m k)	1900 Birr / m^3
	Insulation Cover	0.8 mm Thick Galvanized Pre Painted Steel (1m*2m)	100.00 Birr / m^2
	Manufacturing Cost		50% of Material Cost
3	Piping(Length= 6 m)		
	Material	1" Galvanized Steel 1 1/4" Galvanized Steel 1 ½" Galvanized Steel 2" Galvanized Steel 2 ½ "Galvanized Steel	75 Birr 95 Birr 120 Birr 180 Birr 200 Birr
4	Elbows and Fittings	Elbows, Tees 1 ¼ " Elbows, Tees 2 " Elbows, Tees	 2.5Birr / pcs 8 Birr / pcs
5	Labour and Installation Cost		10 % of Collector Cost
6	Operating Cost (Maintenance & Pumping Cost)		5% of Investment Cost
7	Pump (Electric Drive)	MEC-A 1/40A (with full accessories) MEC-A 1/100D (with full accessories) MEC-A 01/40G (with full accessories) MEC-A 1/50B (with full accessories)	8,000.00 Birr 11,500.00 Birr 8,000.00 Birr 9,200.00 Birr

Table 10. 2 Total Cost Break Down for all systems per Collector

Total Cost Break Down per Collector				
Type of Cost	**Addis Ababa Tannery [Birr/Collector]**	**Dire Tannery [Birr/Collector]**	**Ethiopian Tannery [Birr/Collector]**	**Jimma Hospital [Birr/Collector]**
Collector Cost	2500	2500	2500	2500
Pipes Cost (Material + Insulation)	88.25	90.27	84.94	91.23
Fittings Cost	11.47	11.47	11.47	11.47
Storage Tank Cost	210.72	200.52	209.56	272.07
Pump Cost	122.61	154.36	153.11	92
Labour and Installation Cost	250	250	250	250
Total Investment Cost	**3,183.05**	**3,206.62**	**3,209.08**	**3,216.77**
Operating Cost (Maintenance & Pumping Cost)	159.18	160.33	160.45	160.84

The total initial investment cost for the solar water heating system, unit cost of energy and pay back period for the system are summarized as shown below.

Table 10. 3 Project Cost Summary

Project Site	**Total Initial Cost of Solar Water Heating System** [Birr]	**Unit Cost of Solar Energy** [Birr/kWh]	**Unit Cost of Fossil Fuel (Furnace Oil)** [Birr/kWh]	**Pay Back Period** [Years]
Addis Ababa Tannery	830, 776.05	0.3585	0.5475	4.91
Dire Tannery	477, 786.38	0.3730	0.5475	5.14
Ethiopian Tannery	5, 349, 536.36	0.3600	0.5475	4.93
Jimma Hospital	2, 557, 332.15	0.3388	0.5475	4.61

CHAPTER 11

CONCLUSIONS AND RECOMMENDATIONS FOR FUTURE WORK

11.1 Conclusions

It was found that for Addis Ababa tannery of total daily hot water consumption of 32.6 m^3 a total of 261 collectors with four storage tanks of each capacity 6.5 m^3 are needed with initial capital cost of 3,183.05 Birr per collector, which will cost a total of 4,161.00 Birr per collector through out its life time and the life cycle cost saving will be 5,797.00 Birr per collector.

Similarly,
for Dire tannery of total daily hot water consumption of 18.53 m^3 a total of 149collectors with two storage tanks of each capacity 7.4 m^3 are needed with initial capital cost of 3,206.62 Birr per collector, which will cost a total of 4,191.00 Birr per collector through out its life time and the life cycle cost saving will be 5,610.00 Birr per collector.

for Ethiopian tannery of total daily hot water consumption of 250 m^3 a total of 1667collectors with four storage tanks of each capacity 52.1 m^3 are needed with initial capital cost of 3,209.08 Birr per collector, which will cost a total of 4,194.00 Birr per collector through out its life time and the life cycle cost saving will be 5,824.00 Birr per collector.

for Jimma hospital of total daily hot water consumption of 119.24 m^3 a total of 795 collectors with four storage tanks of each capacity 24.8 m^3 are needed with initial capital cost of 3,216.77 Birr per collector, which will cost a total of 4,205.00 Birr per collector through out its life time and the life cycle cost saving will be 6,197.00 Birr per collector.

Since the unit cost of solar energy is less than the unit cost of the fossil fuel in all sites, the large-scale water heating by solar energy is a viable alternative to heating by fossil fuel (furnace oil).

11.2 Recommendations for Future Work

The following points can be recommended for the future work.

- The same work can also be done using parabolic trough collectors or vacuum tube collectors system.
- Parametric studies can be done using the flat-plate, vacuum tube or concentric type solar collectors.
- Optimizing of the system.

REFERENCE

1. Abebayehu Assefa and Demiss Alemu : **The Viability of Solar Energy for Domestic Water Heating in Ethiopian Cities**, Zede, No.9, Addis Ababa, 1992.
2. ASRAE, **Thermal Hand Book**.
3. Beckman, W.A., Klein, S. A., Duffie, J.A.: **A Design Procedure for Solar Water Heating System**, Solar Energy, Volume 18, pp.113, 1976.
4. Brandemuehl, M.J. and Beckman, W.A.: **Economic Evaluation and Optimization of Solar Water heating Systems**, Solar Energy, Vol. 23, No. 1, 1979.
5. Caprari, **Electric Drive Pump Catalogue**. “EMU General Importer PLC.”
6. Collares-Pereira, Gordan, J. M., Rabi and Zarmi, Y.: **Design and Optimization of Solar Industrial Hot Water System**, Solar Energy, Vol. 32, 1984.
7. Demiss Alemu: **Optimal Design of Solar Water Heating System**, Zede, No.15, Addis Ababa, 1998.
8. Demiss Alemu: **Practice and Prospects of Solar Water Heating in Ethiopia**, Energy conference, Addis Ababa, 2002.
9. Dimitrios Panapakidis: **Solar Water Heating Systems Study Reliability, Quantitative Survey and Life Cycle Cost Method**, MSc. thesis, Department of Mechanical eng., University of Strathclyde in Glasgow.
10. Duffie, J. A. and Beckman W. A. (1991) **Solar Engineering of Thermal Processes.** 2nd edition, J. Wiley and Sons, New York.
11. Fisch, M.N., Guigas, M. and Dalenback, J.O.: **A Review of Large-Scale Solar Heating System in Europe**, Solar Energy, Vol. 63, No. 6, pp. 355-366, 1998.
12. GPG Solar (**Dealer of Flat-Plate collector solar water heater**).
13. Hottel, H.C. and Woertz, B.B.: **Performance of Flat-Plate Solar-Heat Collectors**. Trans. ASME, 64, 91 (1942).
14. Ian Mc. Chesney in association with East Harbour Management Services Ltd. and Enercon Ltd.: **Developing the Market for Larger Scale Solar Water Heating Applications in New Zealand**, Report to the Energy Efficiency and Conservation Authority (EECA), New Zealand, June 2005.

15. **International Journal of Climatology** 26: 75–89 (2006), Published online 7 November 2005 in Wiley InterScience (www.interscience.wiley.com).
16. John R. Howell, Richard B. Bannerot, Grary C. Vliet: **Solar Thermal Energy System**, USA, 1982.
17. **Proceedings of Energy Conference 2002** UNCC, Addis Ababa, September 2002.
18. RAI, G.D.: **Solar Energy Utilization**, fifth edition, Delhi, 2001.
19. Sodha, M.S., Tiwari, G.N., Sawhney, R.L., Sharma, A.K., Singh, A.K. and Goya, R.K.: **Sizing of a Multi-Tank Solar Water Heater**, Int. J. Energy Res., 22, 777 - 790 (1998), India.
20. Tsilingiris, P.T.: **Solar Water-Heating Design – A New Simplified Dynamic Approach**, Solar Energy, Vol. 57, No. 1 pp. 19-28,1996.
21. Vonal.com (**Manufacturer of Flat-Plate Solar Collectors in Ethiopia**).

ANNEX A

TEMPERATURE PLOTS FOR THE FOUR SEASONS WITH REPRESENTATIVE MONTHS

a) Addis Ababa Tannery

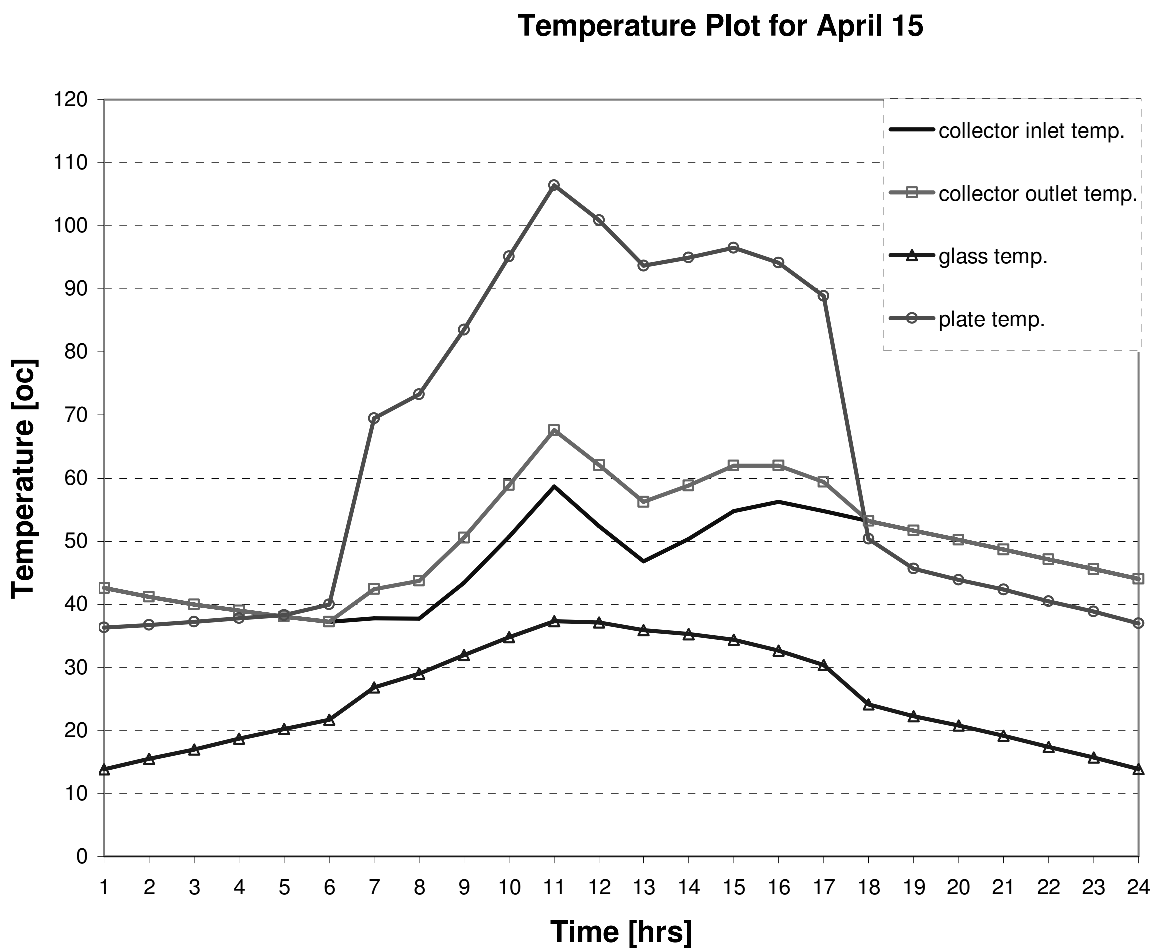

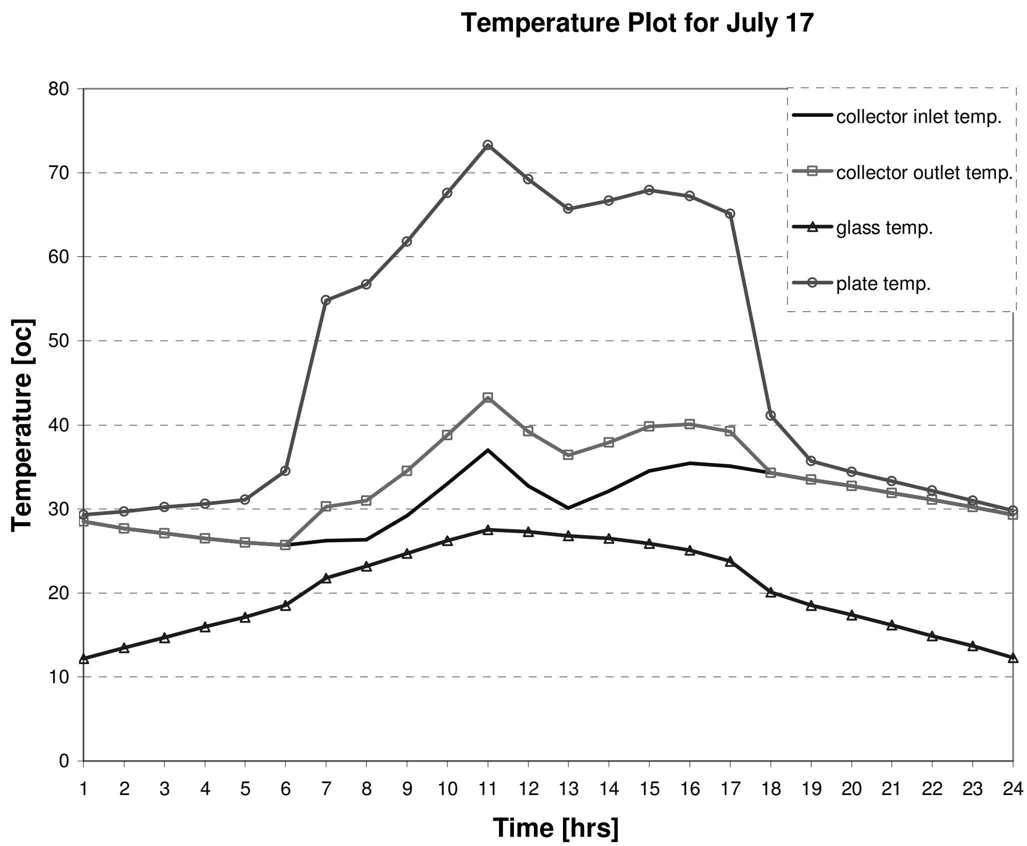
Temperature Plot for July 17
Temperature [oc]
Time [hrs]
collector inlet temp.
collector outlet temp.
glass temp.
plate temp.

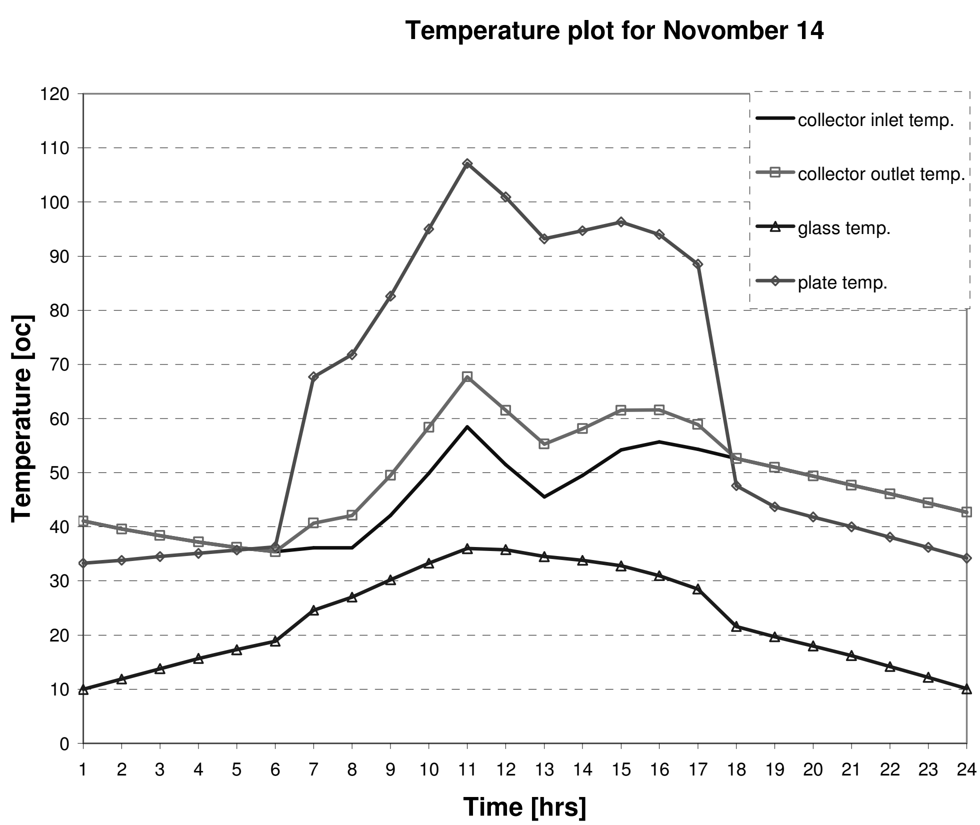
Temperature plot for Novomber 14
Temperature [oc]
Time [hrs]
collector inlet temp.
collector outlet temp.
glass temp.
plate temp.

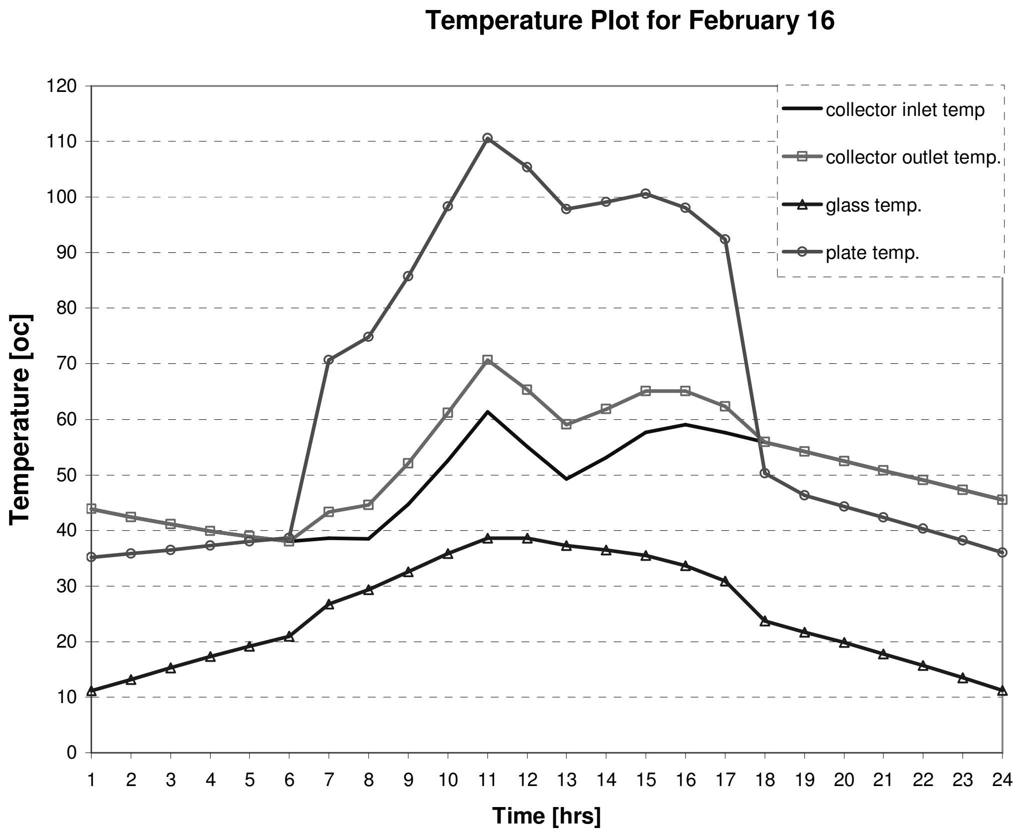
Temperature Plot for February 16
Temperature [oc]
Time [hrs]
collector inlet temp
collector outlet temp.
glass temp.
plate temp.
0
10
20
30
40
50
60
70
80
90
100
110
120
1 2 3 4 5 6 7 8 9 10 11 12 13 14 15 16 17 18 19 20 21 22 23 24

b) Dire Tannery

Temperature Plot for April 15

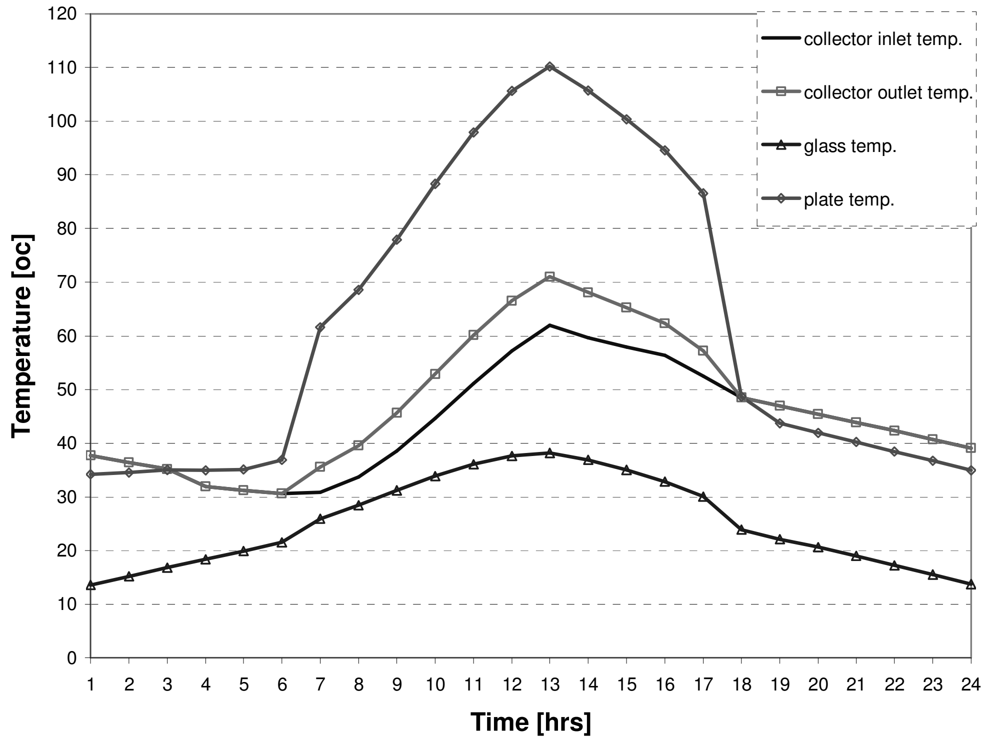

Temperature Plot for July 17

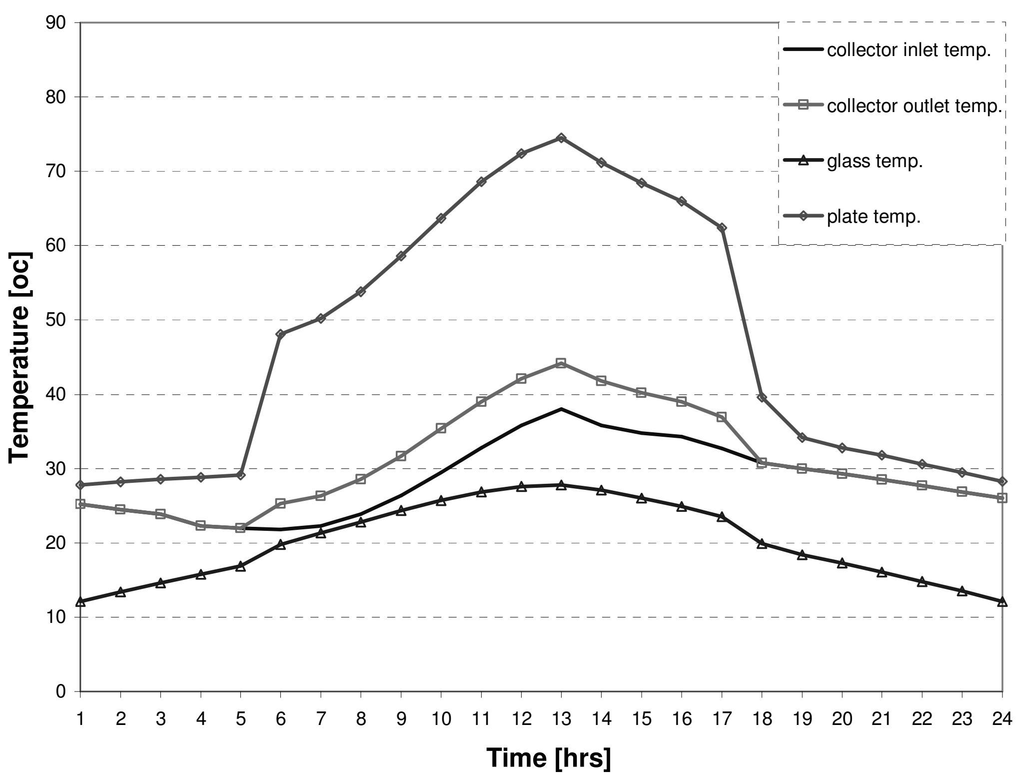

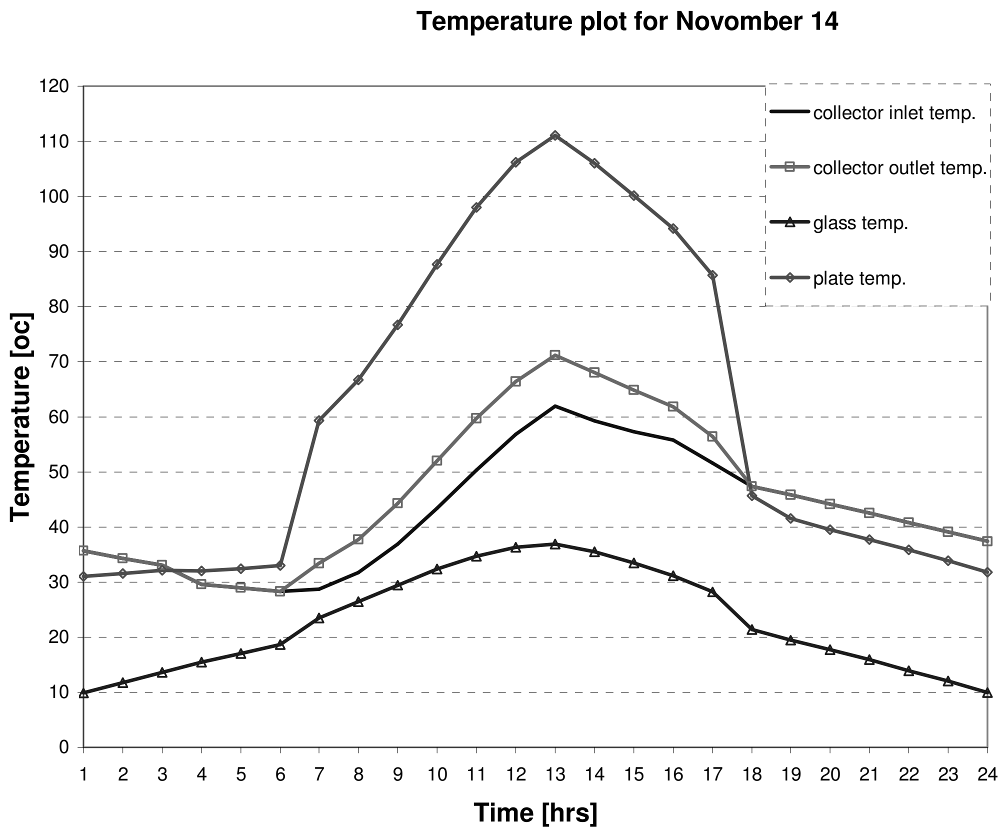
Temperature plot for Novomber 14
Temperature [oc]
Time [hrs]
collector inlet temp.
collector outlet temp.
glass temp.
plate temp.

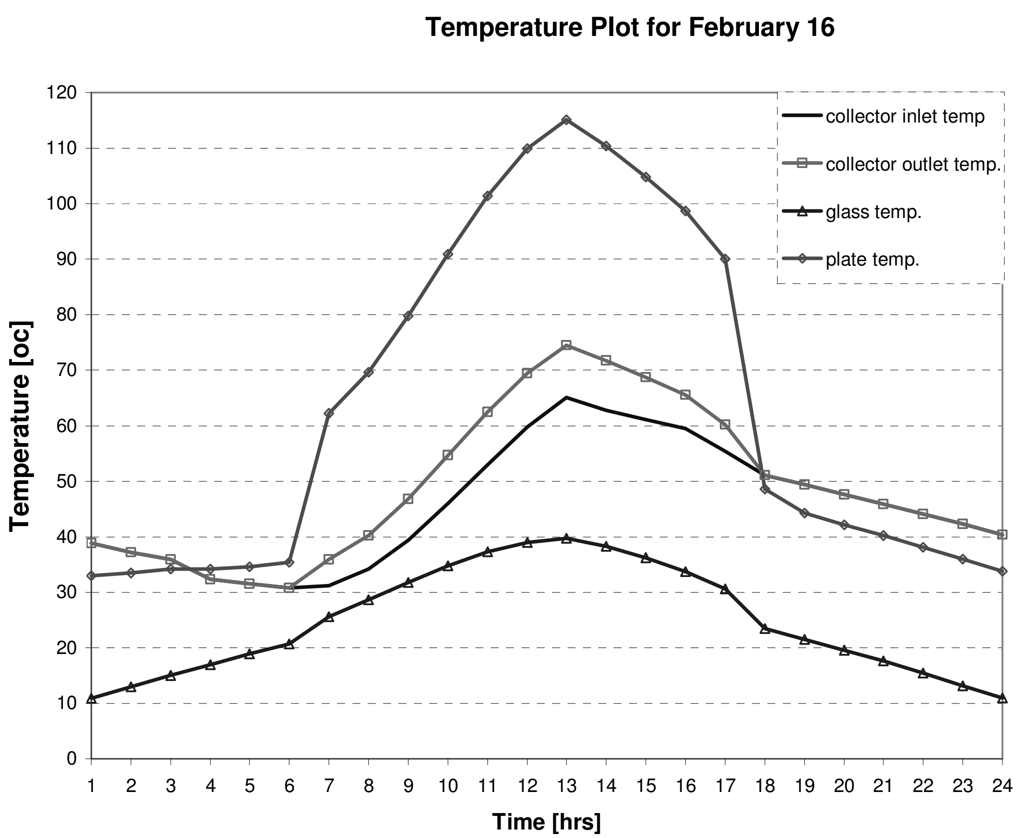
Temperature Plot for February 16
Temperature [oc]
Time [hrs]
collector inlet temp
collector outlet temp.
glass temp.
plate temp.

c) Ethiopian Tannery

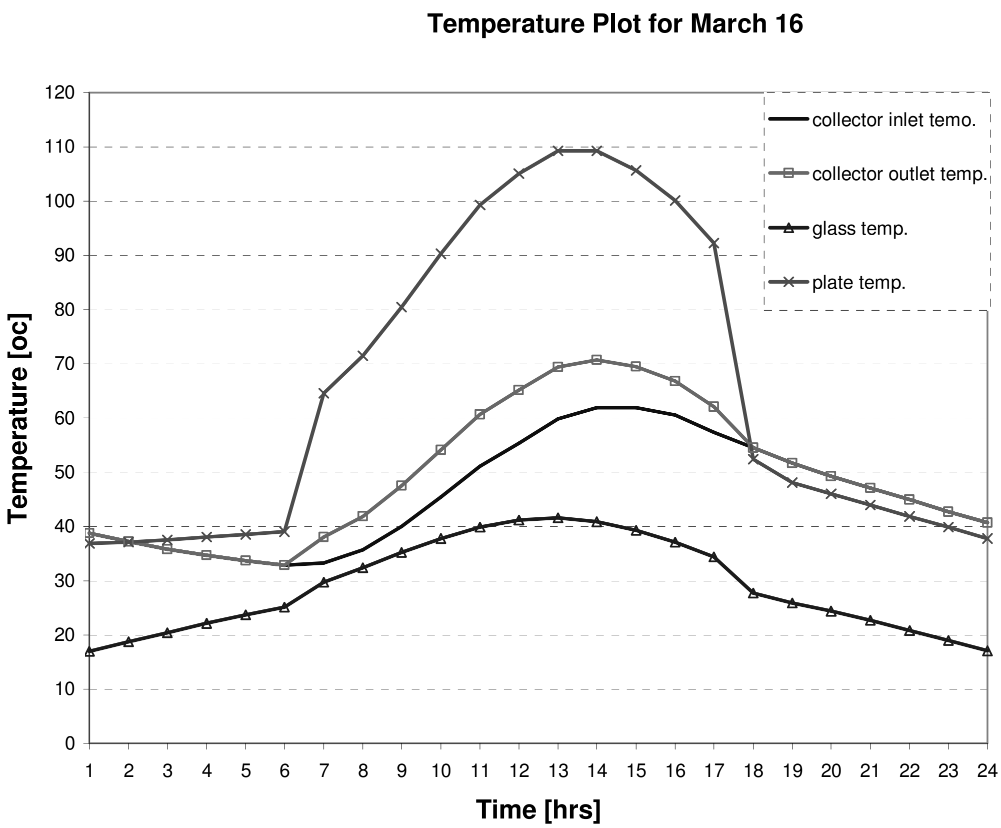

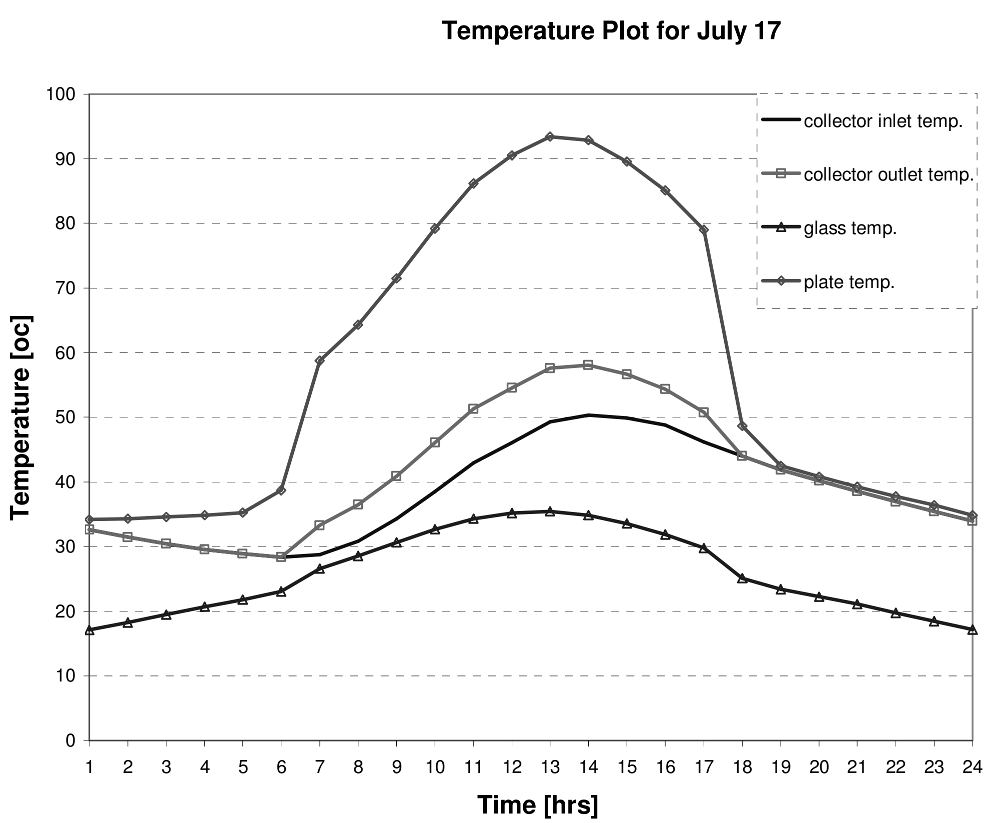

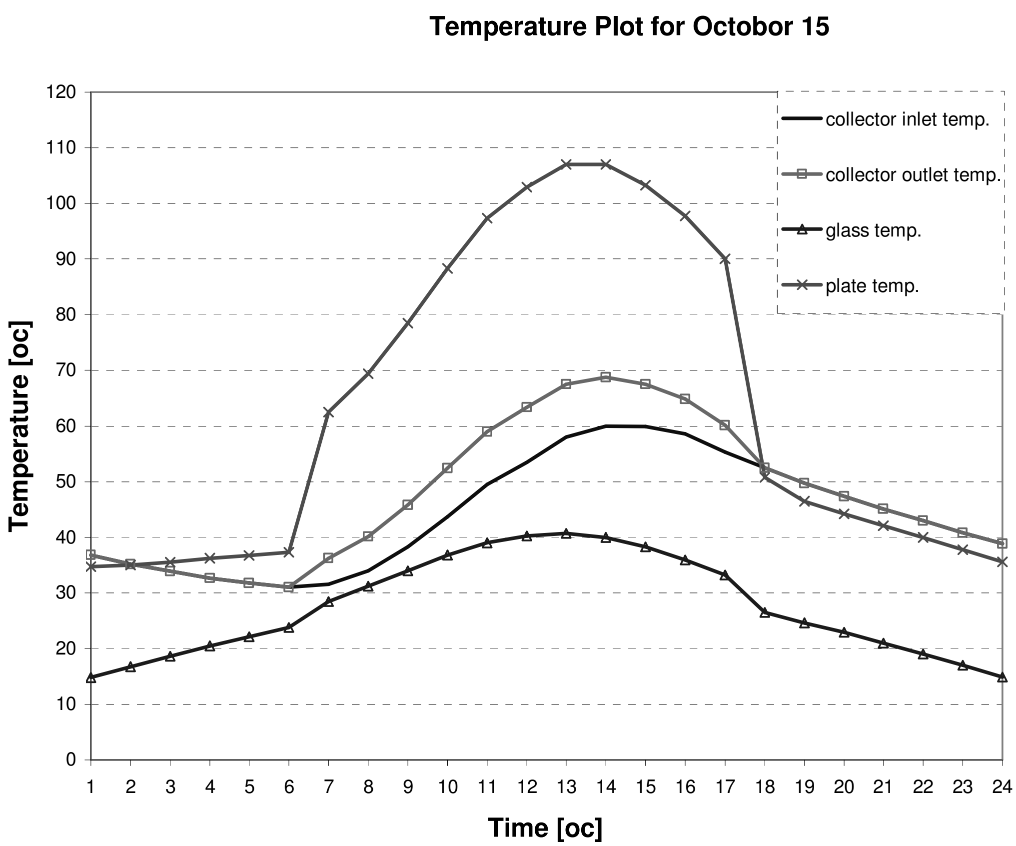
Temperature Plot for Octobor 15
Temperature [oc]
Time [oc]
collector inlet temp.
collector outlet temp.
glass temp.
plate temp.
0
10
20
30
40
50
60
70
80
90
100
110
120
1 2 3 4 5 6 7 8 9 10 11 12 13 14 15 16 17 18 19 20 21 22 23 24

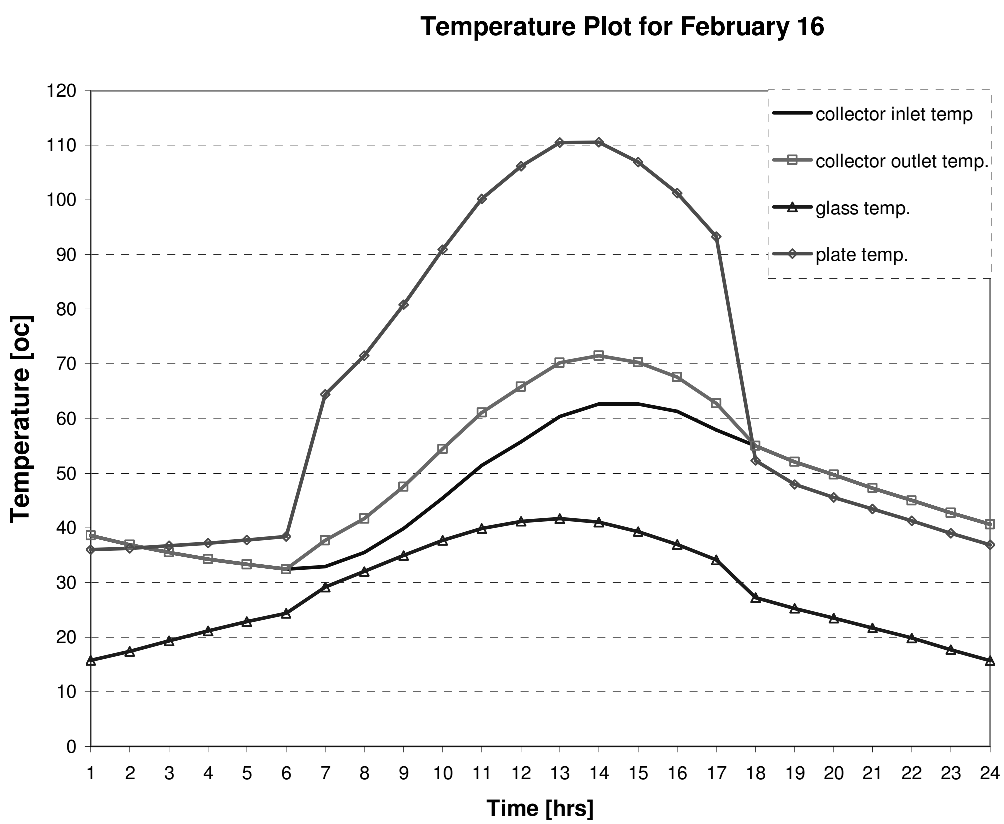
Temperature Plot for February 16
Temperature [oc]
Time [hrs]
collector inlet temp
collector outlet temp.
glass temp.
plate temp.
0
10
20
30
40
50
60
70
80
90
100
110
120
1 2 3 4 5 6 7 8 9 10 11 12 13 14 15 16 17 18 19 20 21 22 23 24

d) Jimma Hospital

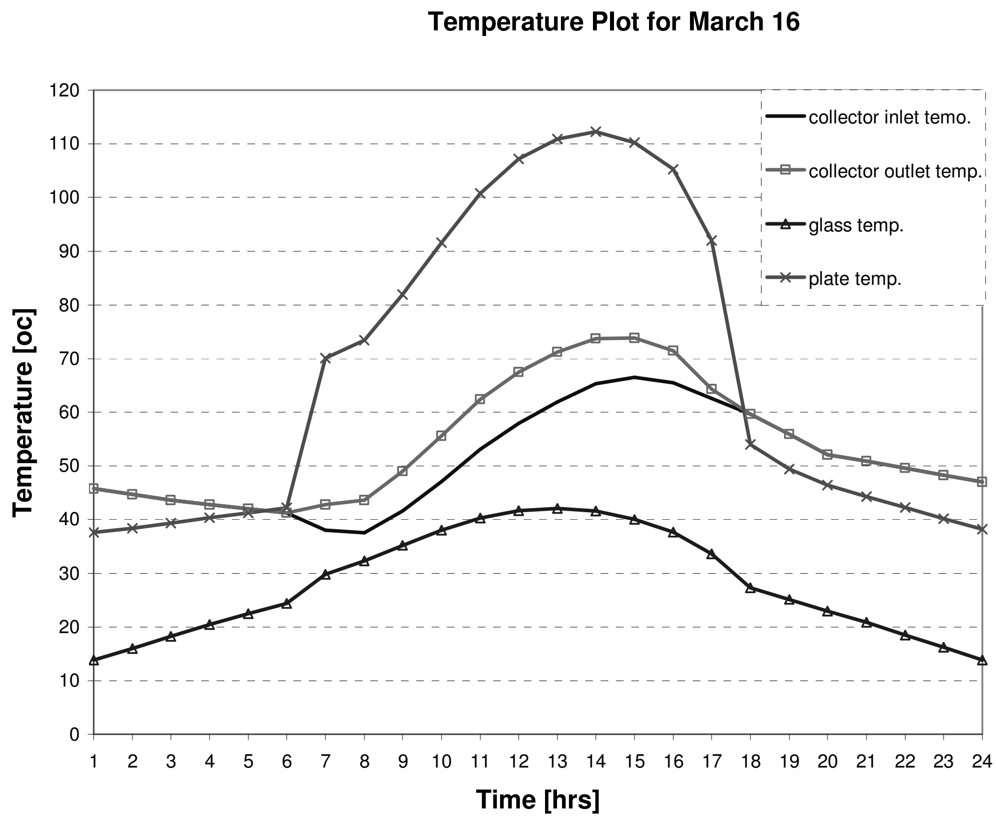

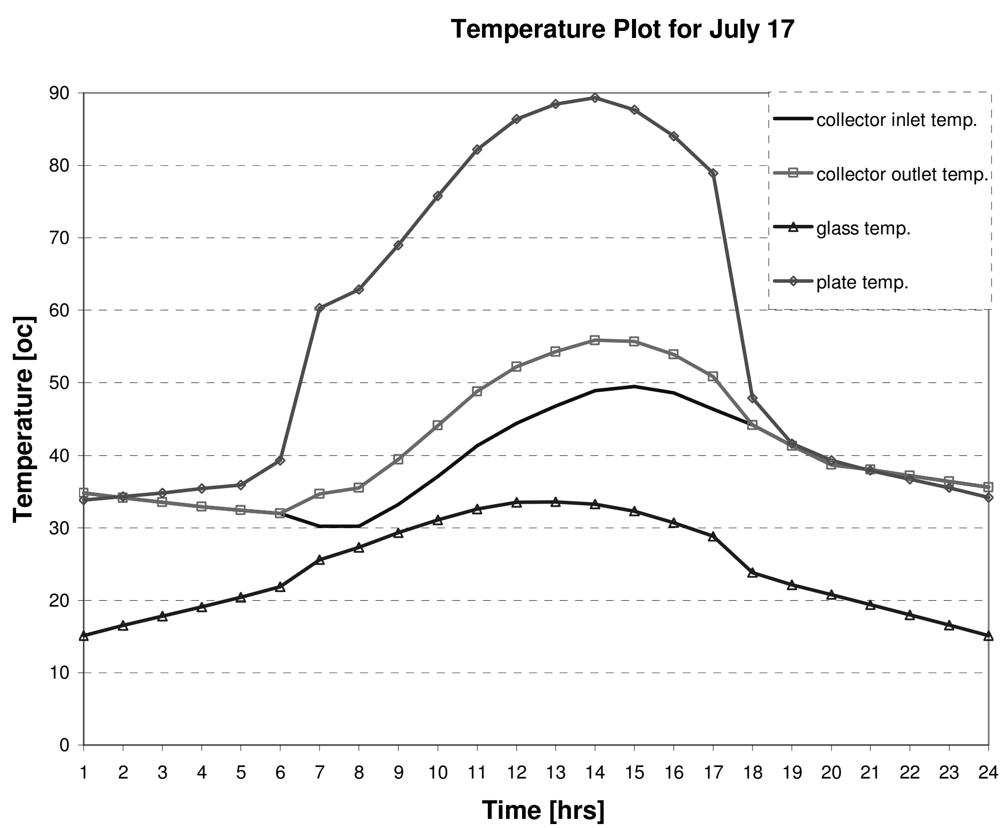

Temperature Plot for Novomber 14

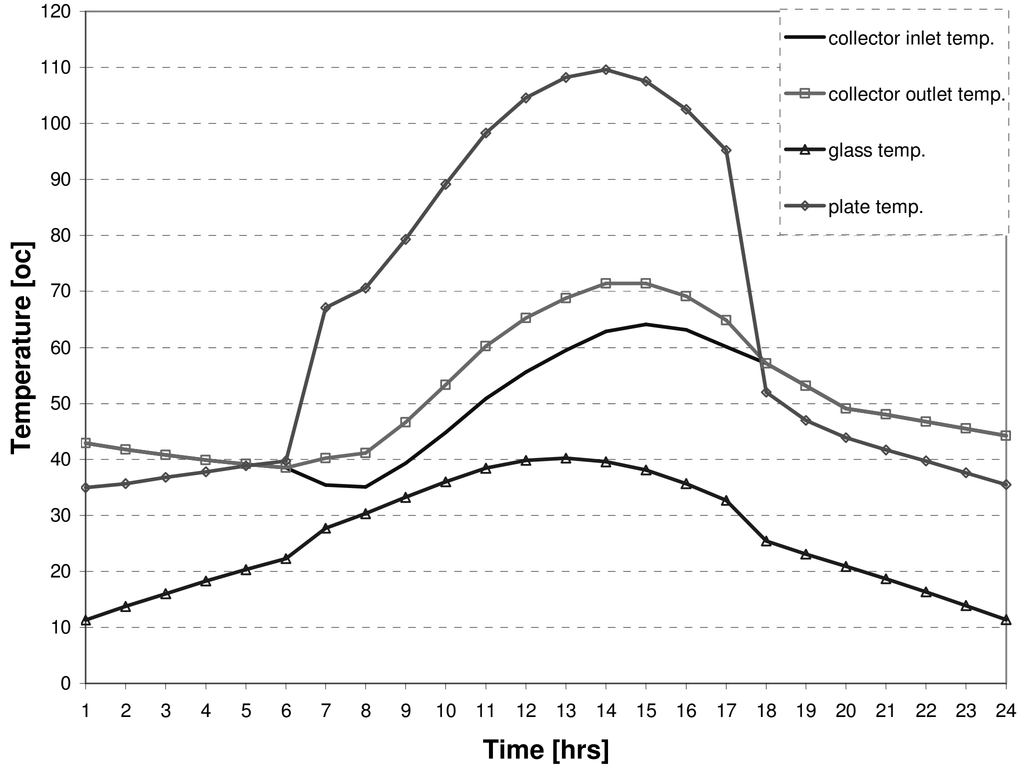

Temperature Plot for February 16

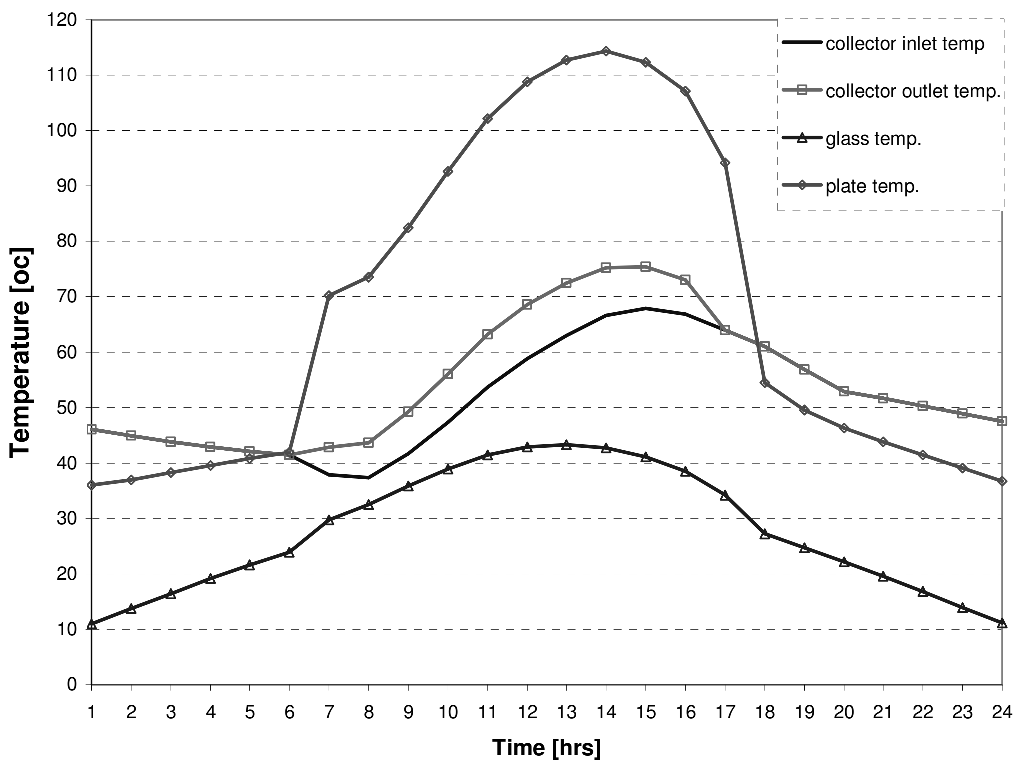

ANNEX B

SOLAR WATER HEATING SYSTEM LAYOUT

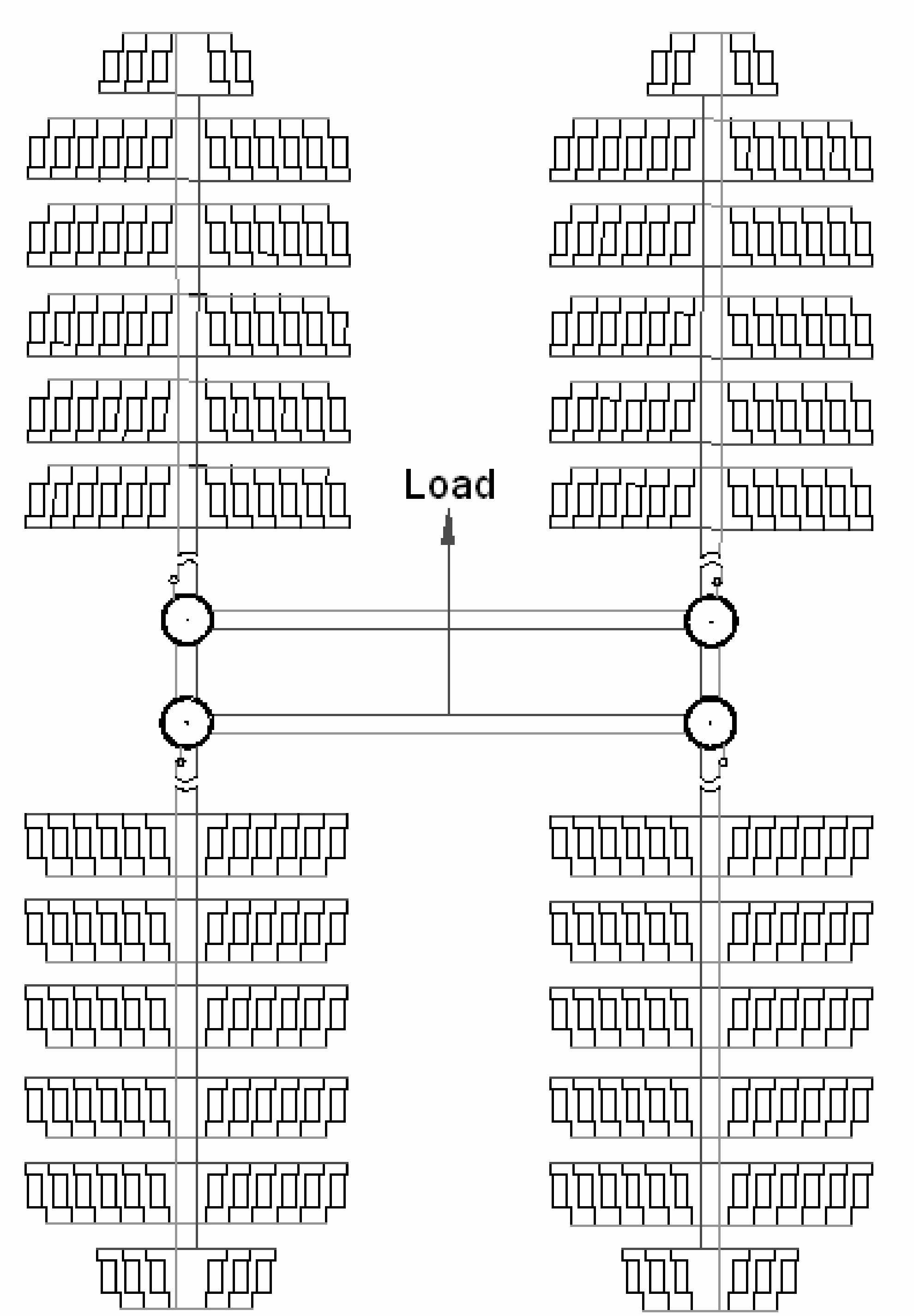

Figure B.1 Addis Ababa Tannery Solar Water Heating System Layout

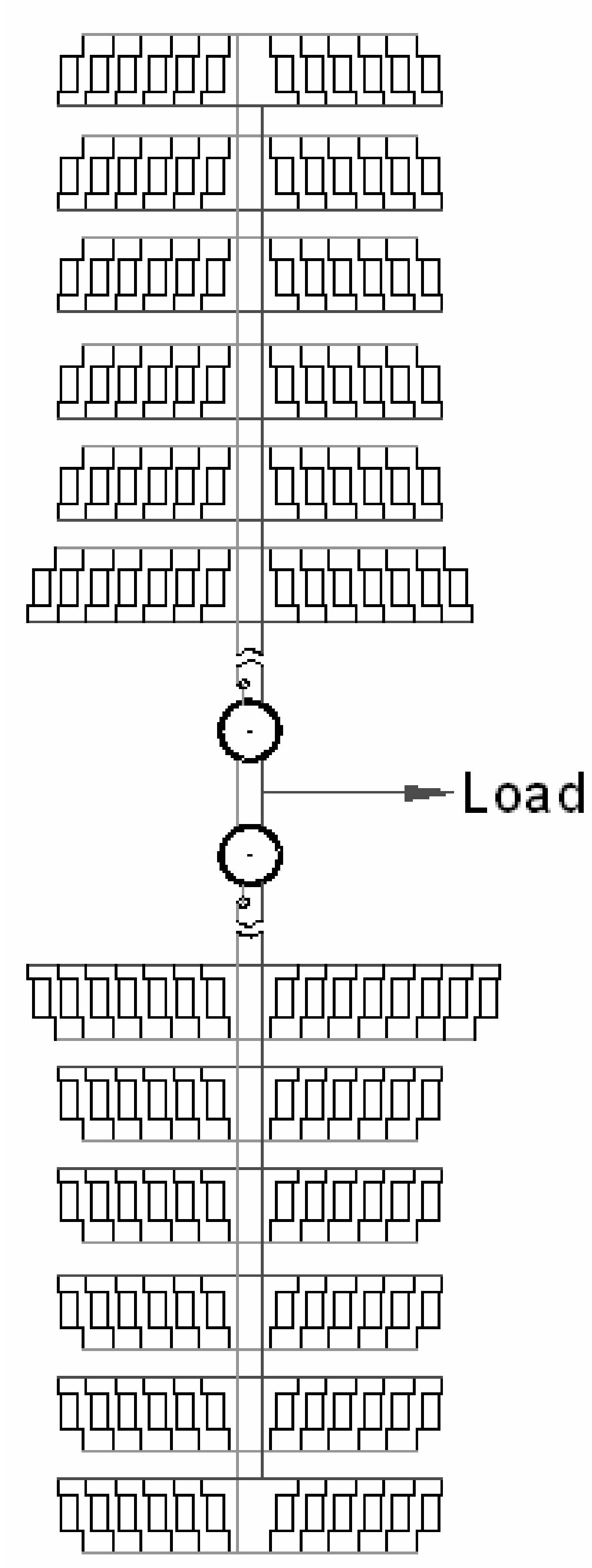

Figure B.2 Dire Tannery Solar Water Heating System Layout

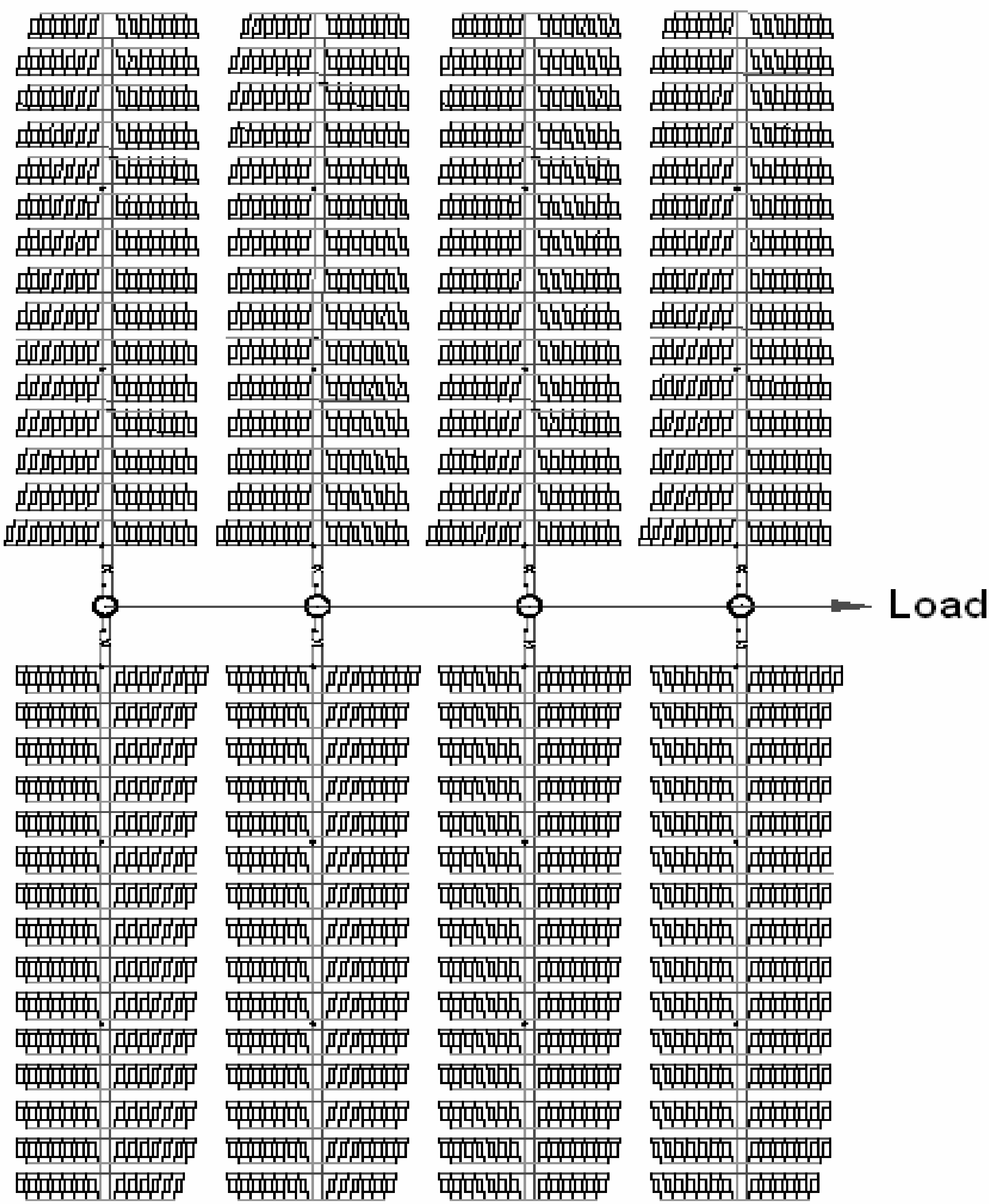

Figure B.3 Ethiopian Tannery Solar Water Heating System Layout

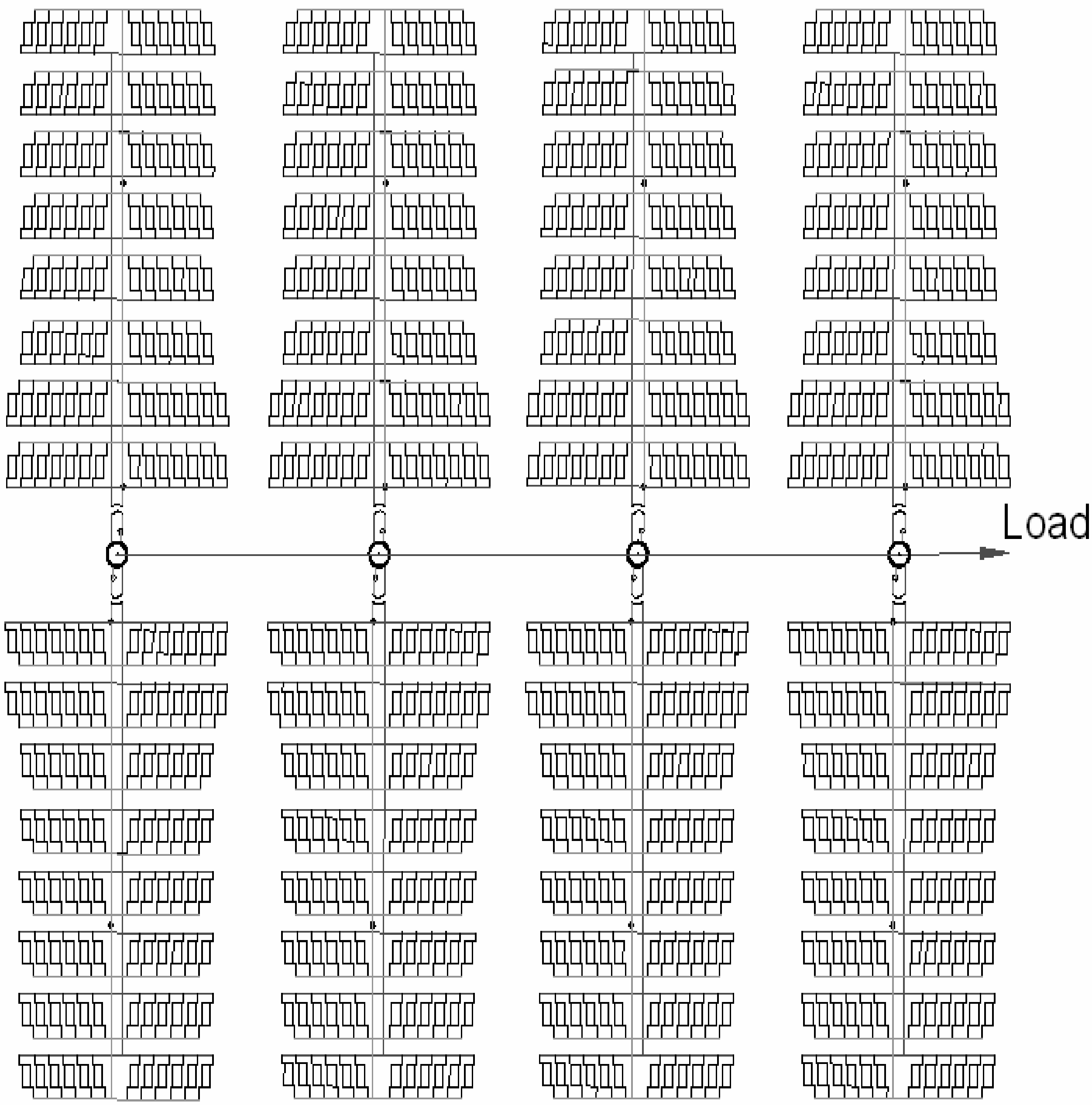

Figure B.4 Jimma Hospital Solar Water Heating System Layout

ANNEX C

PROPERTIES OF VARIOUS MATERIALS

Table C.1 Thermal Conductivities of Absorber Materials

Material	**Thermal Conductivity ($Wm^{-1} K^{-1}$)**
Copper	385
Aluminium	205
Mild Steel	54
Stainless steel	24
Acrylic	0.20
Polyethylene	0.30 – 0.44
Polypropylene	0.20
PVC(Polyvinyl Formal)	0.16

Table C. 2 Properties of Sealing Materials

Materials	**Working temp. Range(^{o} c) Min**	**Max**	**Elongation to Failure(%)**	**Resistance to Compre -ssion Set**	**Resistance to Creep**	**Resistance to Weathering**	**Resistance to Water**
Acrylic	-40	130	400	3	2	4	1
Butyl	-50	125	800	2-3	2	4	2-4
Chloroprene (Neoprene)	-20	130	600	3-4	2-3	4	3
Chlorosulphonated Polyethylene	-40	120	500	1-2	2	4	3-4
EPDM	-40	150	600	3-4	2	4	4
Fluroelastomers	-40	230	300	3-4	3	4	4
Silicone	-60	230	700	2-4	3	4	3-4
Urethanes	-50	100	700	1-4	3	4	1-2

(4=excellent, 3=good, 2=fair, 1=poor)

Table C. 3 Properties of Insulation Materials

Materials	**Thermal Conductivity @ 25 ºc ($Wm^{-1}K^{-1}$)**	**Maximum Service Temperature (º C)**
Glass Fibre	0.032	343
Mineral Fibre	0.036-0.055	649-1037
Calcium Silicate	0.055 (@90 º c)	649
Perlite	0.048	816
Foamed Glass	0.058	
Polystyrene Foam	0.029-0.039	74
Polyurethane Foam	0.023	104
Isocyanurate Foam	0.025	121
Phenolic Foam	0.033	135
Cellular Plastic	0.040	100

Table C. 4 Lists Properties of Some Selective Coatings

Coating	**Type**	**Absorptance α**	**Emittance ε_p**
Black Chrome	Electroplated	0.96	0.10
Black Nickel	Electroplated	0.90	0.10
Black Copper	Copper oxide	0.87-0.92	0.07-0.35
Black Anodize	Alulminium oxide	0.94	0.07
Solar Foil	Black chrome over copper	0.96	0.10
Enersorb*	Urethane paint	0.97	0.90
Nextel*	Paint	0.98	0.89

* Non-Selective